

E. WOLF, PROGRESS IN OPTICS 44
© 2004
ALL RIGHTS RESERVED

X

Multistep Parametric Processes in Nonlinear Optics

BY

SOLOMON M. SALTIEL^{1,2}, ANDREY A. SUKHOUKOV¹, AND YURI S. KIVSHAR¹

¹ NONLINEAR PHYSICS GROUP AND CENTER FOR ULTRA-HIGH BANDWIDTH DEVICES FOR OPTICAL SYSTEMS (CUDOS),
RESEARCH SCHOOL OF PHYSICAL SCIENCES AND ENGINEERING, AUSTRALIAN NATIONAL UNIVERSITY, CANBERRA ACT
0200, AUSTRALIA

HOME PAGE: WWW.RSPHYSSE.ANU.EDU.AU/NONLINEAR

² FACULTY OF PHYSICS, UNIVERSITY OF SOFIA, 5 J. BOURCHIER BLD, SOFIA BG-1164, BULGARIA

Abstract

We present a comprehensive overview of different types of parametric interactions in nonlinear optics which are associated with simultaneous phase-matching of several optical processes in quadratic nonlinear media, the so-called *multistep parametric interactions*. We discuss a number of possibilities of double and multiple phase-matching in engineered structures with the sign-varying second-order nonlinear susceptibility, including (i) uniform and non-uniform quasi-phase-matched (QPM) periodic optical superlattices, (ii) phase-reversed and periodically chirped QPM structures, and (iii) uniform QPM structures in non-collinear geometry, including recently fabricated two-dimensional nonlinear quadratic photonic crystals. We also summarize the most important experimental results on the multi-frequency generation due to multistep parametric processes, and overview the physics and basic properties of multi-color optical parametric solitons generated by these parametric interactions.

CONTENTS¹

	PAGE
1 Introduction	3
2 Single-phase-matched processes	4
3 Multistep phase-matched interactions	5
3.1 Third-harmonic multistep processes	7
3.2 Wavelength conversion	13
3.3 Two-color multistep cascading	17
3.4 Fourth-harmonic multistep cascading	19
3.5 OPO and OPA Multistep parametric processes	21
3.6 Other types of multistep interactions	24
3.7 Measurement of the $\chi^{(3)}$ -tensor components	25
4 Phase-matching for multistep cascading	27
4.1 Uniform QPM structures	27
4.2 Non-uniform QPM structures	29
4.3 Quadratic 2D nonlinear photonic crystals	32
5 Multi-color parametric solitons	36
5.1 Third-harmonic parametric solitons	37
5.2 Two-color parametric solitons	37
5.3 Solitons due to wavelength conversion	39
5.4 Other types of multi-color parametric solitons	40
6 Conclusions	41
7 Acknowledgements	41

¹Run LaTeX twice for up-to-date contents.

§ 1. Introduction

Energy transfer between different modes and phase-matching relations are the fundamental concepts in nonlinear optics. Unlike nonparametric nonlinear processes such as self-action and self-focusing of light in a nonlinear Kerr-like medium, parametric processes involve several waves at different frequencies and they require special relations between the wave numbers and wave group velocities to be satisfied, the so-called *phase-matching conditions*.

Parametric coupling between waves occurs naturally in nonlinear materials without the inversion symmetry, when the lowest-order nonlinear effects are presented by *quadratic nonlinearities*, often called $\chi^{(2)}$ nonlinearities because they are associated with the second-order contribution ($\sim \chi^{(2)} E^2$) to the nonlinear polarization of a medium. Conventionally, the phase-matching conditions for most parametric processes in optics are implemented either by using anisotropic crystals (the so-called perfect phase-matching), or they occur in fabricated structures with a periodically reversed sign of the quadratic susceptibility (the so-called quasi-phase-matching or QPM). The QPM technique is one of the leading technologies these days, and it employs the spatial scales ($\sim 1 \div 30 \mu\text{m}$) which are compatible with the operational wavelengths of optical communication systems.

Nonlinear effects produced by quadratic intensity-dependent response of a transparent dielectric medium are usually associated with parametric frequency conversion such as the second harmonic generation (SHG). The SHG process is one of the most well-studied parametric interactions which may occur in a quadratic nonlinear medium. Moreover, recent theoretical and experimental results demonstrate that quadratic nonlinearities can also produce many of the effects attributed to nonresonant Kerr nonlinearities via cascading of several second-order parametric processes. Such second-order cascading effects can simulate third-order processes and, in particular, those associated with the intensity-dependent change of the medium refractive index [Stegeman, Hagan, and Torner \[1996\]](#). Importantly, the effective (or induced) cubic nonlinearity resulting from a cascaded SHG process in a quadratic medium can be of the several orders of magnitude higher than that usually measured in centrosymmetric Kerr-like nonlinear media, and it is practically instantaneous.

The simplest type of the phase-matched parametric interaction is based on the simultaneous action of two second-order parametric sub-processes that belong to a single second-order interaction. For example, the so-called two-step cascading associated with type I SHG includes the generation of the second harmonic (SH), $\omega + \omega = 2\omega$, followed by the reconstruction of the fundamental wave through the down-conversion frequency mixing process, $2\omega - \omega = \omega$. These two sub-processes depend only on a single phase-matching parameter Δk . In particular, for the nonlinear $\chi^{(2)}$ media with a periodic modulation of the quadratic nonlinearity, for the QPM periodic structures, we have $\Delta k = k_2 - 2k_1 + G_m$, where $k_1 = k(\omega)$, $k_2 = k(2\omega)$ and G_m is a reciprocal vector of the periodic structure, $G_m = 2\pi m/\Lambda$, where Λ is the lattice spacing and m is integer. For a homogeneous bulk $\chi^{(2)}$ medium, we have $G_m = 0$.

Multistep parametric interactions and multistep cascading presents a special type of the second-order parametric processes that involve *several* different second-order nonlinear interactions; they are characterized by at least two different phase-matching parameters. For example, two parent processes of the so-called third-harmonic cascading are: (i) second-harmonic generation, $\omega + \omega = 2\omega$, and (ii) sum-frequency mixing, $\omega + 2\omega = 3\omega$. Here, we may distinguish five harmonic sub-processes, and the multistep interaction results in their simultaneous action.

Different types of the multistep parametric processes include third-harmonic cascaded generation, two-color parametric interaction, fourth-harmonic cascading, difference-frequency generation, etc. Various applications of the multistep parametric processes have been mentioned in the literature. In particular, the multistep parametric interaction can support multi-color solitary waves, it usually leads to larger accumulated nonlinear phase shifts, in comparison with the simple cascading, it can be effectively employed for the simultaneous generation of higher-order harmonics in a single quadratic crystal, and also for the generation of a cross-polarized wave and frequency shifting in fiber optics gratings. Generally, simultaneous phase-matching of several parametric processes cannot be achieved by the traditional methods such as those based on the optical birefringence effect. However, the situation becomes different for the media with a periodic change of the sign of the quadratic nonlinearity, as occurs in the QPM structures or two-dimensional nonlinear photonic crystals.

In this review paper, we describe the basic principles of simultaneous phase-matching of two (or more) parametric processes in different types of one- and two-dimensional nonlinear quadratic optical lattices. We divide different types of phase-matched parametric processes studied in nonlinear optics into *two major classes*, as shown in Fig. 1, and discuss different types of parametric interactions associated with simultaneous phase-matching of several optical processes in quadratic (or $\chi^{(2)}$) nonlinear media, the so-called multistep parametric interactions. In particular, we overview the basic principles of double and multiple phase-matching in engineered structures with the sign-varying second-order nonlinear susceptibility, including different types of QPM optical superlattices, non-collinear geometry, and two-dimensional nonlinear quadratic photonic crystals (which can be considered as two-dimensional QPM lattices). We also summarize the most important experimental results on the multi-frequency generation

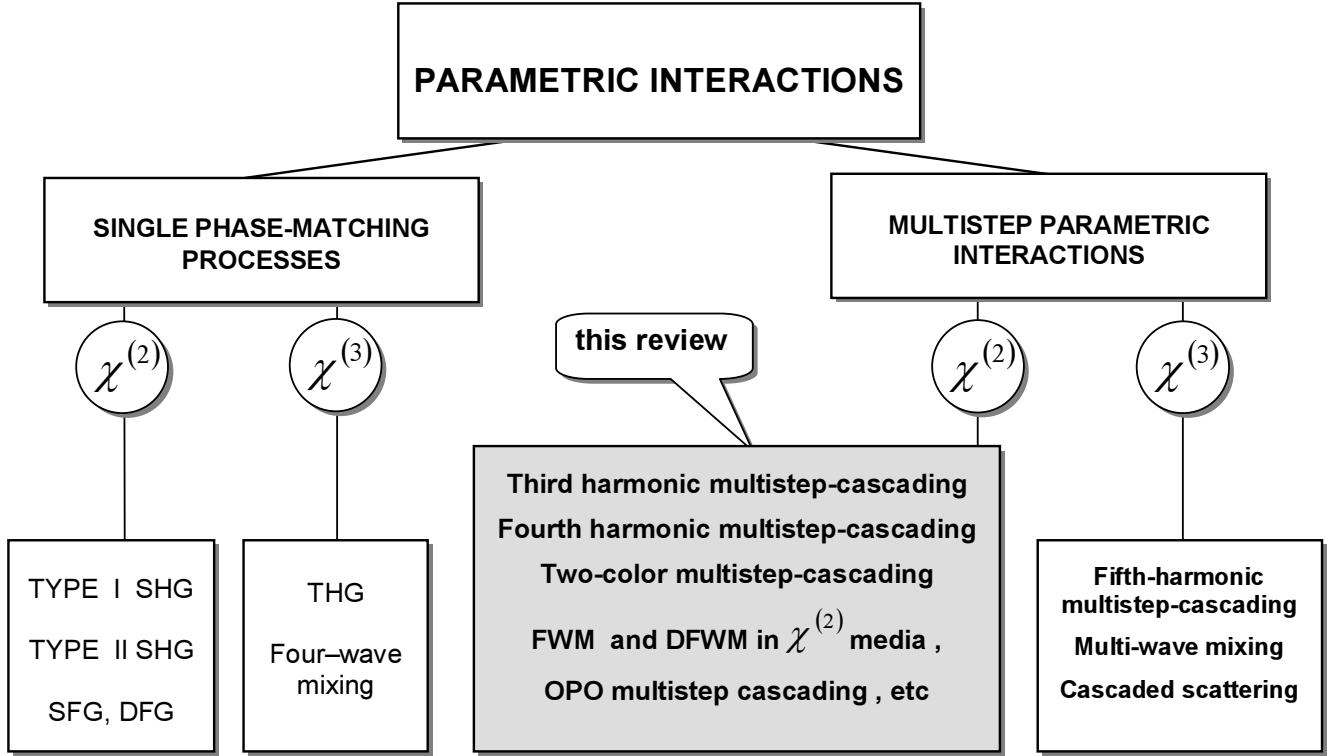


Figure 1: Different types of parametric processes in nonlinear optics, and the specific topics covered by this review paper. SHG: second-harmonic generation; SFG and DFG: sum- and difference-frequency generation, THG: third-harmonic generation; FWM: four-wave mixing; DFWM: degenerate FWM; OPO: optical parametric oscillator.

due to multistep parametric processes, and overview the physics and basic properties of multi-color optical solitons generated by these parametric interactions.

§ 2. Single-phase-matched processes

One of the simplest and first studied parametric process in nonlinear optics is the second-harmonic generation (SHG). The SHG process is a special case of a more general three-wave mixing process which occurs in a dielectric medium with a quadratic intensity-dependent response. The three-wave mixing and SHG processes require only one phase-matching condition to be satisfied and, therefore, they both can be classified as *single phase-matched processes*.

In this section, we discuss briefly these single phase-matched processes, and consider parametric interaction between three continuous-wave (CW) waves with the electric fields $E_j = \frac{1}{2}[A_j \exp(-i\mathbf{k}_j \cdot \mathbf{r} + i\omega_j t) + \text{c.c.}]$, where $j = 1, 2, 3$, with the three frequencies satisfying the energy-conservation condition, $\omega_1 + \omega_2 = \omega_3$. We assume that the phase-matching condition is nearly satisfied, with a small mismatch Δk among the three wave vectors; i.e., $\Delta k = k_3(\omega_3) - k_1(\omega_1) - k_2(\omega_2)$. In general, the three waves do not propagate along the same direction, and the beams may walk off from each other as they propagate inside the crystal. If all three wave vectors point along the same direction (as, e.g., in the case of the QPM materials), the waves have the same phase velocity and exhibit no walk-off.

The theory of $\chi^{(2)}$ -mediated three-wave mixing is available in several books devoted to nonlinear optics ([Shen \[1984\]](#); [Butcher and Cotter \[1992\]](#); [Boyd \[1992\]](#)). The starting point is the Maxwell wave equation written as

$$\nabla \times \nabla \times \mathbf{E} + \frac{1}{c^2} \frac{\partial^2 \mathbf{E}}{\partial t^2} = -\frac{1}{\epsilon_0 c^2} \frac{\partial^2 \mathbf{P}}{\partial t^2}, \quad (2.1)$$

where ϵ_0 is the vacuum permittivity and c is the speed of light in a vacuum. The induced polarization is written in the frequency domain as

$$\tilde{\mathbf{P}}(\mathbf{r}, \omega) = \epsilon_0 \chi^{(1)} \tilde{\mathbf{E}} + \epsilon_0 \chi^{(2)} \tilde{\mathbf{E}} \tilde{\mathbf{E}} + \dots, \quad (2.2)$$

where a tilde denotes the Fourier transform. Using the slowly varying envelope approximation and neglecting the walk-off, one can derive the following set of three coupled equations describing the parametric interaction of three waves under type II phase matching:

$$ik_1 \frac{dA_1}{dz} - \omega_1^2 \Gamma A_3 A_2^* e^{-i\Delta kz} = 0, \quad (2.3)$$

$$ik_2 \frac{dA_2}{dz} - \omega_2^2 \Gamma A_3 A_1^* e^{-i\Delta kz} = 0, \quad (2.4)$$

$$ik_3 \frac{dA_3}{dz} - \omega_3^2 \Gamma A_1 A_2 e^{i\Delta kz} = 0, \quad (2.5)$$

where $\Gamma = d_{\text{eff}}^{(2)}/c^2$, and $d_{\text{eff}}^{(2)}$ is a convolution of the second-order susceptibility tensor $\hat{\chi}^{(2)}$ and the polarization unit vectors of the three fields, $d_{\text{eff}}^{(2)} = \frac{1}{2} \langle \mathbf{e}_3 \hat{\chi}^{(2)} \mathbf{e}_1 \mathbf{e}_2 \rangle$.

In the case of type I SHG, only a single beam at the pump frequency ω_1 is incident on the nonlinear crystal, and a new optical field at the frequency $2\omega_1$ is generated during the SHG process. We can adapt Eqs. (2.3)–(2.5) to this case with minor modifications. More specifically, we set $\omega_3 = 2\omega_1$ and $A_1 = A_2$. The first two equations then become identical, and one of them can be dropped. The type I SHG process is thus governed by the following set of two coupled equations:

$$ik_1 \frac{dA_1}{dz} - k_1 \sigma A_3 A_1^* e^{-i\Delta kz} = 0, \quad (2.6)$$

$$ik_3 \frac{dA_3}{dz} - 2k_1 \sigma A_1^2 e^{i\Delta kz} = 0, \quad (2.7)$$

where $\sigma = (\omega_1/n_1 c) d_{\text{eff}}^{(2)}$ is the nonlinearity parameter and $\Delta k = k_3 - 2k_1$ is the phase-mismatch parameter.

Both the three-wave mixing and SHG processes present an example of a single-phase-matched parametric process because it is controlled by a single phase-matching parameter Δk . This kind of parametric processes can be described as a two-step cascading interaction which includes: (i) the generation of the second-harmonic (SH) wave, $\omega + \omega = 2\omega$, followed by (ii) the reconstruction of the fundamental wave through the down-conversion frequency mixing process, i.e. $2\omega - \omega = \omega$. Respectively, the first sub-process is responsible for the generation of the SH field, with the most efficient conversion observed at $\Delta k = 0$, while the second sub-process, also called cascading, can be associated with an effective intensity-dependent change of the phase of the fundamental harmonic ($\sim d^2/\Delta k$), which is similar to that of the cubic nonlinearity (DeSalvo, Hagan, Sheik-Bahae, Stegeman, Vanstryland, and Vanherzele [1992]; Stegeman, Hagan, and Torner [1996]; Assanto, Stegeman, Sheik-Bahae, and Vanstryland [1995]). This latter effect is responsible for the generation of the so-called quadratic solitons, two-wave parametric soliton composed of the mutually coupled fundamental and second-harmonic components (Sukhorukov [1988]; Torner [1998]; Kivshar [1997]; Etrich, Lederer, Malomed, Peschel, and Peschel [2000]; Torruellas, Kivshar, and Stegeman [2001]; Boardman and Sukhorukov [2001]; Buryak, Di Trapani, Skryabin, and Trillo [2002], and references therein).

Multistep parametric interactions and multistep cascading effects discussed in this review paper are presented by different types of phase-matched parametric interactions in quadratic (or $\chi^{(2)}$) nonlinear media which involve several different parametrically interacting waves, e.g. as in the case of the frequency mixing and sum-frequency generation. However, all such interactions can also be associated with the two major physical mechanisms of the wave interaction discussed for the SH process above: (i) parametric energy transfer between waves determined by the phase-mismatch between the wave vectors of the interacting waves, and (ii) phase changes due to this parametric interaction. Below, we discuss these interactions for a number of physically important examples.

§ 3. Multistep phase-matched interactions

Table 1: Examples of multistep parametric interactions involving SHG.

No.	Multistep parametric process	Cascading steps	$\chi^{(2)}$	Equivalent order	high-parametric process
1	Type I third-harmonic multistep process	$\omega + \omega = 2\omega; \omega + 2\omega = 3\omega$			$\omega + \omega + \omega = 3\omega$
2	Type II third-harmonic multistep process	$\omega + \omega = 2\omega; \omega_{\perp} + 2\omega = 3\omega$			$\omega + \omega + \omega_{\perp} = 3\omega$

No.	Multistep parametric process	Cascading steps	$\chi^{(2)}$	Equivalent high-order parametric process
3	3:1 frequency conversion and division	$3\omega \rightarrow 2\omega + \omega ; \omega = 2\omega - \omega$		
4	Fourth-harmonic multistep process	$\omega + \omega = 2\omega ; 2\omega + 2\omega = 4\omega$		$\omega + \omega + \omega + \omega = 4\omega$
5	Type I & Type II two-color multistep process	$\omega + \omega = 2\omega ; 2\omega - \omega = \omega_{\perp}$		$\omega + \omega - \omega = \omega_{\perp}$
6	Type I & Type II two-color multistep process	$\omega + \omega = 2\omega ; \omega_{\perp} + \omega_{\perp} = 2\omega$		
7	wavelength conversion	$\omega + \omega = 2\omega ; 2\omega - \omega_a = \omega_b$		$\omega + \omega - \omega_a = \omega_b$
8	Self-doubling OPO	$\omega_p \rightarrow \omega_i + \omega_s ; \omega_s + \omega_s = \omega_{s,SH}$		
9	Self-sum-frequency generation OPO	$\omega_p \rightarrow \omega_i + \omega_s ; \omega_s + \omega_p = \omega_{SFG}$		
10	Internally pumped OPO	$\omega_{p/2} + \omega_{p/2} = \omega_p ; \omega_p \rightarrow \omega_i + \omega_s$		

In the table above, the symbol ω_{\perp} stands for a wave polarized in the plane perpendicular to that of the wave with the main carrier frequency ω .

In this part, we consider the nonlinear parametric interactions that involve several processes, such that each of the processes is described by an independent phase-matching parameter. In the early days of nonlinear optics, the motivation to study this kind of parametric interactions was to explore various possibilities for the simultaneous generation of several harmonics in a single nonlinear crystal (see, e.g., [Akhmanov and Khokhlov \[1964, 1972\]](#)) as well as to use the cascading of several parametric processes for measuring higher-order susceptibilities in nonlinear optical crystals (see, e.g., [Yablonovitch, Flytzanis, and Bloembergen \[1972\]](#); [Akhmanov, Dubovik, Saltiel, Tomov, and Tunkin \[1974\]](#); [Akhmanov \[1977\]](#); [Kildal and Iseler \[1979\]](#); [Bloembergen \[1982\]](#)). More recently, these processes were proved to be efficient for the higher-order harmonic generation, for building reliable standards for the third-order nonlinear susceptibility measurements (see, e.g., [Bosshard, Gubler, Kaatz, Mazerant, and Meier \[2000\]](#) and references therein), and also for generating multi-color optical solitons. Additionally, it is expected that the multistep parametric processes and multistep cascading will find their applications in optical communication devices, for wavelength shifting and all-optical switching (see discussions below). Another class of applications of the multistep phase-matched parametric processes is the construction of optical parametric oscillators (OPOs) and optical parametric amplifiers (OPAs) with complimentary phase-matched processes in the same nonlinear crystal where the main phase-matched parametric process occurs. In this way, the OPOs and OPAs may possess additional coherent tunable outputs (see Sec. 3.5 below). On the basis of the third-harmonic multistep cascading process $\{\omega + \omega = 2\omega; \omega + 2\omega = 3\omega\}$, real advances have been made in the development of the nonlinear optical systems for division by three. The multistep parametric interactions governed by several phase-mismatching parameters can also occur in centrosymmetric nonlinear media (see, e.g., [Akhmanov, Martynov, Saltiel, and Tunkin \[1975\]](#); [Reintjes \[1984\]](#); [Astinov, Kubarych, Milne, and Miller \[2000\]](#); [Crespo, Mendonca, and Dos Santos \[2000\]](#); [Misoguti, Backus, Durfee, Bartels, Murnane, and Kapteyn \[2001\]](#)).

The first proposal for simultaneous phase-matching of two parametric processes can be found in the pioneering book of Akhmanov and Khokhlov ([Akhmanov and Khokhlov \[1964, 1972\]](#)) who derived and investigated the condition for the THG process in a single crystal with the quadratic nonlinearity through the combined action of the SHG and SFG parametric processes. For the efficient frequency conversion, both the parametric processes, i.e. SHG and SFG, should be phase matched simultaneously. Some earlier experimental attempts to achieve simultaneously two phase-matching conditions for the SHG and SFG processes were not very successful ([Sukhorukov and Tomov \[1970\]](#), [Orlov, Sukhorukov, and Tomov \[1972\]](#)). Recent development of novel techniques for efficient phase matching, including the QPM technique, make many of such multistep processes readily possible.

The multistep parametric processes investigated so far can be divided into several groups, as shown in Fig. 1 and Table 1. These processes include: third-harmonic multistep cascading; fourth-harmonic multistep cascading; two-color multistep cascading; FWM and DFWM in $\chi^{(2)}$ media, OPO and OPA multistep cascading. We will review these groups separately.

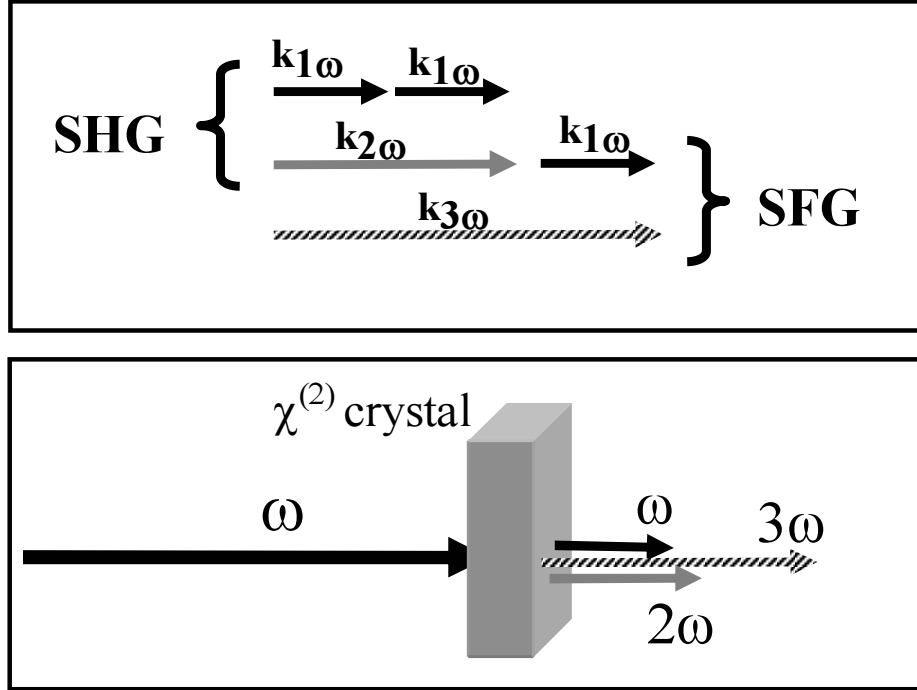


Figure 2: Schematic of the THG multistep cascading.

Table 1 does not provide a complete list of all possible types of the multistep parametric processes. Here, we pick up only several examples for each type of the multistep process. As follows from Table 1, some of the parametric processes simulate some known higher-order processes but occur through several steps. However, some other multistep parametric processes have no such simpler analogues. Below in the review paper, we discuss some of those processes in more details. For example, the THG multistep cascading is considered in Sec. 3.1, while the two-color multistep cascading is discussed in Sec. 3.3. The last three lines in Table 1 are the examples of the multistep cascading processes in optical parametric oscillators and amplifiers, and they will be discussed in Sec. 3.5.

To illustrate the physics responsible for the use of the terminology "multistep interaction" or "multistep cascading", we just point out the simultaneous action of SHG and SFG (line 1 in Table 1); this three-wave interaction involves five simpler parametric sub-processes in a quadratic medium. In order to describe, for example, the nonlinear phase shift of the fundamental wave accumulated in this interaction, we should consider the following chain of parametric interactions: SHG ($\omega + \omega = 2\omega$), SFG ($\omega + 2\omega = 3\omega$), DFM ($3\omega - \omega = 2\omega$), and, finally, another DFM ($2\omega - \omega = \omega$).

3.1. THIRD-HARMONIC MULTISTEP PROCESSES

The multistep parametric interaction involving the THG process is one of the most extensively studied multistep cascading schemes (see Fig. 2). The two simpler parametric interactions are the SHG process, $\omega + \omega = 2\omega$, and the SFG process, $\omega + 2\omega = 3\omega$. Each of these sub-processes is characterized by an independent phase matching parameter, namely $\Delta k_{\text{SHG}} = k_{2\omega} - 2k_{1\omega}$ and $\Delta k_{\text{SFG}} = k_{3\omega} - k_{2\omega} - k_{\omega}$.

This kind of the multistep cascading appears in many schemes of parametric interactions in nonlinear optics, including: (i) efficient generation of the third harmonic in a single quadratic crystal; (ii) measurement of unknown $\chi^{(3)}$ tensor components using known $\chi^{(2)}$ components of the crystal as a reference; (iii) accumulation of a large nonlinear phase shift by the fundamental wave; (iv) propagation of multi-color solitons; (v) frequency division; (vi) generation of entangled and squeezed photon states, etc.

3.1.1. Efficient generation of a third-harmonic wave

First we consider the process of efficient generation of a third-harmonic wave. In the approximation of plane waves, this process is described by the following system of coupled equations for the slowly varying amplitudes A_1 , A_2 ,

and A_3 of the fundamental, second-, and third-harmonic waves, respectively:

$$\begin{aligned}\frac{dA_1}{dz} &= -i\sigma_1 A_2 A_1^* e^{-i\Delta k_{\text{SHG}} z} - i\sigma_3 A_3 A_2^* e^{-i\Delta k_{\text{SFG}} z}, \\ \frac{dA_2}{dz} &= -i\sigma_2 A_1^2 e^{i\Delta k_{\text{SHG}} z} - i\sigma_4 A_3 A_1^* e^{-i\Delta k_{\text{SFG}} z}, \\ \frac{dA_3}{dz} &= -i\sigma_5 A_2 A_1 e^{i\Delta k_{\text{SFG}} z} - i\gamma A_1^3 e^{i\Delta k_{\text{THG}} z},\end{aligned}\quad (3.1)$$

where $\Delta k_{\text{SHG}} = k_2 - 2k_1 + G_p$ and $\Delta k_{\text{SFG}} = k_3 - k_2 - k_1 + G_q$, $\sigma_{1,2} = (2\pi/\lambda_1 n_{1,2})d_{\text{eff,I}}$ and $\sigma_j = (\omega_{j-2}/\omega_1)(2\pi/\lambda_1 n_{j-2})d_{\text{eff,II}}$ (where $j = 3, 4, 5$). Here, the parameters $d_{\text{eff,I}}$ and $d_{\text{eff,II}}$ are the effective quadratic nonlinearities corresponding to the two steps of the multistep parametric process; its values depend on the crystal orientation (see, e.g., [Dmitriev *et al.* \[1999\]](#)) and the method of phase matching (PM). The parameter γ is found as $\gamma = (3\pi/4\lambda_1 n_3)\chi_{\text{eff}}^{(3)}$ (for calculation of $\chi_{\text{eff}}^{(3)}$ in crystals see [Yang and Xie \[1995\]](#)). The complementary wave vectors G_p and G_q are two vectors of the QPM structure that can be used for achieving double phase matching. A solution of this system (see, e.g., [Kim and Yoon \[2002\]](#); [Qin, Zhu, Zhang, and Ming \[2003\]](#)) gives maximum for THG in several different situations, when (i) $\Delta k_{\text{SHG}} \rightarrow 0$; (ii) $\Delta k_{\text{SFG}} \rightarrow 0$; (iii) $\Delta k_{\text{THG}} = \Delta k_{\text{SHG}} + \Delta k_{\text{SFG}} = k_3 - 3k_1 \rightarrow 0$; and (iv) simultaneously $\Delta k_{\text{SHG}} \rightarrow 0$ and $\Delta k_{\text{SFG}} \rightarrow 0$. The latter condition, for which both SHG and SFG steps should be simultaneously phase matched, corresponds to the highest efficiency for THG. The intensity of the third-harmonic (TH) wave is proportional to the fourth power of the crystal length,

$$|A_3(L)|^2 = \frac{1}{4}\sigma_2^2\sigma_5^2|A_1|^6L^4. \quad (3.2)$$

This expression should be compared with the analogous result for the centrosymmetric media:

$$|A_3(L)|^2 = \gamma^2|A_1|^6L^2. \quad (3.3)$$

The advantage of the single-crystal phase-matched cascaded THG becomes clear if we note that, in average, $(\sigma_2\sigma_5 L)^2$ is in $10^4 - 10^6$ times larger than γ^2 , even for the sample length as small as 1 mm.

Table 2: Experimental results on cascaded THG processes

Nonlinear crystal	λ_ω [μm]	Phase-matched steps	Phase matching method	L [cm]	Regime	$\eta, \%$	Refs.
LiTaO ₃	1.44	$\Delta k_{\text{SHG}} \approx 0; \Delta k_{\text{SFG}} \approx 0$	QPOS	1.5	Pulsed (8 ns)	27%	a
LiTaO ₃	1.570	$\Delta k_{\text{SHG}} \approx 0; \Delta k_{\text{SFG}} \approx 0$	QPOS	0.8	Pulsed (8 ns)	23%	b, c
LiTaO ₃	1.342	$\Delta k_{\text{SHG}} \approx 0; \Delta k_{\text{SFG}} \approx 0$	SHG-QPM 1st-ord. SFG-QPM 3rd-ord.	1.8	quasi-cw (30 ns)	19.3 %	d
LiTaO ₃	1.342	$\Delta k_{\text{SHG}} \approx 0; \Delta k_{\text{SFG}} \approx 0$	SHG-QPM 1st-ord. SFG-QPM 3rd-ord.	1.2	Pulsed (90 ns)	10.2%	e
β -BBO	1.055	$\Delta k_{\text{THG}} \approx 0;$ $\Delta k_{\text{SFG}} = -\Delta k_{\text{SHG}} \neq 0$	BPM	0.3	Pulsed (350 fs)	6%	f, g
LiTaO ₃	1.442	$\Delta k_{\text{SHG}} \approx 0; \Delta k_{\text{SFG}} \approx 0$	QPOS	0.6	Pulsed (10 ns)	5.8%	h
KTP	1.8	$\Delta k_{\text{SHG}} \neq 0; \Delta k_{\text{SFG}} \approx 0$	BPM		Pulsed (35 ps)	5%	i
LiTaO ₃	1.064	$\Delta k_{\text{SHG}} \approx 0; \Delta k_{\text{SFG}} \approx 0$	PR-QPM	1.2	quasi-cw (150 ns)	2.8%	j
KTP	1.618	$\Delta k_{\text{THG}} \approx 0;$ $\Delta k_{\text{SFG}} = -\Delta k_{\text{SHG}} \neq 0$	BPM	0.11	Pulsed (22 ps)	2.4%	k, l
SBN	1.728	$\Delta k_{\text{SHG}} \approx 0; \Delta k_{\text{SFG}} \approx 0$	QPOS	0.75	Pulsed (15 ps)	1.6%	m
d-LAP	1.055	$\Delta k_{\text{THG}} \approx 0;$ $\Delta k_{\text{SFG}} = -\Delta k_{\text{SHG}} \neq 0$	BPM	0.1	Pulsed (350 fs)	1.2%	f, g

Nonlinear crystal	λ_ω [μm]	Phase-matched steps	Phase matching method	L [cm]	Regime	$\eta, \%$	Refs.
β -BBO	1.05	$\Delta k_{\text{THG}} \approx 0$; $\Delta k_{\text{SFG}} = -\Delta k_{\text{SHG}} \neq 0$	BPM	0.72	Pulsed (5 ps)	0.8%	n
KTP waveguide	1.234	$\Delta k_{\text{SHG}} \approx 0$; $\Delta k_{\text{SFG}} \approx 0$	QPM	0.26	Pulsed (9 ns)	0.4% ²	o
KTP	1.32	$\Delta k_{\text{SHG}} \neq 0$; $\Delta k_{\text{SFG}} \approx 0$	BPM	0.47	pulsed (200 fs)	0.17%	p,q
LiNbO ₃ waveguide	1.619	$\Delta k_{\text{SHG}} \approx 0$; $\Delta k_{\text{SFG}} \approx 0$	SHG- QPM 1st-ord. SFG- QPM 3rd-ord.		pulsed (7 ps)	0.055%	r
LiNbO ₃	1.534	$\Delta k_{\text{SHG}} \neq 0$; $\Delta k_{\text{SFG}} \approx 0$	QPM	0.6	Pulsed (9 ns)	0.016% ³	s
KTP waveguide	1.65	$\Delta k_{\text{SHG}} \approx 0$; $\Delta k_{\text{SFG}} \approx 0$	SHG- QPM 1st-ord. SFG- QPM 3rd-ord.	0.35	pulsed (6 ps)	0.011%	t
β -BBO	1.053	$\Delta k_{\text{THG}} \approx 0$; $\Delta k_{\text{SFG}} = -\Delta k_{\text{SHG}} \neq 0$	BPM	0.7	Pulsed (45 ps)	0.007%	u
LiNbO ₃ 2D-NPC	1.536	$\Delta k_{\text{SHG}} \approx 0$; $\Delta k_{\text{SFG}} \approx 0$	2D-QPM	1	pulsed (5 ns)	0.01% ⁴	v
LiNbO ₃	3.561	$\Delta k_{\text{SHG}} \approx 0$; $\Delta k_{\text{SFG}} \approx 0$	QPM	2	CW	$10^{-4}\%$ [W ⁻²]	w
KTP	1.55	$\Delta k_{\text{SHG}} \approx 0$; $\Delta k_{\text{SFG}} \approx 0$	QPOS	1	CW	$3.10^{-5}\%$ [W.cm ⁻²]	x
Y:LiNbO ₃	1.064	$\Delta k_{\text{SHG}} \approx 0$; $\Delta k_{\text{SFG}} \approx 0$	SHG-QPM 9th-ord. SFG-QPM 33rd-ord.	0.5	pulsed (100 ns)	$10^{-5}\%$	y

References:

^a Zhang, Wei, Zhu, Wang, Zhu, and Ming [2001]
^b Qin, Zhu, Zhu, and Ming [1998]
^c Zhu, Zhu, and Ming [1997]
^d He, Liu, Luo, Jia, Du, Guo, and Zhu [2002]
^e Luo, Zhu, He, Zhu, Wang, Liu, Zhang, and Ming [2001]
^f Banks, Feit, and Perry [1999]
^g Banks, Feit, and Perry [2002]
^h Chen, Zhang, Zhu, Zhu, Wang, and Ming [2001]
ⁱ Takagi and Muraki [2000]
^j Liu, Du, Liao, Zhu, Zhu, Qin, Wang, He, Zhang, and Ming [2002]
^k Feve, Boulanger, and Guillien [2000]
^l Boulanger, Feve, Delarue, Rousseau, and Marnier [1999]
^m Zhu, Xiao, Fu, Wong, and Ming [1998]
ⁿ Qiu and Penzkofer [1988]
^o Gu, Makarov, Ding, Khurjin, and Risk [1999]
^p Mu, Gu, Makarov, Ding, Wang, Wei, and Liu [2000]
^q Ding, Mu, and Gu [2000]
^r Baldi, Trevino-Palacios, Stegeman, Demicheli, Ostrowsky, Delacourt, and Papuchon [1995]
^s Gu, Korotkov, Ding, Kang, and Khurjin [1998]
^t Sundheimer, Villeneuve, Stegeman, and Bierlein [1994b]
^u Tomov, Van Wonterghem, and Rentzepis [1992]
^v Broderick, Brattalean, Monroe, Richardson, and de Sterke [2002]
^w Pfister, Wells, Hollberg, Zink, Van Baak, Levenson, and Bosenberg [1997]
^x Fradkin-Kashi, Arie, Urenski, and Rosenman [2002]

²backward THG³backward THG⁴Type II cascaded THG

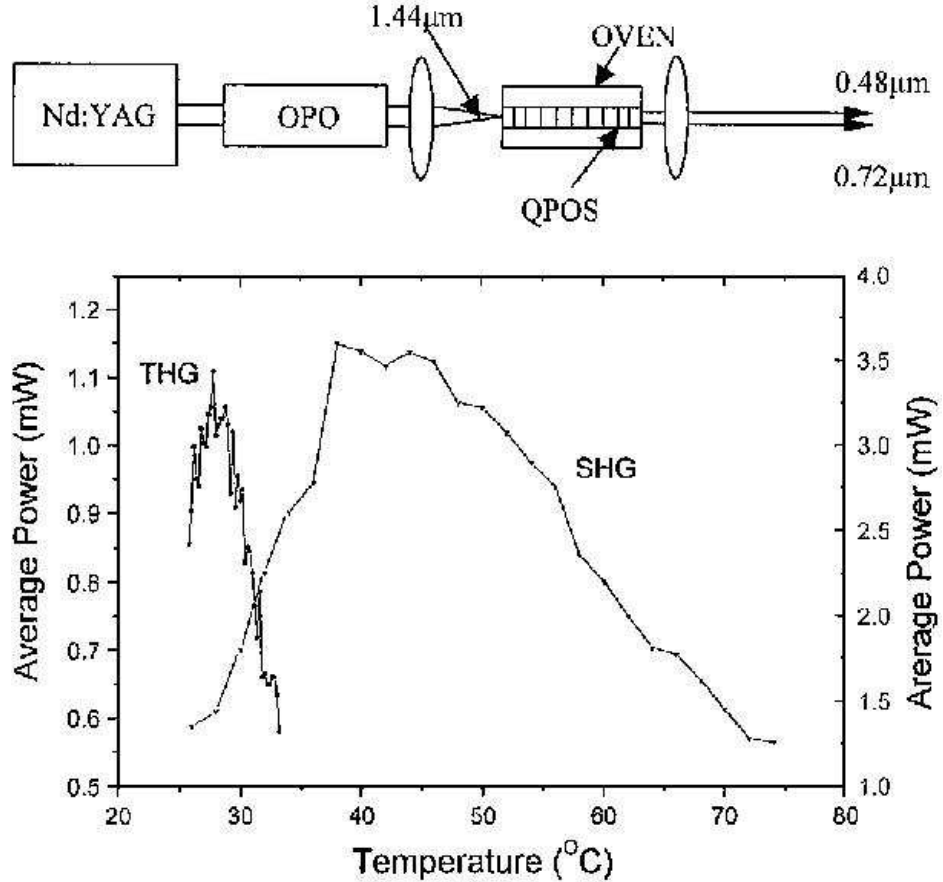


Figure 3: (above) Schematic of the experimental setup. (below) Average powers of the second harmonic (right scale) and third harmonic (left scale) vs. temperature. Average power of the fundamental wave is 4.8 mW (Zhang, Wei, Zhu, Wang, Zhu, and Ming [2001]).

^y Volkov, Laptev, Morozov, Naumova, and Chirkin [1998]

Abbreviations:

QPOS – quasi periodical optical superlattices; BPM – birefringence phase matching; PR-QPM – phase reversed QPM structure (see Chou, Parameswaran, Fejer, and Brener [1999]); 2D-NPC – two-dimensional photonic crystals; 2D-QPM – two-dimensional QPM structure.

Introducing normalized efficiency (measured in units of $W^{-1}cm^{-2}$) for the first and second steps in separate crystals as $\eta_{0,1}$ and $\eta_{0,2}$, respectively, we obtain

$$\eta_{3\omega} = \frac{1}{4} \eta_{0,1} \eta_{0,2} P_1^2 L^4 \quad (3.4)$$

The results for THG in a single quadratic crystal under the condition of double phase matching were reported for the efficiency exceeding 20%, as shown in Table 2. Figure 3 shows the phase matching curves in the experiment (Zhang, Wei, Zhu, Wang, Zhu, and Ming [2001]) where 27% THG efficiency has been achieved. The two PM curves are not perfectly overlapped. We may expect that with an improvement of the superlattice structure the achieved efficiencies will be higher. Numerical solution of the system (3.1) shows that, in general, the third-harmonic output has an oscillating behavior as a function of the length or input power, and generally it does not reach the efficiency of 100%. However, as shown in Egorov and Sukhorukov [1998]; Chirkin, Volkov, Laptev, and Morozov [2000] and Zhang, Zhu, Yang, Qin, Zhu, Chen, Liu, and Ming [2000], the total conversion of the fundamental wave into the third-harmonic wave is possible if the ratio σ_2/σ_5 is optimized.

In other cases, where only one phase-matched condition is satisfied, the THG conversion efficiency is not so large, and it should be compared to that of the direct THG process in a cubic medium. The efficiency of a cascaded THG

process is inversely proportional to the square of the wave vector mismatch of the unmatched process. It is important to note that in such cases, even when only one of the phase-matched parameters Δk_{SHG} or Δk_{SFG} is close to zero (such conditions can be easily realized in the birefringent phase matching in bulk quadratic media or in an uniform QPM structure) the THG process has the behavior of the phase matched process with the characteristic dependence $[\sin(x)/x]^2$ for the TH intensity vs. tuning and a cubic dependence on the input intensity. The dependence of the sample thickness is quadratic but not periodic function as for the totally non phase matched processes.

Situation (iii), that is, tuning where $\Delta k_{\text{SHG}} + \Delta k_{\text{SFG}} = 0$, also corresponds to the phase-matching condition for direct THG where the fundamental wave is converted directly into a third-harmonic wave. In such a case, both the cascade process and direct process $k_3 = 3k_1$ contribute to the third harmonic wave. However, a relative contribution of the two processes could be different. In some cases, the direct THG process is stronger (see, e.g., [Feve, Boulanger, and Guillien \[2000\]](#)), in other cases the cascading THG process is dominant (see, e.g., [Banks, Feit, and Perry \[2002\]](#); [Bosshard, Gubler, Kaatz, Mazerant, and Meier \[2000\]](#)).

We wonder why the whole process is phase matched when both steps are mismatched? The reason is that in the case (iii) we have the situation similar to that of the quasi-phase-matching effect (see, e.g., [Reintjes \[1984\]](#); [Banks, Feit, and Perry \[1999\]](#); [Durfee, Misoguti, Backus, Kapteyn, and Murnane \[2002\]](#)). Indeed, if the first step is mismatched, inside a nonlinear medium it generates a periodically modulated polarization at the frequency 2ω ($P(2\omega)$) and the modulation period is exactly a mismatch of the second step. Thus, in the regions where the phase of the polarization $P(2\omega)$ is reversed, we have the minimum generation of second- and third-harmonic waves, and the generated TH components interfere constructively with the propagating third-harmonic wave along the length of the crystal. This leads to a quadratic dependence of the THG efficiency on the crystal length.

For the cascaded THG processes, the optimal focusing is an important issue when the goal is the maximum conversion efficiency. If only one of the steps is phase matched, the optimal focusing is in the input face when SFG is phase matched, or at the output face when SHG is phase matched ([Rostovtseva, Sukhorukov, Tunkin, and Saltiel \[1977\]](#); [Rostovtseva, Saltiel, Sukhorukov, and Tunkin \[1980\]](#)). If both the steps are phase matched, the optimum focusing position is in the center of the nonlinear medium ([Ivanov, Koynov, and Saltiel \[2002\]](#)).

In Table 2, we summarize the experimental results obtained for the efficient single-crystal THG processes. Conditions at which the third-harmonic wave included in double phase-matched interaction can be transformed with 100% efficiency into the 2ω wave or ω wave were found by [Komissarova and Sukhorukov \[1993\]](#); [Komissarova, Sukhorukov, and Tereshkov \[1997\]](#); and [Egorov and Sukhorukov \[1998\]](#). [Volkov and Chirkin \[1998\]](#) show that the same parametric interaction can be used for 100% conversion from 2ω wave into 3ω wave. Considering the situations with nonzero SH and TH boundary conditions it has to be taken into account that, as shown by [Alekseev and Ponomarev \[2002\]](#), the spatial evolution of three light waves participating simultaneously in SHG and SFM under the conditions of QPM double phase matching becomes chaotic at large propagation distances for many values of the complex input wave amplitudes. Thus, the possibility of transition to chaos exists in the application of an additional pump at frequency 2ω in order to increase the efficiency of THG [[Egorov and Sukhorukov \[1998\]](#)]. As shown in [Longhi \[2001b\]](#) for the multistep cascading process $\{\omega + \omega = 2\omega; \omega + 2\omega = 3\omega\}$ in a cavity, the formation of spatial patterns is possible. Another application of the multistep cascading interaction and, in particular, the THG multistep cascading is the generation of the entangled and squeezed quantum states (see Sec. 3.5 below). The conditions for the simultaneous phase matching of both SHG and SFG processes were considered by [Pfister, Wells, Hollberg, Zink, Van Baak, Levenson, and Bosenberg \[1997\]](#); [Grechin and Dmitriev \[2001a\]](#), for uniform QPM structures; by [Zhu and Ming \[1999\]](#), for quasi-periodic optical superlattices; by [Fradkin-Kashi and Arie \[1999\]](#) and [Fradkin-Kashi, Arie, Urenski, and Rosenman \[2002\]](#), for the generalized Fibonacci structures; and by [Saltiel and Kivshar \[2000a\]](#), for the two-dimensional nonlinear photonic crystals. This topic will be discussed below in Sec. 4.

3.1.2. Nonlinear phase shift in multistep cascading

The multistep parametric process, that combines two phase-matched interaction SHG ($\omega + \omega = 2\omega$) and SFG ($2\omega + \omega = 3\omega$), is described by the system of equations (3.1), and it can be used for all-optical processing and formation of parametric solitons. Indeed, the nonlinear phase shift (NPS) accumulated by the fundamental wave in the multistep cascading process is in several times larger than that in the standard cascading interaction that involves only one phase matched process ([Koynov and Saltiel \[1998\]](#)).

To illustrate this result, we consider the fundamental wave with the frequency ω entering a second-order nonlinear media under appropriate phase-matching conditions. As the first step, the wave with frequency 2ω is generated via the type I SHG process, and then, as the second step, the third-harmonic wave is generated via the SFG process ($2\omega + \omega = 3\omega$). Both the processes, SHG and SFG, are assumed to be nearly phase matched. The generated second- and third-harmonic waves are down-converted to the fundamental wave ω via the processes $(2\omega - \omega)$; $(3\omega - 2\omega)$, and $(3\omega - \omega, 2\omega - \omega)$, contributing all to the nonlinear phase shift that the fundamental wave collects. As follows

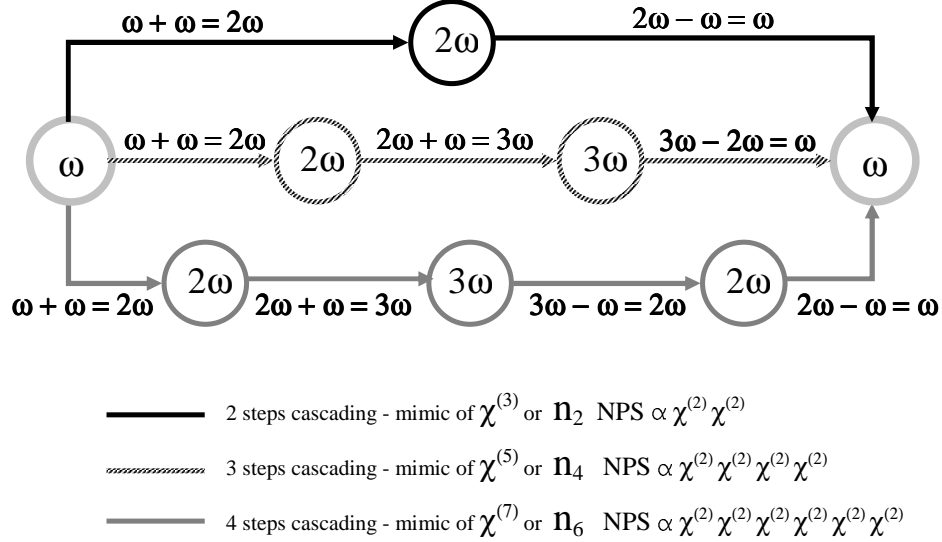


Figure 4: Schematic of the possible channels for the phase modulation of the fundamental wave (Koynov and Saltiel [1998]).

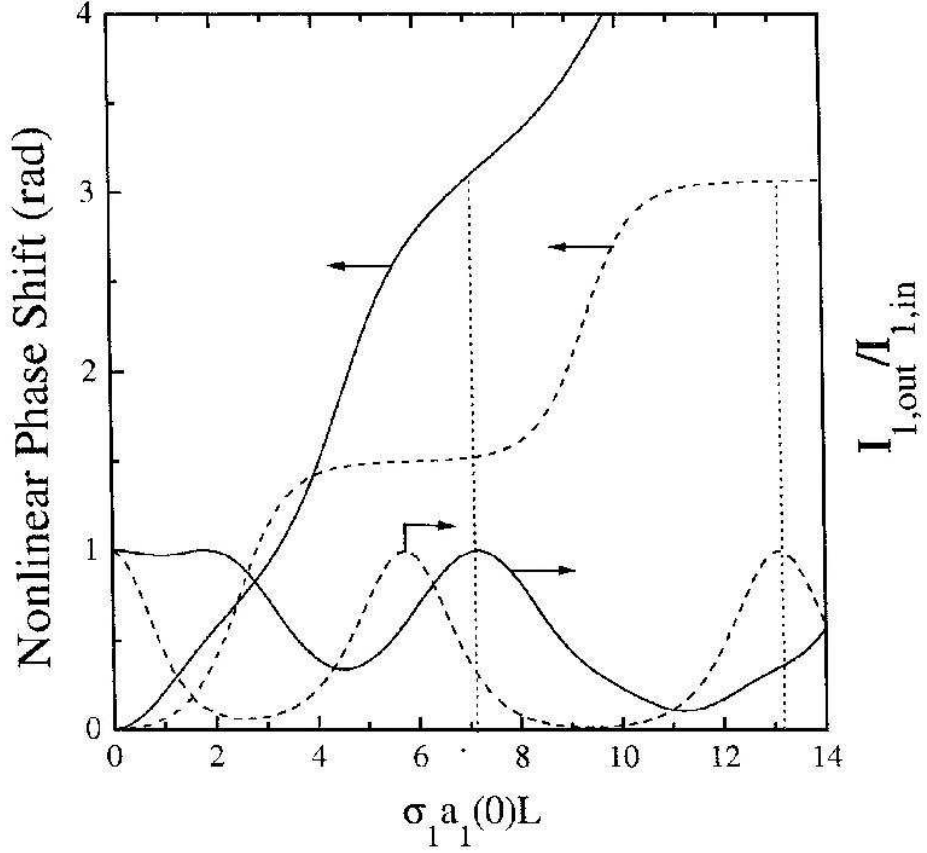


Figure 5: Nonlinear phase shift and depletion of the fundamental wave as a function of its normalized input amplitude: solid line – multistep cascading, dash line – type I SHG case (Koynov and Saltiel [1998]).

from numerical calculations, the total NPS is a result of the simultaneous action of two-, three-, and four-step $\chi^{(2)}$ cascading, and it can exceed the value of π for relatively low input intensities. The possible channels for the phase modulation and NPS of the fundamental wave are shown in Fig. 4. The interpretation of the analytical

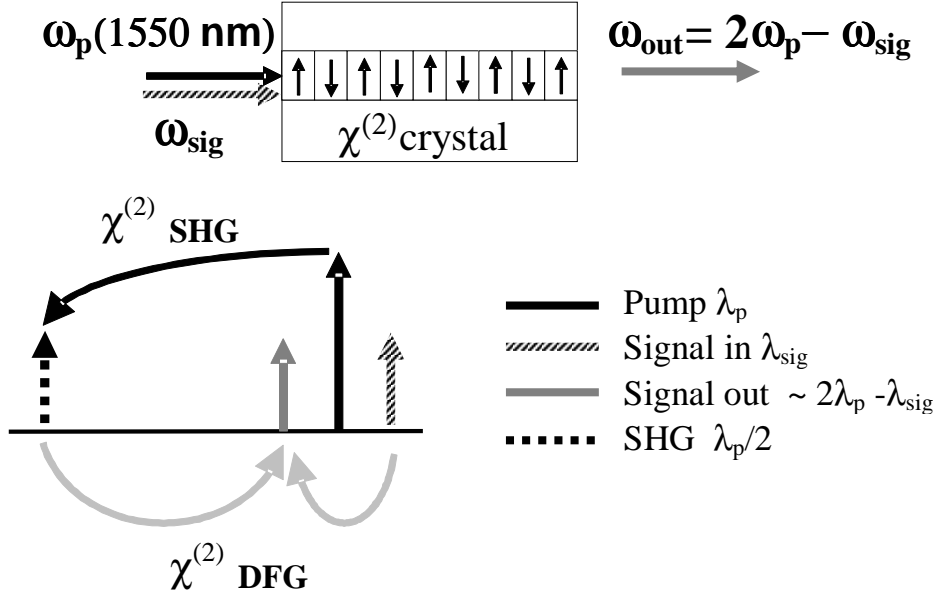


Figure 6: Wavelength conversion of optical communication channels in a periodically-poled nonlinear crystal using SHG/DFG multistep cascading.

result obtained in the fixed-intensity approximation (Koynov and Saltiel [1998]) shows that the effective cascaded fifth-order and higher-order nonlinearities are involved into the accumulation of a total NPS, and the signs of the contributions from different processes can be controlled by a small change of the phase matching conditions. Schematically, the role of the multistep cascading with three and four steps can be interpreted as equivalent of a contribution from the higher-order nonlinear corrections n_4 and n_6 to the refractive index, and they can be linked to the cascaded $\chi^{(5)}$ and $\chi^{(7)}$ processes, respectively. Indeed, for a relatively low intensity of the fundamental wave, the refractive index can be written in the form of expansion,

$$n(E) = n_0 + n_2 E^2 + n_4 E^4 + n_6 E^6 + \dots \quad (3.5)$$

The advantage of the multistep cascading for accumulating large nonlinear phase shift over the conventional two-step cascading is illustrated in Fig. 5 obtained by numerical integration of the system (3.1). This result is also useful for studying the multi-color solitons supported by this type of multistep parametric interaction (Kivshar, Alexander, and Saltiel [1999]; Huang [2001]). We note again the THG multistep cascading can be efficient only if the two processes can be simultaneously phase-matched. Due to dispersion in a bulk material, generally it is impossible to achieve double phase matching. However, due to the recent progress in the design of the QPM structures, the double phase matching can be achieved in nonlinear photonic materials (Zhang, Wei, Zhu, Wang, Zhu, and Ming [2001]; Luo, Zhu, He, Zhu, Wang, Liu, Zhang, and Ming [2001]; Fradkin-Kashi, Arie, Urenski, and Rosenman [2002]), although there exist a number of technical problems to be solved.

3.2. WAVELENGTH CONVERSION

So far we discussed only the multistep cascading process that allows to generate the third harmonic by combining the SHG and SFG phase-matched parametric interactions in a single crystal. Let now consider another single-crystal multistep process that combines SHG and DFM and mimic in this way the four-wave mixing (FWM) process with two input waves ω_p and ω_{sig} , resulting in the generation of a signal at $\omega_{\text{out}} = 2\omega_p - \omega_{\text{sig}}$. The idea of this type multistep cascading is illustrated in Fig. 6. Usually, the difference $\lambda_{\text{sig}} - \lambda_p$ is smaller than 50 nm (with $\lambda_p \sim 1550\text{nm}$) that leads to the result that when SHG process is phase matched the DFM process is very close to exact phase matching. Here we have the situation of double phase matched multistep cascading. This allows a very efficient conversion from λ_{sig} to $\lambda_{\text{sig}} - \lambda_p/2$ which is in $10^4 \div 10^5$ times larger than what can be obtained with the direct FWM process. To be more specific, let us consider the parametric interaction shown in Fig. 6 which is

described by the system of parametrically coupled equations,

$$\begin{aligned}\frac{dA_p}{dz} &= -i\sigma_1 A_2 A_p^* e^{-i\Delta k_{\text{SHG}} z}, \\ \frac{dA_2}{dz} &= -i\sigma_2 A_p^2 e^{i\Delta k_{\text{SHG}} z} - i\sigma_3 A_{\text{sig}} A_{\text{out}} e^{i\Delta k_{\text{DFG}} z}, \\ \frac{dA_{\text{out}}}{dz} &= -i\sigma_4 A_2 A_{\text{sig}}^* e^{-i\Delta k_{\text{DFG}} z}, \\ \frac{dA_{\text{sig}}}{dz} &= -i\sigma_5 A_2 A_{\text{out}}^* e^{-i\Delta k_{\text{DFG}} z},\end{aligned}\tag{3.6}$$

where $\Delta k_{\text{SHG}} = k_2 - 2k_1 + G_m$ and $\Delta k_{\text{DFG}} = k_2 - k_{\text{sig}} - k_{\text{out}}$, σ_1 to σ_5 are the coupling coefficients proportional to the second-order nonlinearity parameter d_{eff} . The vector G_m is one of the QPM vectors used for achieving the phase matching (Fejer, Magel, Jundt, and Byer [1992]) in the QPM structure. If the birefringence phase matching is used, then $G_m = 0$. Two phase-matching parameters, i.e. Δk_{SHG} and Δk_{DFG} , are involved into this parametric cascaded interaction. However, if the signal wavelength is sufficiently close to that of the pump, i.e. $|\lambda_{\text{sig}} - \lambda_p| \ll \lambda_p$, the tuning curves for the two processes practically overlap, and we have the situation in which if one of the parametric processes is phase matched, the other one is also phase matched. In other words, in this case the signal wavelength is sufficiently close to that of the pump, and we work under the conditions of double phase matching. If we neglect the depletion, the amplitude of the phase-matched SH wave can be found as $A_2(z) = -i\sigma_2 A_p^2 z$. Then, the output signal can be written in the form,

$$|A_{\text{out}}(L)|^2 \simeq 4\sigma_2^2 \sigma_4^2 |A_p^2|^2 |A_{\text{sig}}|^2 \frac{\sin^4(\Delta k_{\text{DFG}} L/2)}{(\Delta k_{\text{DFG}})^4}.\tag{3.7}$$

In the limit $\Delta k_{\text{DFG}} \rightarrow 0$, the efficiency becomes

$$|A_{\text{out}}(L)|^2 = \frac{1}{4} \sigma_2^2 \sigma_4^2 |A_p^2|^2 |A_{\text{sig}}|^2 L^4,\tag{3.8}$$

or

$$\eta_{\text{out}} = \frac{1}{4} \eta_0^2 P_p^2 L^4,\tag{3.9}$$

where η_0 is the normalized efficiency measured in $W^{-1}cm^{-2}$; it depends on the overlap integral between the interacting modes and the effective nonlinearity d_{eff} , and it is the same normalized value that describes the efficiency of the first step, the SHG process (Chou, Brener, Fejer, Chaban, and Christman [1999]). From Eq. (3.7) it follows that the output signal is a linear function of the input signal—the property important for communications. Also, the efficiency is proportional to the fourth power of the crystal length L . Detailed theoretical description of this cascading process can be found in Gallo, Assanto, and Stegeman [1997]; Gallo and Assanto [1999]; Chen, Xu, Zhou, and Tang [2002].

For the DFG process, the width of the phase-matching curve depends on the type of the crystal, its length, and the phase-matching method. Several proposal for increasing the phase-matching region have been suggested, including the use of the phase-reversed QPM structures (Chou, Parameswaran, Fejer, and Brener [1999]); the pump deviation from the exact phase matching (Chou, Brener, Parameswaran, and Fejer [1999]); the periodically chirped (phase modulated) QPM structures (Asobe, Tadanaga, Miyazawa, Nishida, and Suzuki [2003]); the phase shifting domain (Liu, Sun, and Kurz [2003]). In particular, the paper Gao, Yang, and Jin [2004] reports that the use of sinusoidally chirped QPM superlattices provides broader bandwidth and more flat response compared to homogeneous and segmented QPM structures.

Novel cascaded $\chi^{(2)}$ wavelength conversion schemes are based on the SFG and DFG processes and the use of two pump beams, as proposed and demonstrated in Xu and Chen [2004]; Chen and Xu [2004]. The conversion efficiency is enhanced by 6 dB, as compared with the conventional cascaded SHG+DFG wavelength conversion configuration. The cascading steps in this SFG+DFG wavelength conversion method are $\omega_{\text{SF}} = \omega_{p1} + \omega_{p2}$, and $\omega_{\text{out}} = \omega_{\text{SF}} - \omega_{\text{sig}}$, so that the effective third-order interaction is the totally nondegenerate FWM process: $\omega_{\text{out}} = \omega_{p1} + \omega_{p2} - \omega_{\text{sig}}$.

The second-order cascading wavelength conversion is one of the best examples of the richness of the multistep cascading phenomena. In the initial stage of development, this concept was experimentally demonstrated in the media employing two types of the phase matching techniques, i.e. the birefringence phase matching in a bulk crystal (e.g. Tan, Banfi, and Tomaselli [1993]; Banfi, Datta, Degiorgio, Donelli, Fortusini, and Sherwood [1998]) and periodically-poled nonlinear LiNbO₃ crystal (Banfi, Datta, Degiorgio, Donelli, Fortusini, and Sherwood [1998]). Since that, this parametric process was extensively investigated not only as an interesting multistep parametric

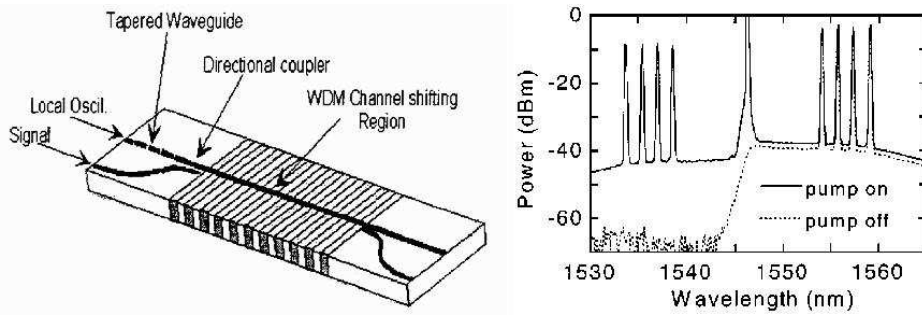


Figure 7: Right: periodically poled LiNbO_3 crystal for the cascaded wavelength conversion. Left: wavelength conversion with 1545 nm pump and four inputs in the range 1555-1560 nm (Chou, Brener, Lenz, Scotti, Chaban, Shmulovich, Philen, Kosinski, Parameswaran, and Fejer [2000]).

effect that may occur in different nonlinear media (see Table 3), but also as a proposal for realistic all-optical communication devices (Chou, Brener, Fejer, Chaban, and Christman [1999]; Chou, Brener, Lenz, Scotti, Chaban, Shmulovich, Philen, Kosinski, Parameswaran, and Fejer [2000]; Kunimatsu, Xu, Pelusi, Wang, Kikuchi, Ito, and Suzuki [2000]). Nowadays, there is a real progress in the suggesting this device for optical communication industry (Cardakli, Gurkan, Havstad, Willner, Parameswaran, Fejer, and Brener [2002]; Cardakli, Sahin, Adamczyk, Willner, Parameswaran, and Fejer [2002]), because of clear advantages over all other devices used for the wavelength shifting. Indeed, one such device can simultaneously shift several channels. As is shown in Fig. 6, the spectra of the shifted signal is a mirror image of the origin. This feature can be used to invert the signal chirp for dispersion management in transmission systems. A successful experimental demonstration of this property has been reported recently in Kunimatsu, Xu, Pelusi, Wang, Kikuchi, Ito, and Suzuki [2000]: a 600-fs pulse transmission over 144 km using midway frequency inversion with this type second-order cascaded wavelength conversion resulted in a negligible pulse distortion.

The waveguide made in the LiNbO_3 crystals (see Fig. 7) are by now the most suitable nonlinear structures for the cascaded simulation of the FWM wavelength shifting. The important features of this device is an almost perfect linear dependence between the input and output signals for more than 30 dB of the dynamic range, instantaneous memoryless transparent wavelength shifting that can be used at rates of several tera-Hertz, and transparent crosstalk-free operation (Cardakli, Sahin, Adamczyk, Willner, Parameswaran, and Fejer [2002]). Additionally, Couderc, Lago, Barthelemy, De Angelis, and Gringoli [2002] demonstrated that the wavelength conversion multistep cascading system can support parametric solitons in the waveguiding regime, we discuss these results in more detail in Sec. 5.3 below. Experimental works reporting the second-order cascaded wavelength conversion are summarized in Table 3.

Table 3: Experimental results on the multistep SHG and DFM cascading

Nonlinear crystal	$\lambda_p(\lambda_{s_{max}})$ [μm]	L [cm]	Regime	Phase matching method	Refs.
BBO	1.064 (1.090)	1	Pulsed (30ps)	BPM	a
MBA-NP	1.064 (1.090)	0.32	Pulsed (30ps)	BPM	b
LiNbO_3 waveguide	1.533 (1.535)	1	CW&Pulsed (7ps)	QPM	c
LiNbO_3	1.8 (1.863)	1.9	Pulsed (20 ps)	QPM	d
NPP	1.148 (1.158)	0.28	Pulsed (20 ps)	NCPM	e
LiNbO_3 waveguide	1.562 (1.600)	4	CW	QPM	f
Ti: LiNbO_3 waveguide	1.103 (1.107)	5.8	Pulsed (20 ps)	NCPM	g, h
LiNbO_3 waveguide	1.545 (1.580)	5	CW	QPM	i
Ti: LiNbO_3 waveguide	1.556 (1.565)	7.8 (8.6)	CW & pulsed (6 ps)	QPM	j

Nonlinear crystal	$\lambda_p(\lambda_{s_{max}})$ [μm]	L [cm]	Regime	Phase matching method	Refs.
LiNbO ₃ waveguide	1.565 (1.585)	2	CW	QPM	k
LiNbO ₃ waveguide	1.542 (1.562)	1	CW & pulsed	QPM	l
LiNbO ₃ waveguide	1.550 (1.560)		CW	QPM	m
LiNbO ₃ waveguide	1.553 (1.565)	6	CW	QPM	n
Ti:LiNbO ₃ waveguide	1.557 (1.553)	6	CW	QPM	o
LiNbO ₃ waveguide	1.532 (1.565)	2	CW	QPM	p
LiNbO ₃ waveguide	1.537 (1.570)	4.5	CW	QPM	q
LiNbO ₃ waveguide	1.558..1.568 (1.600)	3.4	CW	PM QPM ⁵	r
MgO:LiNbO ₃ waveguide	1.543(1.573)	5	CW	QPM	s
Ti:LiNbO ₃ waveguide	1.55(1.62)	3	CW	QPM ⁶	t
LiNbO ₃ waveguide	1.545(1.580)	5	CW	QPM	u

References:

^a Tan, Banfi, and Tomaselli [1993]
^b Nitti, Tan, Banfi, and Degiorgio [1994]
^c Trevino-Palacios, Stegeman, Baldi, and De Micheli [1998]
^d Banfi, Datta, Degiorgio, and Fortusini [1998]
^e Banfi, Datta, Degiorgio, Donelli, Fortusini, and Sherwood [1998]
^f Chou, Brener, Fejer, Chaban, and Christman [1999]
^g Cristiani, Banfi, Degiorgio, and Tartara [1999]
^h Banfi, Cristiani, and Degiorgio [2000]
ⁱ Chou, Brener, Lenz, Scotti, Chaban, Shmulovich, Phalen, Kosinski, Parameswaran, and Fejer [2000]
^j Schreiber, Suche, Lee, Grundkotter, Quiring, Ricken, and Sohler [2001]
^k Cristiani, Liberale, Degiorgio, Tartarini, and Bassi [2001]
^l Ishizuki, Suhara, Fujimura, and Nishihara [2001]
^m Cardakli, Sahin, Adamczyk, Willner, Parameswaran, and Fejer [2002]
ⁿ Harel, Burkett, Lenz, Chaban, Parameswaran, Fejer, and Brener [2002]
^o Cristiani, Degiorgio, Soccia, Carbone, and Romagnoli [2002]
^p Zeng, Chen, Chen, Xia, and Chen [2003]
^q Zhou, Xu, and Chen [2003]
^r Asobe, Tadanaga, Miyazawa, Nishida, and Suzuki [2003]
^s Bracken and Xu [2003]
^t Gao, Yang, and Jin [2004]
^u Sun and Liu [2003]

⁵phase modulated QPM⁶three types of QPM grating are compared: homogeneous, segmented gratings and sinusoidally chirped

3.3. TWO-COLOR MULTISTEP CASCADING

By two-color multistep cascading in a quadratic medium we understand the multi phase-matched parametric interaction between several waves which possess two frequencies (or wavelengths) only. One of the ways to introduce a parametric process involving more than one phase-matched interaction with two wavelengths is to consider a vectorial interaction between the waves with different polarizations, or degenerate interaction between allowed modes in a waveguide. We denote two waves at the fundamental frequency (FF) (at $\lambda = \lambda_{\text{fund}}$) as A and B, and the two waves of the second harmonic (SH) field (at $\lambda_{\text{sh}} = \lambda_{\text{fund}}/2$), as S and T. Each pair of the eigenmodes [(A,B) and (S,T)] can be, for example, two orthogonal polarization states or two different waveguide modes at the fundamental and second-harmonic wavelengths, respectively. There exists a finite number of possible multistep parametric interactions that can couple these waves. For example, if we consider the AA-S&AB-S cascading, then the multistep cascading is composed of the following sub-processes. First, the fundamental wave A generates the SH wave S via the type I SHG process. Then, by the down-conversion process SA-B, the other fundamental eigenmode B is generated. At last, the initial FF wave A is reconstructed by the processes SB-A or AB-S, SA-A. When we deal with two orthogonal polarizations, the two principal second-order processes AA-S and AB-S are governed by two different components (or two different combinations of the components) of the $\chi^{(2)}$ susceptibility tensor, thus introducing additional degrees of freedom into the parametric interaction. The classification of different types of the multistep parametric interactions has been introduced by [Kivshar, Sukhorukov, and Saltiel \[1999\]](#) and [Saltiel, Koynov, Deyanova, and Kivshar \[2000\]](#).

Table 4: Two-color multistep cascading processes

Multistep-cascading schemes	No of waves	SHG processes	Equivalent cascading schemes	WC/SC	Refs.
AA-S:AB-S	3	Type I & Type II	BB-S:AB-S; AA-T:AB-T; BB-T:AB-T	SC	a,b,c
AA-S:AB-T	4	Type I & Type II	BB-S:AB-T; AA-T:AB-S; BB-T:AB-S	WC	d,e
AA-S:BB-S	3	Type I & Type I	AA-T:BB-T	WC	f,g,h,i
AA-S:AA-T	3	Type I & Type I	BB-S:BB-T	SC	h,j
AB-S:AB-T	4	Type II & Type II		SC	
AA-S:BB-S:AB-S	3	Type I & Type II	AA-T:BB-T:AB-T		k,l,m

^a [Saltiel and Deyanova \[1999\]](#)

^b [Saltiel, Koynov, Deyanova, and Kivshar \[2000\]](#)

^c [Petrov, Albert, Etchepare, and Saltiel \[2001\]](#); [Petrov, Albert, Minkovski, Etchepare, and Saltiel \[2002\]](#)

^d [DeRossi, Conti, and Assanto \[1997\]](#)

^e [Pasiskevicius, Holmgren, Wang, and Laurell \[2002\]](#)

^f [Assanto, Torelli, and Trillo \[1994\]](#)

^g [Kivshar, Sukhorukov, and Saltiel \[1999\]](#)

^h [Grechin, Dmitriev, and Yur'ev \[1999\]](#); [Grechin and Dmitriev \[2001b\]](#)

ⁱ [Grechin and Dmitriev \[2001b\]](#)

^j [Trevino-Palacios, Stegeman, Demicheli, Baldi, Nouh, Ostrowsky, Delacourt, and Papuchon \[1995\]](#)

^k [Trillo and Assanto \[1994\]](#)

^l [Towers, Sammut, Buryak, and Malomed \[1999\]](#); [Towers, Buryak, Sammut, and Malomed \[2000\]](#)

^m [Boardman and Xie \[1997\]](#); [Boardman, Bontemps, and Xie \[1998\]](#)

Different types of the multistep parametric interactions can be divided into two major groups. The first group is composed by the parametric interactions with two common waves in both cascading processes, and the two processes are strongly coupled (SC). For the other group, both the parametric processes share one common wave, and these processes are weakly coupled (WC). The same classification can be applied to other types of the multistep

parametric interactions. In Table 4, we present an updated classification of two-color multistep parametric processes and the publications where they are analyzed.

The first analysis of the multistep parametric interactions of this type has been carried out by [Assanto, Torelli, and Trillo \[1994\]](#) and [Trillo and Assanto \[1994\]](#). These authors studied the simultaneous phase-matching of two SHG processes of the type AA-S and BB-S, where S denotes the SH wave whereas A and B stand for the the FF waves polarized in the perpendicular planes. The two orthogonal FF fields interact through the generated SH wave. All-optical operations and the polarization switching can be performed on the base of this scheme. [Kivshar, Sukhorukov, and Saltiel \[1999\]](#) demonstrated that this two-color parametric interaction can support two-color spatial solitary waves. [Trevino-Palacios, Stegeman, Demicheli, Baldi, Nouh, Ostrowsky, Delacourt, and Papuchon \[1995\]](#) considered the interference between the parametric processes AA-S and AA-T, where S and T are two different modes of the waveguide at the frequency 2ω . In both the cases mentioned above, two different parametric processes share one and the same fundamental wave. However, it is possible that the multistep cascading interaction involves the SHG process of the type AB-S. Such a four-wave multistep cascading process was considered by [DeRossi, Conti, and Assanto \[1997\]](#). The two SHG processes were AB-S and AA-T, where (A,B) and (S,T) are pairs of the modes at the frequencies ω and 2ω , respectively. [DeRossi, Conti, and Assanto \[1997\]](#) concluded that a devise based on this type of multistep cascading can operate as an all-optical modulator or as an all-optical switch, with a good switching contrast at $1.55 \mu\text{m}$.

Another interesting process of the multistep interaction was considered by [Boardman and Xie \[1997\]](#); [Boardman, Bontemps, and Xie \[1998\]](#) who studied the parametric mode coupling in a nonlinear waveguide placed in a magnetic field. In this case, the simultaneous coexistence of six SHG processes is possible, namely, ooo, ooe, oee, eee, eeo, and eoo. The exact number of allowed parametric interactions depends on the symmetry point group of the material. It was shown that, by controlling a ratio of the input fundamental components, one of the SH components can be controlled and switched off. Importantly, repulsive and collapsing regimes for the interacting parametric solitons can be produced by switching the direction of the magnetic field.

[Saltiel and Deyanova \[1999\]](#) considered the possibility to realize the efficient polarization switching in a quadratic crystal that supports simultaneous phase matching for both Type I and Type II SHG processes (e.g. ooo and oeo). At certain conditions, the fundamental beam involved in such a process can accumulate a large nonlinear phase shift at relatively low input power ([Saltiel, Koynov, Deyanova, and Kivshar \[2000\]](#)). The SHG process that can be realized by two possible pairs of the simultaneously phase-matched processes (ooo, ooe) and (ooe, eee) was studied theoretically in [Grechin, Dmitriev, and Yur'ev \[1999\]](#). The effect of SHG by simultaneous phase-matching of three parametric processes (ooe, eee, and oee) in a crystal of LiNbO_3 was estimated theoretically in [Grechin and Dmitriev \[2001b\]](#). It was shown that, at certain conditions, one can obtain polarization insensitive SHG.

Also, we would like to mention several experimental studies of the two-color multistep cascading interactions. In the paper of [Trevino-Palacios, Stegeman, Demicheli, Baldi, Nouh, Ostrowsky, Delacourt, and Papuchon \[1995\]](#), an interplay of two Type I SHG processes with a common fundamental wave was observed. [Petrov, Albert, Etchepare, and Saltiel \[2001\]](#) and [Petrov, Albert, Minkovski, Etchepare, and Saltiel \[2002\]](#) performed the experiment with a BBO crystal in which, as a result of the simultaneous action of the Type I SHG and Type II SHG interactions, the generation of the wave orthogonally polarized to the input fundamental wave was observed. [Couderc, Lago, Barthelemy, De Angelis, and Gringoli \[2002\]](#) demonstrated that the multistep cascading interaction can support parametric solitons in the waveguiding regime. In this latter case, the multistep interaction simulates an effective nearly-degenerate FWM process and, in this sense, it is almost "two-color". [Pasiskevicius, Holmgren, Wang, and Laurell \[2002\]](#) realized experimentally the simultaneous SHG process that gives two SH waves with the orthogonal polarizations in the blue spectral region by use of the Type II and Type I QPM phase matching in a periodically poled KTP crystal.

As a simple example of the two-color multistep parametric interaction, we consider the cascading of the Type I and Type II SHG processes according to the scheme: BB-S and AB-S. Here, the SH wave is generated by two interactions. Thus, we can expect an increase of the SHG efficiency when both A and B waves (i.e., the ordinary and extraordinary waves) are involved. However, if only one of the waves, say the wave A, is launched at the input, this type of the double phase-matched interaction will lead to the generation of a wave perpendicular to the input wave, through the parametric process SA \rightarrow B. Additionally, the fundamental wave A accumulates a strong

nonlinear phase shift. This parametric interaction is described by the following equations for plane waves,

$$\begin{aligned}\frac{dA}{dz} &= -i\sigma_1 SA^* e^{-i\Delta k_{\text{SHG}}z} - i\sigma_3 SB^* e^{-i\Delta k_{\text{DFG}}z}, \\ \frac{dS}{dz} &= -i\sigma_2 A^2 e^{i\Delta k_{\text{SHG}}z} - i\sigma_4 AB e^{i\Delta k_{\text{DFG}}z}, \\ \frac{dB}{dz} &= -i\sigma_5 SA^* e^{-i\Delta k_{\text{DFG}}z},\end{aligned}\quad (3.10)$$

where A , S , and B are the complex amplitudes of the input fundamental wave, the second-harmonic wave, and the orthogonally polarized wave at the fundamental frequency, σ_1 and σ_2 are defined above, and

$$\sigma_{3,4,5} = \frac{2\pi d_{\text{eff,II}}}{\lambda_1 n_{A,2,B}} \left(\frac{\omega_{1,2,1}}{\omega_1} \right).$$

If we neglect dispersion of the index of refraction, i.e. $n_A \simeq n_B \simeq n_2$, then we can assume that $\sigma_1 \simeq \sigma_2$ and $\sigma_3 \simeq \sigma_5 \simeq \sigma_4/2$. The phase-mismatch parameters are defined as $\Delta k_{\text{SHG}} = k_2 - 2k_A + G_p$ and $\Delta k_{\text{DFG}} = k_2 - k_A - k_B + G_q$, where G_p and G_q are two QPM vectors used for the phase matching.

Solution of this system, with respect of the amplitude of the wave B , has been obtained by Saltiel and Deyanova [1999] in the approximation of nondepleted pump. It gives the following result,

$$B(L) = \frac{i\sigma_1\sigma_3}{D_{-} - \Delta k_{\text{SHG}}} |A|^2 A \sin(D_{-}L) e^{iD_{-}L}, \quad (3.11)$$

where

$$D_{\pm} = \frac{1}{2}(\Delta k_{\text{SHG}} - \Delta k_{\text{DFG}}) \pm \frac{\sigma_1^2}{\Delta k_{\text{SHG}}} |A|^2.$$

Equation (3.11) shows that the generation of the component B by this multistep interaction mimic the FWM process of the type $AAA^* - B$, governed by the cascaded cubic nonlinearity. This effective cubic nonlinearity leads to the accumulation of a nonlinear phase shift by the wave A that, similar to the case of the cascaded THG process, includes a contribution of high-order (> 3) nonlinearities (Saltiel, Koynov, Deyanova, and Kivshar [2000]). Existence of two-color multistep parametric solitons and waveguiding effects are the result of the nonlinear phase shift collected by the interacting waves (Kivshar, Sukhorukov, and Saltiel [1999]).

3.4. FOURTH-HARMONIC MULTISTEP CASCADING

Another fascinating example of the multistep cascading interaction is the fourth-harmonic generation (FHG) in a single crystal with the second-order nonlinearity. There are two possible parametric processes of the second order that lead to the generation of a fourth harmonic. In both the cases the fourth harmonic (FH) amplitude is proportional to the factor $(\chi^{(2)})^3$:

1. SHG + SHG: $\omega + \omega = 2\omega$; $2\omega + 2\omega = 4\omega$;
2. SHG + SFG + SFG: $\omega + \omega = 2\omega$; $2\omega + \omega = 3\omega$; $3\omega + \omega = 4\omega$.

The phase matching conditions define which of these processes will be more effective. Obviously, the former process is easier to realize technically because it requires only two phase-matching conditions to be fulfilled simultaneously, and therefore many papers deal with this case.

The first experiment on the generation of a forth-harmonic wave by cascading was reported in the paper by Akhmanov, Dubovik, Saltiel, Tomov, and Tunkin [1974], where the FHG cascaded process in Lithium Formate crystal was studied. As pointed out by the authors, the generation is due to the simultaneous action of two and three processes with the involvement of the quadratic and cubic nonlinearities. The FHG process in CdGeAs₂ was observed by Kildal and Iseler [1979]. Both these pioneer papers were motivated by the idea to estimate the magnitude of the direct fourth-order nonlinearity in terms of $(\chi^{(2)})^3$. One of the first studies that reported the efficiency of the cascaded FHG process is the paper by Hooper, Gauthier, and Madey [1994] where the efficiency of $3.3 \times 10^{-4}\%$ was obtained in a single LiNbO₃ crystal. The other paper by Sundheimer, Villeneuve, Stegeman, and Bierlein [1994b] reported the efficiency of 0.012%. However, in those experiments only the first step $\omega + \omega = 2\omega$ was phase-matched while the other one was not matched, leading to the overall low conversion efficiency. Somewhat larger efficiency of 0.066% was reported in the work of Baldi, Trevino-Palacios, Stegeman, Demicheli, Ostrowsky, Delacourt, and Papuchon [1995] where a periodically poled LiNbO₃ waveguide was used. Both steps of the multistep parametric interaction, namely $\omega + \omega = 2\omega$ and $2\omega + 2\omega = 4\omega$, were phase matched: the first step was realized

through the first-order QPM process, while the second step was realized through the 7-th order QPM process. As is shown by [Norton and de Sterke \[2003b\]](#) and [Sukhorukov, Alexander, Kivshar, and Saltiel \[2001\]](#), if both steps are phase-matched, the resulting efficiency should be close to 100%. In the second paper, the existence and stability of the normal modes for such a multistep cascading system have been studied. Some possibilities for the double-phase-matched FHG process for certain input wavelengths in single-crystals of LiNbO_3 , LiTaO_3 , KTP, and GaAs have been shown by [Pfister, Wells, Hollberg, Zink, Van Baak, Levenson, and Bosenberg \[1997\]](#) and [Grechin and Dmitriev \[2001a\]](#). The possibility for FHG by double phase-matching in broader spectral region by use of the phase-reversed QPM structure was discussed by [Sukhorukov, Alexander, Kivshar, and Saltiel \[2001\]](#).

In a very interesting experiment, [Broderick, Bratfalean, Monro, Richardson, and de Sterke \[2002\]](#) demonstrated cascaded FHG in a 2D nonlinear photonic crystal with the efficiency 0.01% in a (not optimized) 2D planar QPM structure. Several useful efficient schemes for FHG in 2D nonlinear photonic crystals have been proposed by [Saltiel and Kivshar \[2000a\]](#) and [de Sterke, Saltiel, and Kivshar \[2001\]](#). An optimal design of 2D nonlinear photonic crystals for achieving the maximum efficiency of FHG has been discussed by [Norton and de Sterke \[2003a\]](#) and [Norton and de Sterke \[2003b\]](#). The use of the FHG multistep interaction for the frequency division schemes (4:1) and (4:2) have been discussed in [Dmitriev and Grechin \[1998\]](#) and [Sukhorukov, Alexander, Kivshar, and Saltiel \[2001\]](#).

The basic equations describing the FHG parametric process in a double-phase-matched QPM structure for the interaction of plane waves can be written in the form (see, e.g., [Hooper, Gauthier, and Maday \[1994\]](#))

$$\begin{aligned}\frac{dA_1}{dz} &= -i\sigma_1 A_2 A_1^* e^{-i\Delta k_{\text{SHG}} z}, \\ \frac{dA_2}{dz} &= -i\sigma_2 A_1^2 e^{i\Delta k_{\text{SHG}} z} - i\sigma_6 A_4 A_2^* e^{-i\Delta k_4 z}, \\ \frac{dA_4}{dz} &= -i\sigma_7 A_2^2 e^{i\Delta k_4 z},\end{aligned}\quad (3.12)$$

where A_1 , A_2 and A_4 are the complex amplitudes of the fundamental, second-harmonic, and fourth-harmonic waves, respectively. The parameters σ_1 and σ_2 are defined above, and

$$\sigma_{6,7} = \frac{4\pi}{\lambda_1 n_{2,4}} d_{\text{eff,II}}.$$

As before, if we neglect the index of refraction dispersion ($n_1 \simeq n_2 \simeq n_4$) then we can accept that $\sigma_1 \simeq \sigma_2$ and $\sigma_6 \simeq \sigma_7$. Phase mismatch parameters are $\Delta k_{\text{SHG}} = k_2 - 2k_A + G_p$ and $\Delta k_4 = k_4 - 2k_2 + G_q$, where G_p and G_q are two QPM reciprocal vectors. The role of high order nonlinearities are not included in (3.12) since their contribution is rather small when one works in conditions close to double or triple phase-matching.

Solution of the system (3.12) can be found neglecting the depletion effects. It reveals that the phase-matched FHG wave is generated when either one of the following phase-matching conditions is satisfied,

1. $\Delta k_{\text{SHG}} \rightarrow 0$;
2. $\Delta k_4 \rightarrow 0$;
3. $\Delta k_{\text{SHG}} + \Delta k_4 = k_4 - k_2 - 2k_1 + G_p + G_q \rightarrow 0$; and
4. $2\Delta k_{\text{SHG}} + \Delta k_4 = k_4 - 4k_1 + 2G_p + G_q \rightarrow 0$

The case $\Delta k_{\text{SHG}} \rightarrow 0$ gives the strongest phase-matching process among all those cases, and the generated FH wave exceeds by several orders of magnitude FH generated by other schemes. For the double-phase-matching process (when $\Delta k_{\text{SHG}} \rightarrow 0$ and $\Delta k_4 \rightarrow 0$) the squared amplitude of forth harmonic is given by the expression ([de Sterke, Saltiel, and Kivshar \[2001\]](#)):

$$|A_4(L)|^2 = \frac{1}{9} \sigma_2^4 \sigma_6^2 |A_1|^8 L^6. \quad (3.13)$$

Introducing again the normalized efficiency (measured in $\text{W}^{-1}\text{cm}^{-2}$) for the first and second steps as $\eta_{0,1}$ and $\eta_{0,2}$, respectively, we can obtain the efficiency of the cascaded FHG process,

$$\eta_{4\omega} = \frac{1}{9} \eta_{0,1}^2 \eta_{0,2} P_1^3 L^6. \quad (3.14)$$

Thus, the efficiency of the cascaded FHG process in a single $\chi^{(2)}$ is proportional to the 6-th power of the length and the 3-rd power of the pump, and it can be estimated with the known efficiencies for the separated steps. For the pump intensities at which the depletion effect of the fundamental and second-harmonic waves can not be neglected, the system (3.12) should be solved numerically. As shown in [Zhang, Zhu, Zhu, and Ming \[2001\]](#), the 100% conversion of the fundamental wave into the fourth-harmonic wave is possible independently on the ratio of the nonlinear coupling coefficients σ_2/σ_6 . This behavior is in contrast with the $\chi^{(2)}$ -based cascaded THG process where the 100% conversion is possible only for a specific ratio of the nonlinear coupling coefficients (see Sec. 3.1).

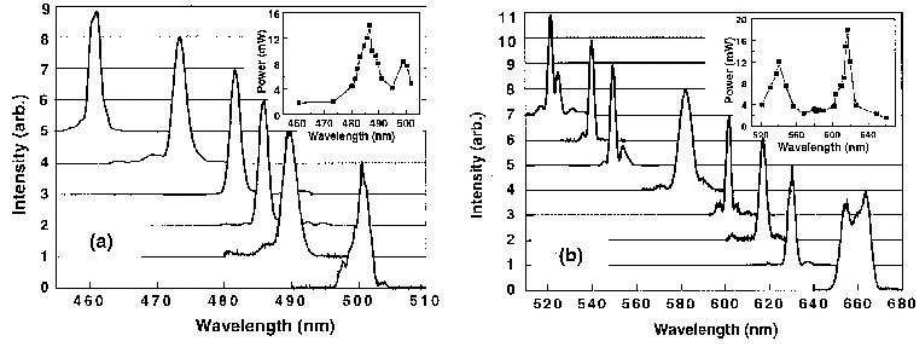


Figure 8: The tuning characteristics of OPO with the simultaneously phase matched SHG and SFG processes. (a) SFG between the signal and pump, and (b) SHG of the signal. Inset: output power vs. wavelength (Zhang, Hebling, Kuhl, Ruhle, Palfalvi, and Giessen [2002]).

3.5. OPO AND OPA MULTISTEP PARAMETRIC PROCESSES

Many studies dealing with optical parametric oscillators (OPOs) and optical parametric amplifiers (OPAs) have observed, in addition to the expected signal and idler waves, other waves at different wavelengths that are coherent and are generated with a good efficiency. These waves were identified as being a result of additional phase-matched (or nearly phase-matched) second-order parametric processes in OPOs and OPAs. In some of the cases, up to five additional waves coming out from the nonlinear crystal were detected and measured. By tuning the wavelength of the signal and idler waves simultaneously, the additional outputs from OPO can be frequency tuned as well. An example is shown in Fig. 8 adapted from Zhang, Hebling, Kuhl, Ruhle, Palfalvi, and Giessen [2002]. The study of the simultaneous phase matching in OPO was started more than 30 years ago. As shown in Ammann, Yarborough, and Falk [1971], in many nonlinear crystals the phase-matching tuning curves for OPO and SHG of the signal and the idler cross and the experimental observations of the corresponding double phase-matching parametric processes are possible.

Plane-wave single-pass theory of the new frequency generation with OPO with the simultaneous frequency doubling of the signal wave in the OPO crystal was presented in Aytur and Dikmelik [1998]. The case of OPO with the simultaneous frequency mixing between the pump and signal waves — in Dikmelik, Akgun, and Aytur [1999] and Morozov and Chirkin [2003]. Moore, Koch, Dearborn, and Vaidyanathan [1998] considered theoretically the simultaneous phased matched tandem of OPOs in a single nonlinear crystal. The signal wave of the first OPO process becomes a pump wave of the second process. The simultaneous action of the parametric generation, $\omega_p \rightarrow \omega_i + \omega_s$, and SFG between the pump and signal wave, $\omega_{SF} = \omega_p + \omega_s$, was also analyzed by Huang, Zhu, Zhu, and Ming [2002], where the main goal was to show that this type of the multistep cascading can be used for the simultaneous generation of three fundamental colors.

Table 5: Experimental results on the OPO and OPA multistep cascading

Nonlinear crystal	λ_{pump} [μm]	Phase matching processes	Phase matching method	L [cm]	Regime	Refs
ADP	1.06	$\omega_1 = \omega_p + \omega_s$	BMP	5	Pulsed (Q pulse)	a
LiNbO ₃	1.06	$\omega_1 = \omega_s + \omega_s$ or $\omega_2 = \omega_i + \omega_i$	BMP	0.38	Pulsed (Q pulse)	b
LiNbO ₃	1.064	$\omega_1 = \omega_s + \omega_s$ $\omega_2 = \omega_1 - \omega_i$	BPM	3(5)	pulsed (35 ps)	c
KTP	0.79	$\omega_1 = \omega_s + \omega_s$ $\omega_2 = \omega_p + \omega_s$ $\omega_3 = \omega_p + \omega_i$	BPM	0.115	pulsed (115 fs)	d
LiNbO ₃	0.532	$\omega_p = \omega_p/2 + \omega_p/2$	NCPM	3.2	CW	e

Nonlinear crystal	λ_{pump} [μm]	Simultaneously PM processes	Phase matching method	L [cm]	Regime	Refs
BBO	0.74-0.89	$\omega_1 = \omega_p + \omega_i$	BPM	0.4	pulsed (150 fs)	f
KTP	0.82-0.92	$\omega_1 = \omega_s + \omega_s$ $\omega_2 = \omega_p + \omega_s$ $\omega_3 = \omega_p + \omega_i$	NCPM	0.2	pulsed (120 fs)	g
LiNbO ₃	1.064	$\omega_1 = \omega_p + \omega_p$ $\omega_2 = \omega_p + \omega_s$ $\omega_3 = \omega_p + 2\omega_s$	QPM	1.5	Pulsed (7 ns)	h
LiNbO ₃	0.532	$\omega_p = \omega_p/2 + \omega_p/2$	NCPM	0.75	CW	i
LiNbO ₃	0.78-0.80	$\omega_1 = \omega_p + \omega_p$ $\omega_2 = \omega_s + \omega_s$ $\omega_3 = \omega_p + \omega_s$ $\omega_4 = \omega_p + \omega_i$ $\omega_5 = \omega_s + \omega_s + \omega_s$	QPM	0.6	pulsed (2 ps)	j
LiNbO ₃	0.793	$\omega_1 = \omega_p + \omega_s$	QPM	0.08	pulsed (85 fs)	k
β -BBO	0.53	$\omega_1 = \omega_s + \omega_s$ $\omega_{s1} = \omega_1 - \omega_i$ $\omega_{i1} = \omega_p - \omega_{s1}$ $\omega_2 = \omega_{s1} + \omega_{s1}$ $\omega_{s2} = \omega_2 - \omega_i$ $\omega_{i2} = \omega_p - \omega_{s2}$	BPM	0.8	pulsed (1 ps)	l
KTP	0.74-0.76	$\omega_1 = \omega_s + \omega_s$	BPM	0.5	pulsed (150 fs)	m
LiNbO ₃	1.064	$\omega_s \rightarrow \omega_{s2} + \omega_{i2}$	QPM	2.5	pulsed (43 ns)	n
LiNbO ₃	0.79-0.81	$\omega_1 = \omega_s + \omega_s$	QPM	0.1	pulsed (100 fs)	o
KTP	0.827	$\omega_1 = \omega_p + \omega_s$	BPM	0.5	pulsed (170 fs)	p
KTP	0.76-0.84	$\omega_1 = \omega_s + \omega_s$ $\omega_2 = \omega_p + \omega_s$ $\omega_3 = \omega_1 + \omega_i$	QPM	0.05	pulsed (30 fs)	q, r
LiTaO ₃	0.532	$\omega_1 = \omega_p + \omega_s$	QPOS	2	pulsed (40 ps)	s
LiNbO ₃	0.8	$\omega_1 = \omega_p + \omega_s$ $\omega_2 = \omega_s + \omega_s$	QPM	0.05	pulsed (40 fs)	t
LiNbO ₃	1.064	$\omega_1 = \omega_s + \omega_s$ $\omega_2 = \omega_s + \omega_p$ $\omega_3 = \omega_s + \omega_s + \omega_s$ $\omega_4 = \omega_p + \omega_p$ $\omega_5 = \omega_p + \omega_1$	QPM	2	pulsed (17.5 ns)	u
KTA	0.796	$\omega_1 = \omega_s + \omega_s$	BPM	2	pulsed (140 fs)	v
LiNbO ₃	0.79	$\omega_1 = \omega_s + \omega_s$	APQPM	1.8	pulsed (5 ns)	w
β -BBO	0.405 (0.81)	$\omega_1 = \omega_p/2 + \omega_s$ $\omega_2 = \omega_i + \omega_i$	BPM	0.2	pulsed (90 fs)	x

^a Andrews, Rabin, and Tang [1970]

- ^b Ammann, Yarborough, and Falk [1971]
- ^c Bakker, Planken, Kuipers, and Lagendijk [1989]
- ^d Powers, Ellingson, Pelouch, and Tang [1993]
- ^e Schiller and Byer [1993]
- ^f Petrov and Noack [1995]
- ^g Hebling, Mayer, Kuhl, and Szipocs [1995]
- ^h Myers, Eckardt, Fejer, Byer, Bosenberg, and Pierce [1995]
- ⁱ Schiller, Breitenbach, Paschotta, and Mlynek [1996]
- ^j Butterworth, Smith, and Hanna [1997]
- ^k Burr, Tang, Arbore, and Fejer [1997]
- ^l Varanavicius, Dubietis, Berzanskis, Danielius, and Piskarskas [1997]
- ^m Kartaloglu, Koprulu, and Aytur [1997]
- ⁿ Vaidyanathan, Eckardt, Dominic, Myers, and Grayson [1997]
- ^o McGowan, Reid, Penman, Ebrahimzadeh, Sibbett, and Jundt [1998]
- ^p Koprulu, Kartaloglu, Dikmelik, and Aytur [1999]
- ^q Zhang, Hebling, Kuhl, Ruhle, and Giessen [2001]
- ^r Zhang, Hebling, Kuhl, Ruhle, Palfalvi, and Giessen [2002]
- ^s Du, Zhu, Zhu, Xu, Zhang, Chen, Liu, Ming, Zhang, Zhang, and Zhang [2002]
- ^t Zhang, Hebling, Bartels, Nau, Kuhl, Ruhle, and Giessen [2002]
- ^u Xu, Liang, Li, Yao, Lin, Cui, and Wu [2002]
- ^v Kartaloglu and Aytur [2003]
- ^w Kartaloglu, Figen, and Aytur [2003]
- ^x Lee, Zhang, Huang, and Pan [2003]

Abbreviations: BPM – birefringence phase matching; NCPM – noncritical phase matched; QPM – uniformly poled quasi-phase-matched structure; QPOS – quasi-periodical optical superlattices; APQPM – aperiodically poled QPM structure.

In Table 5, we have summarized different experimental results on the multistep cascading processes observed in OPOs and OPAs. For each of this work, we also mention the additional second-order parametric processes.

In the special case when all frequencies become phase related, i.e. $\omega_p : \omega_s : \omega_i = 3 : 2 : 1$, OPO displays the unique properties (Kobayashi and Torizuka [2000]; Longhi [2001b]). As a matter of fact, this case corresponds to the third-harmonic multistep cascading (see Sec. 3.1) but realized in a cavity. The second harmonic of the idler simultaneously generated in the OPO crystal (or by externally frequency doubling) $\omega_{2i} = \omega_i + \omega_i$ will interfere with the signal wave of the frequency ω_i . The resulting beat signal can be used for locking OPO at this particular tuning point and for realizing the frequency divisions (3:2) and (3:1), or vice versa. More details about the frequency division with these types OPO can be found in the papers by Lee, Klein, Meyn, Wallenstein, Gross, and Boller [2003]; Douillet, Zondy, Santarelli, Makdissi, and Clairon [2001]; Slyusarev, Ikegami, and Ohshima [1999]; Zondy, Douillet, Tallet, Ressaire, and Le Berre [2001]; Zondy [2003]. For the double phase-matched parametric interactions for the frequencies 3ω ; 2ω ; ω , the total conversion from a 3ω wave to a 2ω wave was predicted when the pump is the 3ω wave (Komissarova and Sukhorukov [1993]), and from a 2ω wave to a 3ω wave, when the pump is the 2ω wave (Volkov and Chirkin [1998]) for the OPA scheme. Additionally, the theoretical studies in Longhi [2001b,a,c] show that OPO, when the signal and idler wave have the frequencies ω and 2ω , respectively, can produce different types of interesting patterns including the spiral and hexagonal patterns. The internally pumped OPOs, due to the simultaneous action of the SHG process and the parametric down-conversion, also shows the formation of spatial patterns and the parametric instability dynamics (Lodahl and Saffman [1999]; Lodahl, Bache, and Saffman [2000, 2001]).

Additionally, the multistep cascaded OPOs and OPAs can be an efficient tool for generating the entangled and squeezed photon states. In particular, Smithers and Lu [1974] considered the quantum properties of light generated during simultaneous action of the parametric processes $\omega_p \rightarrow \omega_i + \omega_s$ and $\omega_1 = \omega_i + \omega_p$. The theoretical predictions by Marte [1995b,a]; Eschmann and Marte [1997] suggest that, due to the multistep cascading in internally pumped OPO, this type of OPO can be an excellent source for generating twin photons with the sub-Poissonian statistics, and the generated SH wave exhibits a perfect noise reduction. Several other phase-matched schemes for generating the entangled and squeezed photon states have been proposed by Chirkin [2002]; Nikandrov and Chirkin [2002b] and Chirkin and Nikandrov [2003] who utilizes OPA with two simultaneously phase-matched processes, $2\omega = \omega + \omega$ and $3\omega = 2\omega + \omega$. In the theoretical study (Nikandrov and Chirkin [2002a]), a possibility of generating squeezed light with the utilization of a single quadratic crystal was compared with that of two different crystals for each step. The conclusion is that a single-crystal cascaded method is more efficient. New possibilities for the generation of

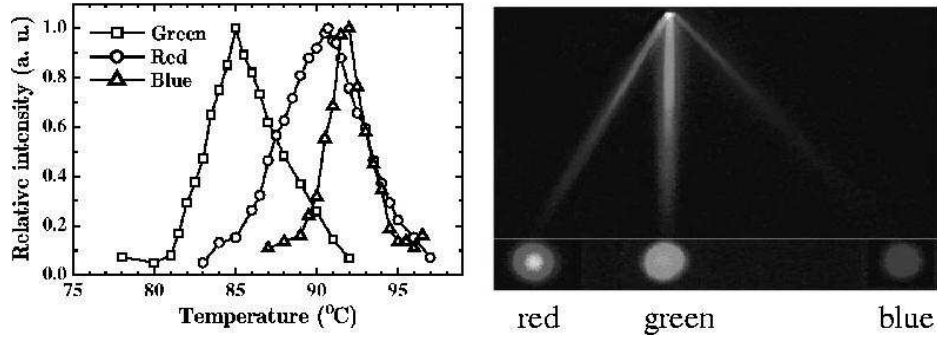


Figure 9: Left: the phase matching curves for three simultaneously phase-matched processes in a single aperiodically-poled LiTaO_3 crystal. Right: visible red, green and blue outputs from a nonlinear crystal diffracted by a prism (Liao, He, Liu, Wang, Zhu, Zhu, and Ming [2003]).

squeezed polarized light have been discussed by [Dmitriev and Singh \[2003\]](#) who considered the five-wave generation via the four simultaneously phase-matched parametric processes.

3.6. OTHER TYPES OF MULTISTEP INTERACTIONS

The multistep parametric interactions allow building compact frequency converters with several visible beams as the output. [He, Liao, Liu, Du, Xu, Wang, Zhu, Zhu, and Ming \[2003\]](#) reports on the simultaneous generation of all three "traffic signal lights". The simultaneous generation of a pair blue and green waves have been achieved in [Capmany, Bermudez, Callejo, Sole, and Dieguez \[2000\]](#) by exploring self-doubling and self-frequency mixing active media.

Table 6: Experiments on the simultaneous generation of several visible beams

Nonlinear crystal	λ_p [μm]	COLORS	PM method	L [cm]	Regime	Ref.
KTP waveguide	1.023 0.716	RED, GREEN, BLUE	BPM/QPM	0.45	CW	a
KTP waveguide	1.650	RED, GREEN, BLUE	QPM	0.35	pulsed (6 ps)	b
LiNbO_3 waveguide	1.620	RED, GREEN, BLUE	QPM		pulsed (7 ps)	c
NYAB	1.338 0.807 0.755	RED, GREEN, BLUE	BPM	0.5	CW	d
Nd:LiNbO ₃	1.084 0.744	GREEN, BLUE	APQPM	0.095	CW	e
Nd:LiNbO ₃	1.372 1.084 0.744	RED, OR- ANGE, GREEN, BLUE(2)	APQPM	0.3	CW	f
SBN	1.34 0.88	RED, GREEN, BLUE	APQPM	0.7	CW	g
LiTaO_3	1.342 1.064	RED, GREEN, BLUE	APQPM	1	CW	h

Nonlinear crystal	λ_p [μm]	COLORS	PM method	L [cm]	Regime	Ref.
LiTaO ₃	1.342 1.064	RED, YEL- LOW, GREEN	APQPM	1	CW	i

^a Laurell, Brown, and Bierlein [1993]

^b Sundheimer, Villeneuve, Stegeman, and Bierlein [1994b]

^c Baldi, Trevino-Palacios, Stegeman, Demicheli, Ostrowsky, Delacourt, and Papuchon [1995]

^d Jaque, Capmany, and Garcia Sole [1999]

^e Capmany, Bermudez, Callejo, Sole, and Dieguez [2000]

^f Capmany [2001]

^g Romero, Jaque, Sole, and Kaminskii [2002]

^h Liao, He, Liu, Wang, Zhu, Zhu, and Ming [2003]

ⁱ He, Liao, Liu, Du, Xu, Wang, Zhu, Zhu, and Ming [2003]

Recently, several studies presented successful attempts to obtain the simultaneous generation of red, green and blue radiation (the so-called RGB radiation) from a single nonlinear quadratic crystal. This is an important target for building compact laser-based projection displays. Theoretically, the parametric process for achieving the generation of three primary colors as OPO outputs was considered in Huang, Zhu, Zhu, and Ming [2002]. Liao, He, Liu, Wang, Zhu, Zhu, and Ming [2003] used a single aperiodically-poled LiTaO₃ crystal for generating 671, 532 and 447 nm (see Fig. 9) with three simultaneously phase-matched processes: SHG of 1342 and 1064 nm (the output of the dual-output Nd:YVO₄ laser) and SFG of 671 and 1342 nm. Jaque, Capmany, and Garcia Sole [1999] realized a different method for achieving the three-wavelength output. In their experiments, a nonlinear medium is the Nd:YAl₃(BO₃)₄ crystal that was pumped by a Ti:sapphire laser. The red signal at 669 nm was obtained by self-frequency doubling of the fundamental laser line. The green signal at 505 nm and a blue signal at 481 nm were obtained by self-SFG of the fundamental laser radiation at 1338 nm and the pump radiation (807 nm, for green, and 755 nm, for blue). All three processes were simultaneously phase matched by birefringence phase matching due to an exceptional situation that the three phase-matchings appear extremely close to each other and their tuning curves overlap. The generation of red, green and blue signals by triple phase-matching in LiNbO₃ and KTP periodically poled waveguides was reported also by Sundheimer, Villeneuve, Stegeman, and Bierlein [1994a] and Baldi, Trevino-Palacios, Stegeman, Demicheli, Ostrowsky, Delacourt, and Papuchon [1995]. The experimental efforts to build optical devices with the simultaneous generation of several visible harmonics are summarized in Table 6.

3.7. MEASUREMENT OF THE $\chi^{(3)}$ -TENSOR COMPONENTS

As an important application of the multistep parametric processes in nonlinear optics, we would like to mention the possibility making a calibration link between the second- and third-order nonlinearity in a nonlinear medium. Both THG and FWM processes in non-centrosymmetric nonlinear media can be used for this purpose. Measurements can be done in the phase-matched or non-phase-matched regimes. The non-phase-matched regime allows achieving a higher accuracy, however, it is more complicated since the signal is weak and additional care should be taken to avoid the influence of the respective third-order effect in air. The basic idea of these types of measurements is to compare the THG or FWM signal in several configurations that include a proper choice of the direction and polarization of the input and output waves. In some of the configurations the output signal is generated in result of the direct contribution of the inherent cubic nonlinearity of a sample. In other cases, the signal is generated due to the cascade contribution, while in the third group, the contribution of both direct and cascaded processes is comparable. In this way, we can access the ratio

$$\frac{\chi^{(3)}(-3\omega, \omega, \omega, \omega)}{\chi^{(2)}(-3\omega, 2\omega, \omega)\chi^{(2)}(-2\omega, \omega, \omega)}$$

for the case of the THG multistep interaction, and the ratio

$$\frac{\chi^{(3)}(-\omega_3, \omega_1, \omega_1, -\omega_2)}{\chi^{(2)}(-\omega_3, 2\omega_1, -\omega_2)\chi^{(2)}(-2\omega_1, \omega_1, \omega_1)}$$

for the case of the FWM multistep cascading. Because the information about the $\chi^{(2)}$ components is more available, we can determine quite accurate parameters of the cubic nonlinearity of non-centrosymmetric materials by using this internal calibration procedure which does not require the knowledge of the parameters of the laser beam.

To illustrate that let us consider the phase-matched THG. In condition of non-depletion of the fundamental and second harmonic wave and neglecting the temporal and spatial walk off effect the equations (3.1) has following solution for phase matching $\Delta k_{\text{THG}} = k_3 - 3k_1 \rightarrow 0$:

$$A_3(L) = -i \left(\gamma + \frac{\sigma_2 \sigma_5}{\Delta k_{\text{SFG}}} \right) \frac{\sin(\Delta k_{\text{THG}} L/2)}{\Delta k_{\text{THG}} L/2} |A_1|^3 L. \quad (3.15)$$

Apparent cubic nonlinearity consists two parts direct and cascading:

$$\chi_{\text{tot}}^{(3)} = \chi_{\text{eff,dir}}^{(3)} + \chi_{\text{eff,casc}}^{(3)}, \quad (3.16)$$

with

$$\chi_{\text{eff,casc}}^{(3)} = \frac{16\pi d_{\text{eff,I}} d_{\text{eff,II}}}{\lambda_1 n_1 \Delta k_{\text{SFG}}}.$$

One of the ways to separate the contribution of the two nonlinearities and express of $\chi_{\text{eff,dir}}^{(3)}$ in terms of the product $(d_{\text{eff,I}})(d_{\text{eff,II}})$ is to use the azimuthal (Banks, Feit, and Perry [2002]) or input polarization (Kim and Yoon [2002]) dependence of $\chi_{\text{eff,dir}}^{(3)}$ and $\chi_{\text{eff,casc}}^{(3)}$. The other way is to compare the TH signal obtained under the condition $\Delta k_{\text{THG}} \rightarrow 0$ with the TH signal obtained under one of the conditions $\Delta k_{\text{SHG}} \rightarrow 0$ or $\Delta k_{\text{SFG}} \rightarrow 0$, where the signal is only proportional to the factor $|\chi_{\text{eff,casc}}^{(3)}|^2$ (Akhmanov, Meisner, Parinov, Saltiel, and Tunkin [1977]; Chemla, Begley, and Byer [1974]), and calculate $\chi_{\text{eff,dir}}^{(3)}$; however this procedure gives two possible values due to an indeterminate sign. Considering all symmetry classes Feve, Boulanger, and Douady [2002] found the crystal directions for which the second-order cascade processes give no contribution and, therefore, they are suitable for the measurement of the value of $\chi_{\text{eff,dir}}^{(3)}$.

The parametric interaction that occurs when the degenerated FWM (DFWM) process is in non-centrosymmetric media is special because it consists of the steps of the optical rectification and linear electro-optic effects (Bosshard, Spreiter, Zgonik, and Gunter [1995]; Unsbo [1995]; Zgonik and Gunter [1996]; Biaggio [1999, 2001]). Then, the measured $\chi^{(3)}$ component can be expressed through the squared electro-optic coefficient of the medium. The cascaded $\chi^{(3)}$ contribution in the crystals with a large electro-optic effect leads to a very strong cascaded DFWM effect which can exceed by many times the contribution of the inherent direct $\chi^{(3)}$ nonlinearity (Bosshard, Biaggio, St, Follonier, and Gunter [1999]).

Table 7 presents a summary of the experimental results on the measurement of the cubic nonlinearities by the use of the cascaded THG or cascaded FWM processes.

Table 7: Experimental results for the $\chi^{(3)}$ -tensor components measured through the second-order multistep cascading processes

Nonlinear crystal	$\lambda_{\text{fund}} [\mu\text{m}]$	PM/NPM/ NCPM*	Cascading scheme	Reference
ADP	1.06	PM	THG	Wang and Baardsen [1969]
GaAs	10.6	NPM	FWM	Yablonovitch, Flytzanis, and Bloembergen [1972]
CdGeAs ₂	10.6	PM	THG	Chemla, Begley, and Byer [1974]
KDP	1.064	PM	THG	Akhmanov, Meisner, Parinov, Saltiel, and Tunkin [1977]
α -quartz	1.91	NPM	THG	Meredith [1981]
β -BBO	1.054	PM	THG	Qiu and Penzkofer [1988]
β -BBO	1.053	PM	THG	Tomov, Van Wonterghem, and Rentzepis [1992]
KTP	1.06	PM	DFWM	DeSalvo, Hagan, Sheik-Bahae, Stegeman, Vanstryland, and Vanherzeele [1992]
β -BBO KD*P	1.055	PM	THG	Banks, Feit, and Perry [1999, 2002]
d-LAP				

Nonlinear crystal	λ_{fund} [μm]	PM/NPM/ NCPM*	Cascading scheme	Reference
KTP	1.62	NCPM	THG	Feve, Boulanger, and Guillien [2000]; Boulanger, Feve, Delarue, Rousseau, and Marnier [1999]
DAST#	1.064	PM	DFWM	Bosshard, Biaggio, St, Follonier, and Gunter [1999]
α -quartz	1.064	NPM	THG	Bosshard, Gubler, Kaatz, Mazerant, and Meier [2000]
KNbO ₃	1.318			
KTaO ₃	1.907			
SF59	BK7	2.100		
fused silica				
KNbO ₃	1.06	PM	DFWM	Biaggio [1999, 2001]
DAST				
BaTiO ₃				
AANP#	1.390	NCPM	FWM	Taima, Komatsu, Kaino, Franceschina, Tartara, Banfi, and Degiorgio [2003]
	1.402			
KDP	BBO	1.064	NPM	DFWM
LiNbO ₃		0.532		Ganeev, Kulagin, Ryasnyanskii, Tugushev, and Usmanov [2003]

* PM – phase matched; NPM – non phase-matched; NCPM – noncritically phase-matched;

organic crystals.

§ 4. Phase-matching for multistep cascading

In general, the simultaneous phase-matching of several parametric processes is hard to achieve by using the traditional phase-matching methods, such as those based on the optical birefringence effect, except some special cases discussed above. However, the situation becomes quite different for the nonlinear media with a periodic variation of the sign of the quadratic nonlinearity, as it occurs in the fabricated one-dimensional (1D) QPM structures (Fejer, Magel, Jundt, and Byer [1992]) or two-dimensional (2D) $\chi^{(2)}$ nonlinear photonic crystals (Berger [1998]; Broderick, Ross, Offerhaus, Richardson, and Hanna [2000]; Saltiel and Kivshar [2000a]). In this part of the review, we describe the basic principles of the simultaneous phase-matching of two (or more) parametric processes in different types of 1D and 2D nonlinear optical superlattices.

4.1. UNIFORM QPM STRUCTURES

A bulk homogeneous nonlinear crystal possessing a quadratic nonlinearity is usually homogeneous everywhere. Several methods have been suggested and employed (Fejer [1998]) for creating a periodic change of the sign of the second-order nonlinear susceptibility $d^{(2)}$, as occurs in the QPM structure shown in Fig. 10. From the mathematical point of view, such a periodic sequence of two domains can be described by a simple periodic function,

$$d(z) = d_0 \sum_{m \neq 0} g_m e^{iG_m z}, \quad (4.1)$$

$$g_m = \left(\frac{2}{m\pi} \right) \sin(\pi m D), \quad (4.2)$$

where $G_m = (2\pi m / \Lambda)$ is the reciprocal QPM vector. The uniform QPM structure is characterized by a set of the reciprocal vectors: $\pm 2\pi / \Lambda, \pm 4\pi / \Lambda, \pm 6\pi / \Lambda, \pm 8\pi / \Lambda, \dots$, which can be used to achieve the phase-matching conditions when $\Delta k \rightarrow 0$. The integer number m (that can be both *positive* and *negative*) is called *the order of the wave vector phase-matching*. According to Eq. (4.1), the smaller is the order of the QPM reciprocal wave vector, the larger is the effective nonlinearity. If the filling factor $D = 0.5$, the effective quadratic nonlinearities (proportional to the parameter $d_0 g_m$) that correspond to the even orders QPM vectors vanish. Importantly, such uniform QPM structures can be used for simultaneous phase-matching of two parametric processes when the interacting waves are collinear or non-collinear to the reciprocal wave vectors of the QPM structure.

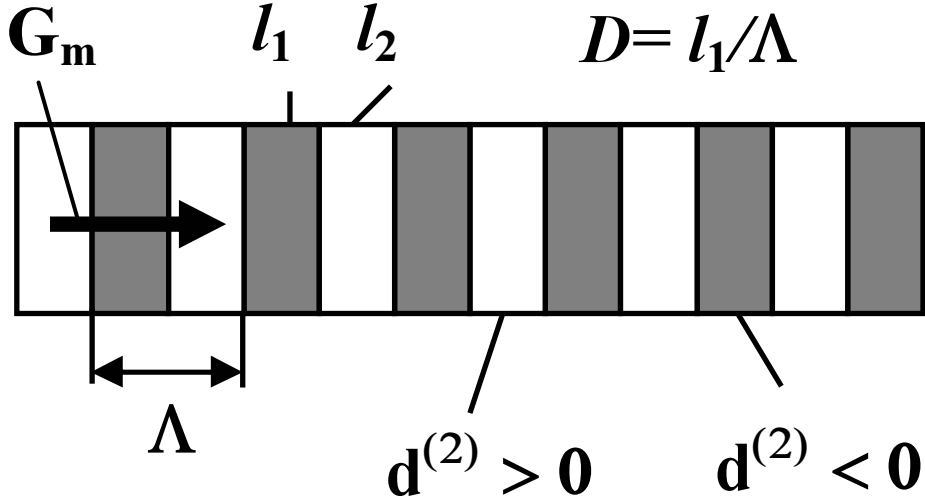


Figure 10: Schematic of the uniform QPM structure: G_m is the reciprocal vector of the m -th order; D is the filling factor, and Λ is the period of the QPM structure.

4.1.1. Collinear case with two commensurable periods

As an example of the multistep QPM interaction, we consider the third-harmonic multistep-cascading process under the condition that the interacting waves are *collinear* to the reciprocal wave vectors of the QPM structure. We denote the mismatches of the nonlinear material without modulation of the quadratic nonlinearity ("bulk mismatches") as Δb_1 and Δb_2 , where $\Delta b_1 = k_2 - 2k_1$ and $\Delta b_2 = k_3 - k_2 - k_1$, and choose the period of the QPM structure in order to satisfy the phase-matching conditions $G_{m_1} = -\Delta b_1$ and $G_{m_2} = -\Delta b_2$. The two parametric processes, SHG and SFG, are characterized by the wave-vector mismatches $\Delta k_1 = k_2 - 2k_1 + G_{m_1}$ and $\Delta k_2 = k_3 - k_2 - k_1 + G_{m_2}$, respectively, and they become simultaneously phase-matched for this particular choice of the QPM period. A drawback of this method is that it can satisfy simultaneously two phase-matching conditions for discrete values of the optical wavelength only. In particular, the values of the fundamental wavelength λ for the double phase-matching condition can be found from the relation

$$\Delta b_2/m_2 - \Delta b_1/m_1 = 0, \quad (4.3)$$

where both Δb_1 and Δb_2 are functions of the wavelength. Equation (4.3) is valid for any pair of the second-order parametric processes. For the third-harmonic multistep-cascading process, Eq. (4.3) is transformed to the following,

$$m_1 [3n(3\omega) - 2n(2\omega) - n(\omega)] - 2m_2 [n(2\omega) - n(\omega)] = 0, \quad (4.4)$$

where the arguments shows the wavelength dependence of the refractive index. For a chosen pair of integer numbers (m_1, m_2) , the required QPM period is found from the relation $\Lambda = 2\pi|m_1/\Delta b_1|$ or $\Lambda = 2\pi|m_2/\Delta b_2|$. Such a method was used for double phase-matching by many researchers for the cascaded single-crystal third- and fourth-harmonic generation (see details and references in Table 2). The highest efficiency achieved with the uniform QPM structure so far is 19.3%, and it is achieved by the use of the combination of SHG (1st-order)/SFG(3rd-order) and is reported in [He, Liu, Luo, Jia, Du, Guo, and Zhu \[2002\]](#).

4.1.2. Non-collinear case

Collinearity between the optical waves and the reciprocal vectors of the QPM structure is an important requirement for achieving a good overlapping of all the beams and a good conversion efficiency. However, phase-matching is possible even in the case when some of the waves propagate under a certain angle to the direction of the reciprocal vectors of the QPM structure, i.e. for the non-collinear case. With this method, the double phase-matching processes can be realized in a broad spectral range ([Saltiel and Kivshar \[2000b\]](#)). Such a type of non-collinear interaction will be efficient for the distances corresponding to the overlap of the interacting beams.

As an example, we consider the THG multistep parametric process in the noncollinear geometry as shown in Fig. 11. in this case, the simultaneous phase-matching of two parametric processes $\omega + \omega = 2\omega$ and $\omega + 2\omega = 3\omega$ is required. We assume the fundamental wave at the input. As shown in Fig. 11, for the first process the phase-

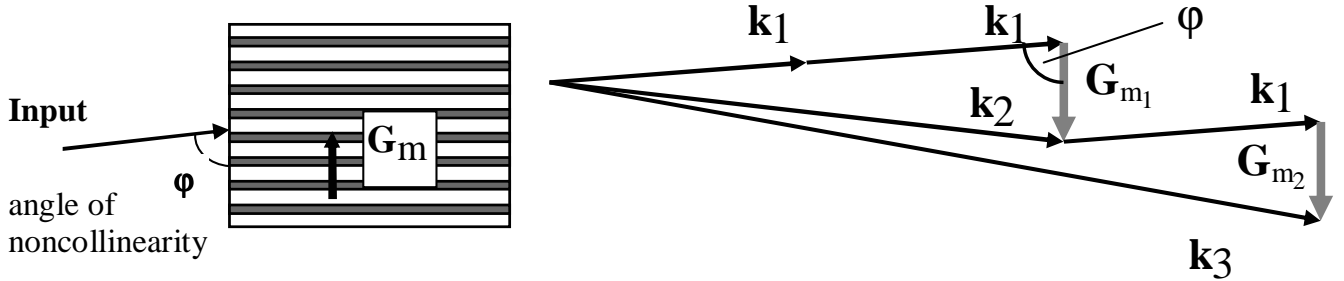


Figure 11: Geometry of the noncollinear cascaded THG parametric process in an uniform QPM structure.

matching can be achieved by the use of the reciprocal vector \mathbf{G}_{m_1} , and the generated SH wave with the wavevector \mathbf{k}_2 is not collinear to the fundamental wave: $2\mathbf{k}_1 - \mathbf{G}_{m_1} = \mathbf{k}_2$. The second process can be phase-matched by using the vector \mathbf{G}_{m_2} : $\mathbf{k}_1 + \mathbf{k}_2 - \mathbf{G}_{m_2} = \mathbf{k}_3$. From Fig. 11, we can derive a result for the period of the QPM structure that allows achieving the double phase-matching of the processes of cascaded THG in a single QPM structure,

$$\Lambda = 2\pi \left[\frac{2m_1(k_3^2 - 9k_1^2) - 3(m_1 + m_2)(k_2^2 - 4k_1^2)}{m_1(m_1 + m_2)(2m_2 - m_1)} \right]^{1/2}. \quad (4.5)$$

The conditions for the double phase-matching for the THG multistep-cascading process in LiTaO₃ for the case when all waves are polarized along the z axis of the crystal were considered by [Saltiel and Kivshar \[2000b\]](#).

4.2. NON-UNIFORM QPM STRUCTURES

Non-uniform QPM structures also allow the simultaneous phase-matching of two parametric nonlinear processes. We consider three types of such non-uniform QPM structures: (i) phase-reversed QPM structures ([Chou, Parameeswaran, Fejer, and Brener \[1999\]](#)), (ii) periodically chirped QPM structures ([Bang, Clausen, Christiansen, and Torner \[1999\]](#)), and (iii) optical superlattices ([Zhu and Ming \[1999\]](#); [Fradkin-Kashi, Arie, Urenski, and Rosenman \[2002\]](#)).

4.2.1. Phase-reversed QPM structures

The idea of *the phase-reversed QPM structures* ([Chou, Parameeswaran, Fejer, and Brener \[1999\]](#)) is illustrated in Fig. 12(a). Such a structure can be explained as a sequence of many equivalent uniform short QPM sub-structures with the length $\Lambda_{ph}/2$ connected in such a way that at the place of the joint two end layers have the same sign of the quadratic nonlinearity. Any two neighboring junctions have the opposite signs of the $\chi^{(2)}$ nonlinearity. In other words, the phase-reversed QPM structure can be thought of as a uniform QPM structure with a change of the domain phase by π characterized by the second (larger) period Λ_{ph} . Modulation of the quadratic nonlinearity $d(z)$ in the phase-reversed QPM structure with the filling factor $D = 0.5$ can be described by the response function

$$d(z) = d_0 (-1)^{\text{int}(2z/\Lambda_Q)} (-1)^{\text{int}(2z/\Lambda_{ph})}, \quad (4.6)$$

and it can be expanded into the Fourier series,

$$d(z) = d_0 \sum_{l=-\infty}^{+\infty} g_l e^{iG_l z} \sum_{m=-\infty}^{+\infty} g_m e^{iF_m z} = d_0 \sum_{l=-\infty}^{+\infty} \sum_{m=-\infty}^{+\infty} g_{lm} e^{iG_{lm} z}, \quad (4.7)$$

where $g_0 = 0$, $g_{l \neq 0} = (2/\pi l)$, $g_{m \neq 0} = (2/\pi m)$, $g_{lm} = g_l g_m$, $G_l = (2\pi/\Lambda_Q)l$, $F_m = (2\pi/\Lambda_{ph})m$, and $G_{lm} = (2\pi/\Lambda_Q)l + (2\pi/\Lambda_{ph})m$.

The phase-reversed QPM structure is characterized by a set of the reciprocal vectors $\{G_{lm}\}$, which are collinear to the normal of the periodic sequence with the magnitude depending on all parameters: $l, m, \Lambda_Q, \Lambda_{ph}$. Two of these vectors can be chosen to phase-match two parametric processes involved into the multistep-cascading, such that $G_{l_1 m_1} = -\Delta b_1$ and $G_{l_2 m_2} = -\Delta b_2$. Then, the two QPM periods satisfying the double-phase-matching condition can be found as follows,

$$\Lambda_Q = \left| \frac{2\pi(l_2 m_1 - l_1 m_2)}{m_2 \Delta b_1 - m_1 \Delta b_2} \right|, \quad \Lambda_{ph} = \left| \frac{2\pi(l_2 m_1 - l_1 m_2)}{l_2 \Delta b_1 - l_1 \Delta b_2} \right|, \quad (4.8)$$

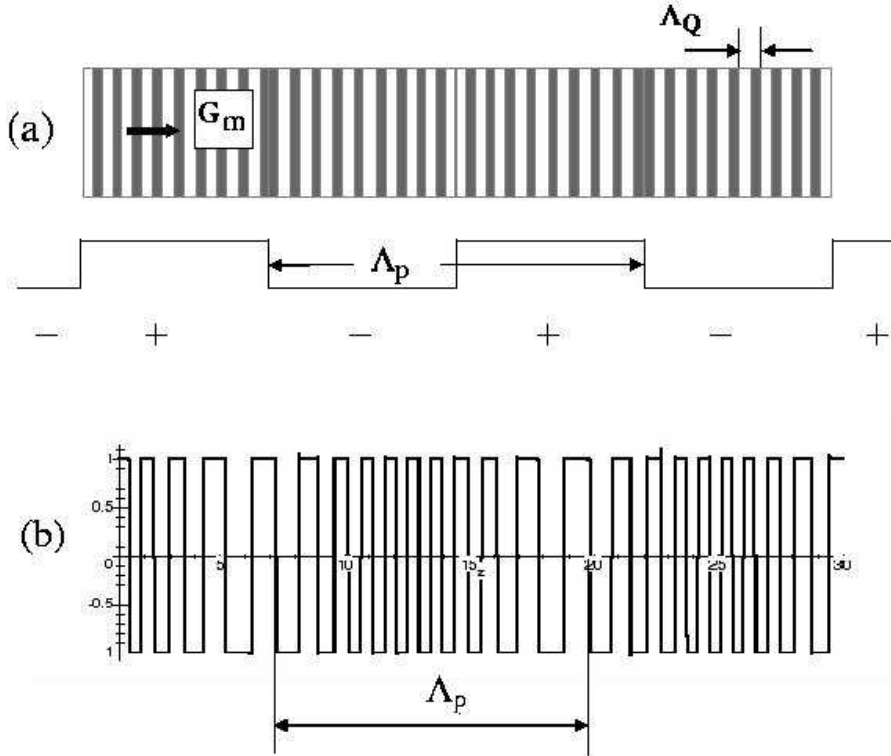


Figure 12: Schematic of the non-uniform QPM structures: (a) phase-reversed QPM structure (Chou, Parameswaran, Fejer, and Brener [1999]), and (b) periodically-chirped QPM structure (Bang, Clausen, Christiansen, and Torner [1999]).

For the case of the THG multistep cascading process, Eqs. (4.8) are transformed into

$$\Lambda_Q = \left| \frac{\lambda(l_2 m_1 - l_1 m_2)}{(m_1 - 2m_2)n(\omega) + 2(m_1 + m_2)n(2\omega) - 3m_1 n(3\omega)} \right|, \quad (4.9)$$

$$\Lambda_{ph} = \left| \frac{\lambda(l_2 m_1 - l_1 m_2)}{(l_1 - 2l_2)n(\omega) + 2(l_1 + l_2)n(2\omega) - 3l_1 n(3\omega)} \right|, \quad (4.10)$$

In addition to Eqs. (4.9) and (4.10), the design shown in Fig. 12(a) impose an additional condition that the ratio $2\Lambda_{ph}/\Lambda_Q$ is an integer number. Nevertheless, the corresponding number of the phase-matched wavelengths is larger than that achieved in the uniform QPM structure for the collinear geometry. The phase-reverse grating with arbitrary ratio $2\Lambda_{ph}/\Lambda_Q$ was considered theoretically by Johansen, Carrasco, Torner, and Bang [2002] in the study of spatial parametric solitons. The study of the effect of arbitrary $2\Lambda_{ph}/\Lambda_Q$ on the efficiency of different types of the frequency conversion processes has not been investigated yet, to the best of our knowledge. Experimentally, the phase-reversed QPM structure was employed for the wavelength conversion (Chou, Parameswaran, Fejer, and Brener [1999]), and for the cascaded single-crystal THG process (Liu, Zhu, Zhu, Qin, He, Zhang, Wang, Ming, Liang, and Xu [2001]; Liu, Du, Liao, Zhu, Zhu, Qin, Wang, He, Zhang, and Ming [2002]).

4.2.2. Periodically chirped QPM structures

Periodically chirped QPM structures, presented schematically in Fig. 12(b), have initially been suggested and designed for increasing an effective (averaged) third-order nonlinearity in quadratic media (Bang, Clausen, Christiansen, and Torner [1999]). We use the terminology "periodically chirped QPM" in the analogy with the chirped QPM structures that has a linear growth of the period Λ_Q along the structure. This type of structure is very suitable for realizing the multiple phase-matching conditions. The properties of the periodically chirped QPM structures have been explored experimentally for achieving a larger bandwidth for the wavelength converters (Asobe, Tadanaga, Miyazawa, Nishida, and Suzuki [2003]; Gao, Yang, and Jin [2004]).

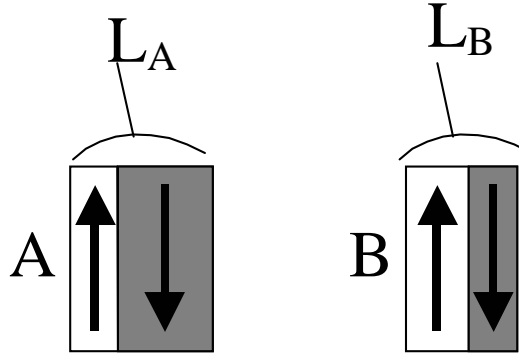


Figure 13: Basic blocks of the quasi-periodic and aperiodic QPM superlattices.

The periodically chirped QPM structure is characterized by the modulated QPM period Λ_Q that is itself a periodic function of z [see Fig. 12(b)]:

$$\Lambda = \Lambda_Q + \varepsilon_0 \cos\left(\frac{2\pi z}{\Lambda_{\text{ch}}}\right), \quad (4.11)$$

Double phase-matching conditions written for this type of structure allow to find two periods of the periodically chirped QPM structure; the results are similar to the formulas that describe the phase-reversed QPM structures,

$$\Lambda_Q = \left| \frac{2\pi(l_2 m_1 - l_1 m_2)}{m_2 \Delta b_1 - m_1 \Delta b_2} \right|, \quad (4.12)$$

$$\Lambda_{\text{ch}} = \left| \frac{2\pi(l_2 m_1 - l_1 m_2)}{l_2 \Delta b_1 - l_1 \Delta b_2} \right|, \quad (4.13)$$

The main advantage of the use of the periodically-chirped QPM structures is the possibility to satisfy the double phase-matching conditions for any wavelength in a broad spectral range, i.e. for any pair of Δb_1 and Δb_2 .

4.2.3. Quasi-periodic and aperiodic optical superlattices

Another method of the double phase-matching, studied extensively both theoretically and experimentally, is based on the use of the quasi-periodic optical superlattices (QPOS) (Zhu and Ming [1999]; Fradkin-Kashi and Arie [1999]; Fradkin-Kashi, Arie, Urenski, and Rosenman [2002]) and aperiodic optical superlattices (Gu, Zhang, and Dong [2000]). In the most of the cases, QPOSs are built with two two-component blocks A and B, as shown in Fig. 13, which are aligned in a Fibonacci-like or more general quasi-periodic sequence. Importantly, each of the blocks consists of two layers with the opposite sign of the quadratic nonlinearity. In order to illustrate the possibility of the double phase-matching in such structures we take, as an example, the structure consisting of two blocks aligned in a generalized sequence (Fradkin-Kashi and Arie [1999]). Modulation of the quadratic nonlinearity can be described by the following Fourier expansion (Birch, Severin, Wahlstrom, Yamamoto, Radnoci, Riklund, Sundgren, and Wallenberg [1990]):

$$d(z) = d_0 \sum_{m,n} f_{m,n} e^{iG_{m,n}z}, \quad (4.14)$$

where the reciprocal vectors are defined as $G_{m,n} = 2\pi(m + n\tau)/S$, where $S = \tau L_A + L_B$.

For phase-matching of two parametric processes with the mismatch parameters Δb_1 and Δb_2 , we solve the system of equations

$$\begin{aligned} G_{m_1, n_1} &= 2\pi(m_1 + n_1\tau)/S = -\Delta b_1, \\ G_{m_2, n_2} &= 2\pi(m_2 + n_2\tau)/S = -\Delta b_2, \end{aligned} \quad (4.15)$$

and find the corresponding value of S and τ . The lengths of the blocks L_A and L_B and a ratio of the sub-layers in each block should be found by maximizing f_{m_1, n_1} and f_{m_2, n_2} . A resulting designed structure allows simultaneous phase-matching in a broad spectral range without constraints on the ratio $\Delta b_2/\Delta b_1$. Equations (4.15) are also valid for the Fibonacci-type QPOS lattices but, because the parameter τ is fixed, the double phase-matching conditions can be satisfied for a limited number of wavelengths (Fradkin-Kashi and Arie [1999]) defined from the equation $\Delta b_1/\Delta b_2 = (m_1 + n_1\tau)/(m_2 + n_2\tau)$.

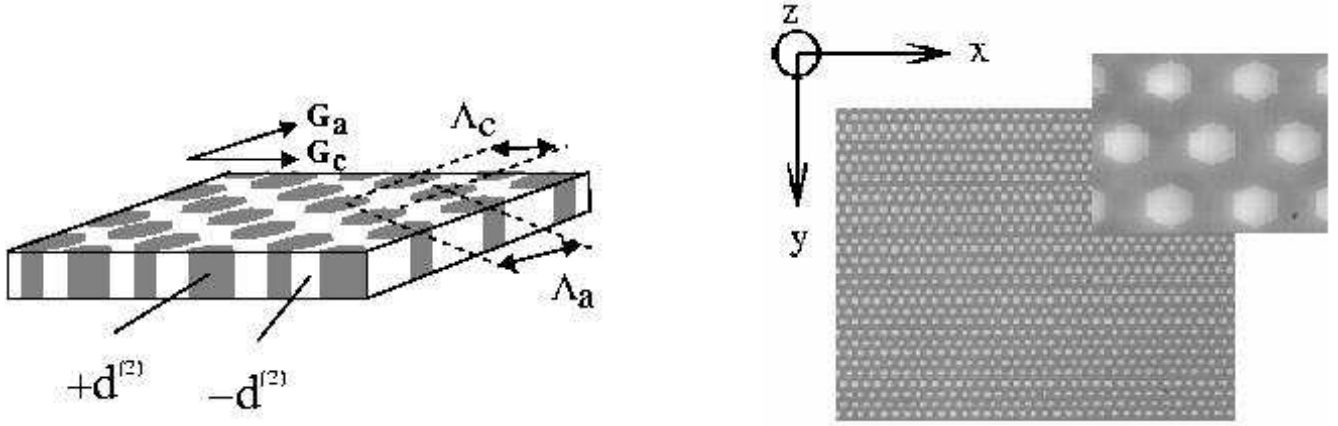


Figure 14: Left: 2D nonlinear quadratic photonic crystal composed of a periodic lattice of domains (gray) with the reversed sign of $\chi^{(2)}$; \mathbf{G}_a and \mathbf{G}_c are the 2D reciprocal vectors. Right: Fabricated 2D hexagonally-poled LiNbO_3 structure with the period $18.05 \mu\text{m}$ (Broderick, Ross, Offerhaus, Richardson, and Hanna [2000]).

In several papers Zhao, Gu, Zhou, and Wang [2003]; Gu, Zhang, and Dong [2000], and Gu, Dong, Zhang, and Yang [1999] studied aperiodic one-dimensional optical superlattices for the simultaneous phase-matching of several parametric processes. In this case, the thickness of the layers and their order can be found by solving an inverse problem maximizing the efficiency of both the processes involved into the multistep-cascading parametric interaction. Experimental results that employed quasi-periodic and aperiodic optical lattices for realizing the multistep parametric interactions are given in Tables 2, 5, and 6.

4.3. QUADRATIC 2D NONLINEAR PHOTONIC CRYSTALS

Nonlinear photonic crystals (NPCs) with a homogeneous change of the linear refraction index and a two-dimensional (2D) periodic variation of the nonlinear quadratic susceptibility have been suggested by Berger [1998, 1999] as a 2D analog of the QPM structures. Both theoretical and experimental results published so far show that this kind of structures can effectively be employed as a host media for realizing many different types of multistep-cascading parametric processes (see, e.g., Broderick, Ross, Offerhaus, Richardson, and Hanna [2000]; Saltiel and Kivshar [2000a]; de Sterke, Saltiel, and Kivshar [2001]; Chowdhury, Hagness, and McCaughan [2000]). Below, we discuss some of the possible application of these 2D structures for multistep parametric interaction and multi-frequency generation.

4.3.1. Phase-matching in two-dimensional QPM structures

A schematic structure of 2D NPC is shown in Fig. 14. A simple way to obtain the phase-matching conditions for 2D NPC is to use a reciprocal lattice formed by the vectors \mathbf{G}_a and \mathbf{G}_c , defined as $|\mathbf{G}_a| = 2\pi/\Lambda_a$ and $|\mathbf{G}_c| = 2\pi/\Lambda_c$. For a hexagonal lattice, $\Lambda_a = \Lambda_c = a\sqrt{3}/2$, where a is the distance between the centers of two neighboring inverted volumes, the so-called lattice spacing. All reciprocal vectors of the 2D NPC crystal are formed by a simple rule, $\mathbf{G}_{m,n} = m\mathbf{G}_c + n\mathbf{G}_a$. Any two vectors of this set can be used to compensate for the bulk mismatch parameters Δb_1 and Δb_2 , however, the phase-matching conditions require, in most of the cases, non-collinear parametric interactions.

The diagrams for calculating the phase-matching conditions for the THG multistep-cascading process are presented in Fig. 15 for (a) the process $\omega + \omega = 2\omega$ which is phase-matched by the reciprocal vector \mathbf{G}_{m_1,n_1} , and (b) the process $\omega + 2\omega = 3\omega$, which is phase-matched by the reciprocal vector \mathbf{G}_{m_2,n_2} . Phase-matching is achieved by choosing the lattice spacing a and the angle of incidence β . 2D NPC can be also used for simultaneous phase-matching of three nonlinear processes, e.g. second-, third-, and fourth-harmonic generation (Saltiel and Kivshar [2000a]), or the generation of a pair of SH waves and the third- (Karaulanov and Saltiel [2003]) or fourth- (de Sterke, Saltiel, and Kivshar [2001]) harmonic generation. Experimentally, the simultaneous second-, third- and fourth-harmonic generation was recently observed in 2D poled bulk LiNbO_3 (Broderick, Ross, Offerhaus, Richardson, and Hanna [2000] and Broderick, Bratfalean, Monro, Richardson, and de Sterke [2002]). The first experiment with phase-matching in 2D NPC made in a poled LiNbO_3 waveguide slab was reported in (Gallo, Bratfalean, Peacock, Broderick, Gawith, Ming, Smith, and Richardson [2003]). As shown in He, Tang, Qin, Dong, Zhang, Kang, Sun,

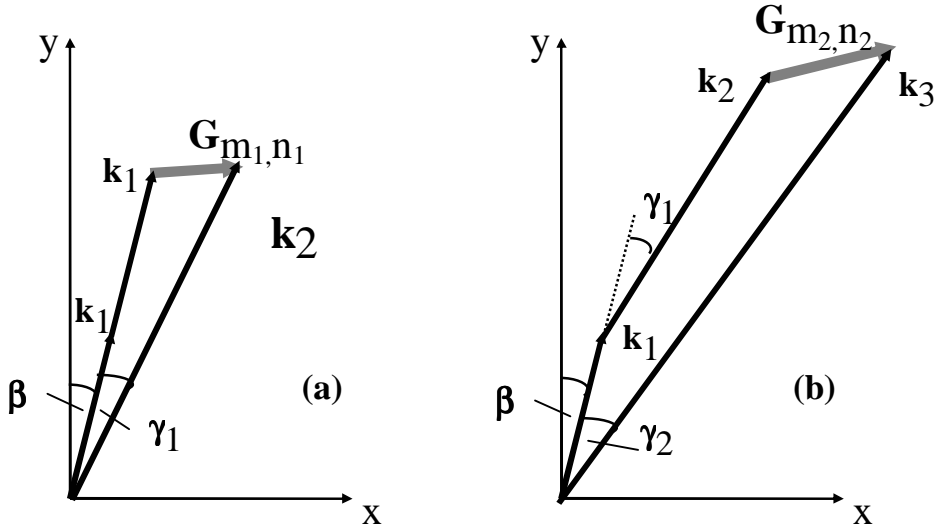


Figure 15: (a,b) Diagrams of the double phase-matching conditions for single-crystal THG in 2D NPC structures.

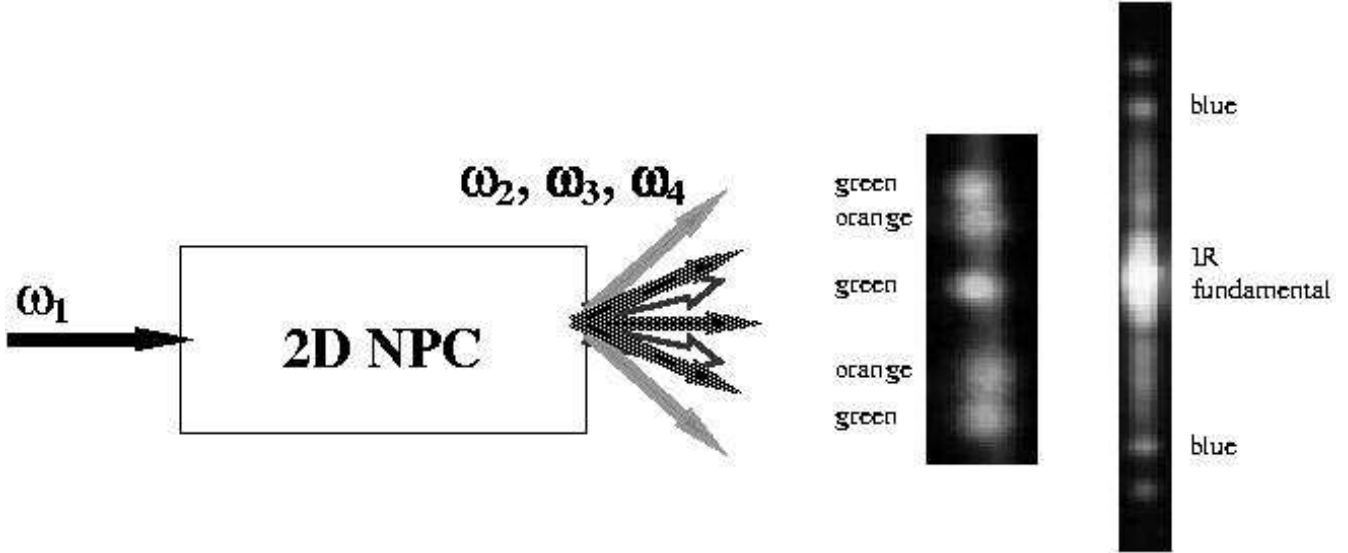


Figure 16: Multiple second- (ω_2), third- (ω_3), and fourth- (ω_4) harmonic generation schemes realized in a 2D NPC structure; orange — SHG (766 nm), green — THG (511nm), blue — FHG (383 nm) (Broderick, Ross, Offerhaus, Richardson, and Hanna [2000]).

and Shen [2003], the method of a direct electron-beam lithography can also be used for creating 2D nonlinear photonic domain-reversed structures.

The shapes of the inverted domain is an important property of the 2D NPC structures, and they can be employed for an effective optimization of the parametric conversion processes. Optimization of the domain shapes for the maximum efficiency of THG and FHG processes was reported by Norton and de Sterke [2003b]. For the case of SHG in Lee and Hagness [2003] the following three types of the domain shapes were compared: hexagonal, circular, and elliptical (aligned to the direction of SHG). The numerical simulation made by the authors revealed that the elliptically-poled domain pattern yields the highest frequency conversion efficiency among these three types of the poling structures. The role of the filling factor for the case of SHG was studied both theoretically and experimentally in Wang and Gu [2001]; Ni, Ma, Wang, Cheng, and Zhang [2003].

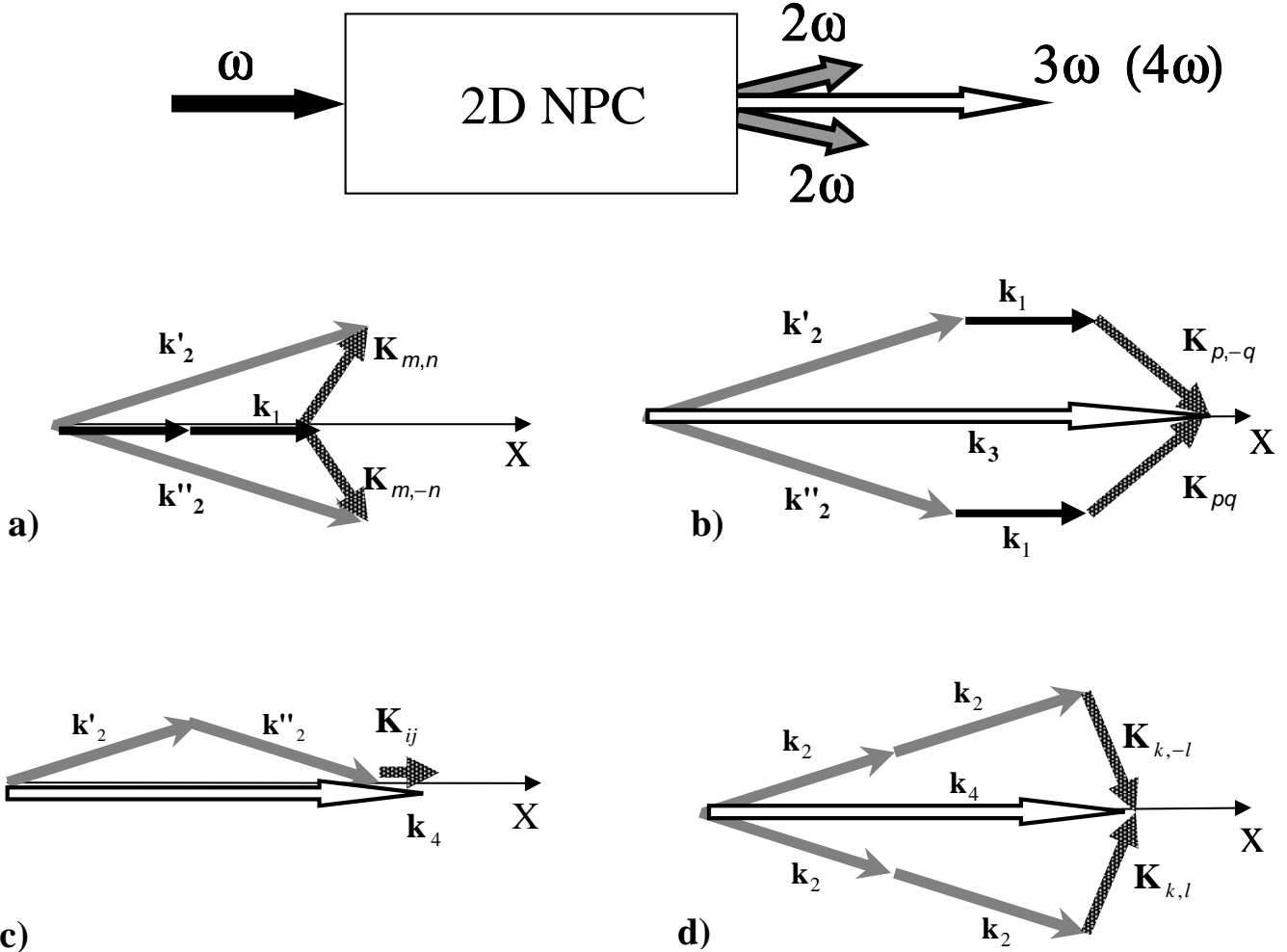


Figure 17: Multi-channel the third- and forth-harmonic generation in 2D NPC structures: (a) the step $\omega + \omega = 2\omega$; (b) the step $\omega + 2\omega = 3\omega$ for THG; (c,d) the step $2\omega + 2\omega = 4\omega$ for FHG; $\mathbf{K}_{p,q}$, $\mathbf{K}_{i,j}$, $\mathbf{K}_{m,n}$, and $\mathbf{K}_{k,l}$ are reciprocal wave-vectors of the lattice.

4.3.2. Multi-channel harmonic generation

In the first experimental work on the harmonic generation in the 2D NPC structures (Broderick, Ross, Offerhaus, Richardson, and Hanna [2000] and Broderick, Bratfalean, Monro, Richardson, and de Sterke [2002]), it was noticed that each generated harmonic has multiple outputs at different angles (see Fig. 16). The reason for that is that each harmonic can be generated by using several different phase-matching conditions. In several papers, an efficient method was suggested to make use of this property and to combine the multiple outputs in order to generate efficient harmonics with the additional advantage of being collinear to the input wave. A phase-matching geometry for THG in 2DNPC, for which generated TH wave is collinear to the input wave, was suggested in Karaulanov and Saltiel [2003]. This scheme uses the fact that the TH wave is generated through two different channels leading to the factor four improvement in comparison with the conventional collinear scheme.

A geometry for the multiple phase-matching of this THG multichannel parametric interaction is presented in Figs. 17(a,b). The process starts with the generation of a pair of the SH waves by employing the wave vectors \mathbf{k}'_2 and \mathbf{k}''_2 . The phase-matching conditions are satisfied by two symmetric reciprocal vectors $\mathbf{K}_{m,n}$ and $\mathbf{K}_{m,-n}$. Each SH wave interacts again with the fundamental wave [see Fig. 17(b)] via a pair of the phase-matched interaction with participation of the reciprocal vectors $\mathbf{K}_{p,q}$ and $\mathbf{K}_{m,-q}$, thus generating a pair of the collinear TH waves with one and the same wave vector \mathbf{k}_3 . The two TH waves interfere constructively in the direction of the input fundamental wave, resulting in the overall higher TH efficiency (in the nondepleted regime).

A scheme for a single-crystal FHG process in a 2D QPM structure where the fundamental and FH waves are collinear was studied in de Sterke, Saltiel, and Kivshar [2001]. The parametric interaction includes cascading of

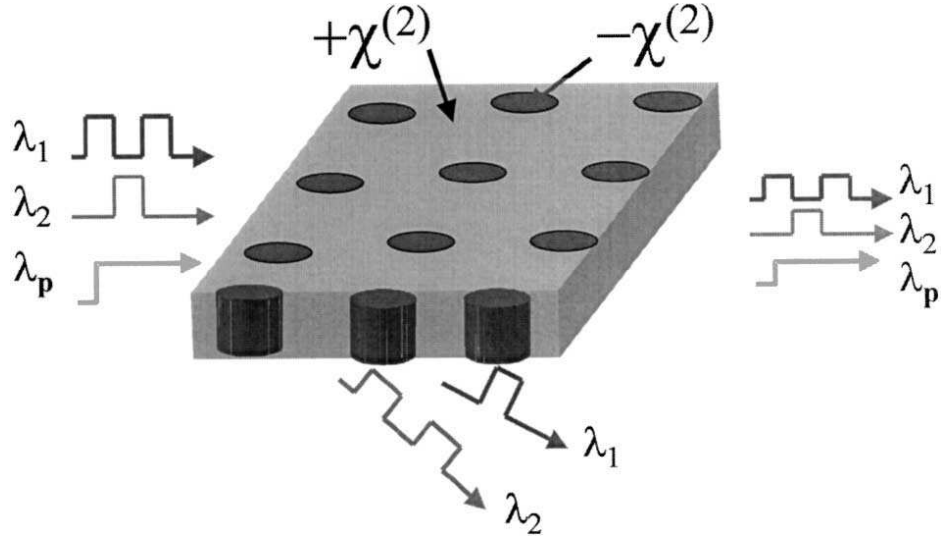


Figure 18: Schematic of the simultaneous optical wavelength interchange in a 2D NPC structure (Chowdhury, Staus, Boland, Kuech, and McCaughan [2001]).

three phase-matched second-order processes that are simultaneously phase-matched. de Sterke, Saltiel, and Kivshar [2001] demonstrated that the FHG efficiency achieved by this scheme is larger than the comparable schemes by a factor that reaches four at low input intensities. The phase-matching geometry for this process is shown in Figs. 17(c,d). Two SH waves are generated at the first step [see Fig. 17(a)], and they interact non-collinearly generating a phase-matched FH wave, which itself is collinear with the fundamental wave [see Fig. 17(c)]. As shown in Norton and de Sterke [2003a], there exist two more FHG channels that are simultaneously phase-matched also leading to the generated FH waves collinear to the input fundamental wave [see Fig. 17(d)]. Thus, in this case the generated FH wave is produced in result of an constructive interference of three FH waves generated at different phase-matching conditions, but propagating in the same direction.

4.3.3. Wave interchange and signal deflection

The first experimental demonstration of the simultaneous optical wavelength interchange by the use of a 2D NPC structure was reported in Chowdhury, Staus, Boland, Kuech, and McCaughan [2001]. A nonlinear 2D lattice fabricated in LiNbO₃ was designed to provide an interchange of the waves with the wavelengths $\lambda_1 = 1535\text{nm}$ and $\lambda_2 = 1555\text{nm}$. The pump was selected at $\lambda_p = 777.2\text{nm}$. The wavelength interchange process takes place by means of the two concurrent difference-frequency generation processes: $\omega_p - \omega_1 = \omega_2$ and $\omega_p - \omega_2 = \omega_1$. The two difference-frequency processes diffract the converted signals from the unconverted ones, as depicted in Fig. 18. The information carried by the input beam 1 will be carried by the output beam 2 and vice versa. In this experiment, one of the main characteristics of the 2D NPC phase-matching, i.e. non-collinearity of the parametric interactions, is used as a real advantage in separating two beams at the output.

Another scheme proposed by Saltiel and Kivshar [2002] is also based on the advantage of non-collinearity of the parametric interactions in the 2D geometry, and it demonstrates how the signal wave can be deflected or split by the pump after the interaction. The phase-matching conditions for this scheme are shown in Fig. 19. The collinear pump and signal are at the same frequency, but they are polarized at the orthogonal directions. If the pump carries some information, the signal will be modulated according to this information after the deflection. This interaction belongs to the two-color multistep cascading processes discussed above. It can also be considered as a spatial analog of the wavelength conversion process discussed above.

In conclusion of this part of the review, we would like to mention that several theoretical studies predicted that the double phase-matched interactions such as the THG multistep parametric process can be realized in photonic bandgap (PBG) structures with the efficiency which should be by several orders higher than that of the conventional nonlinear media of the similar length. In particular, this includes an infinite PBG system as a host of the second-order multistep cascading considered by Konotop and Kuzmiak [1999], cascaded THG in a finite PBG crystal discussed in Centini, D'Aguanno, Scalora, Sibilia, Bertolotti, Bloemer, and Bowden [2001], and a photonic-well

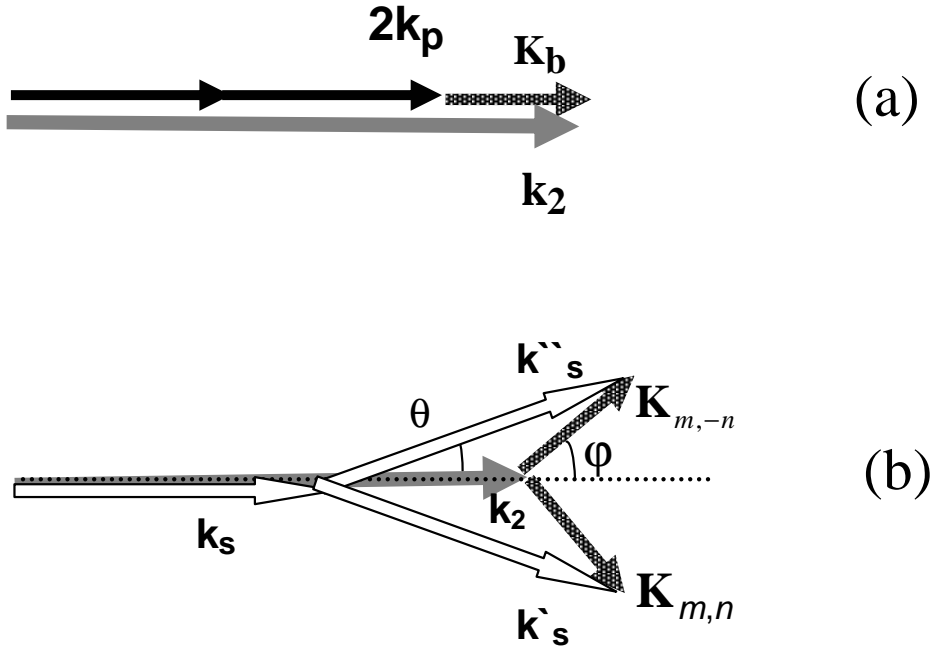


Figure 19: Phase matching for the first (top) and second (below) cascading steps, $y_1p y_{1p} = z_{2p}$, $z_{2p} z_{1s} = z_{1s'}$. Drawings correspond to $n_{1z} < n_{2z} < n_{1y}$ (Saltiel and Kivshar [2002]).

type PBG system analyzed in Shi and Wang [2002]. However, no experimental results on the fabrication of PBG structures with strong nonlinear properties were reported yet.

In conclusion, the part 4 presented a brief overview of different techniques for achieving the simultaneous phase-matching of several nonlinear parametric processes in optical structures with a modulated second-order nonlinear susceptibility. In all those cases, the double phase-matched interaction becomes possible in a wide region of the optical wavelengths provided the QPM structure used to achieve the phase-matching conditions possesses *one extra parameter* (e.g., the modulation period in the chirped QPM structures, or the second dimension, in the case of 2D nonlinear photonic crystals). Some of the possible applications of the double phase-matching processes include the simultaneous generation of several optical frequencies in a single-crystal structure, multi-port frequency conversion, etc. The results presented above look encouraging for experimental feasibility of the predicted effects in the recently engineered 1D and 2D periodic optical superlattices.

§ 5. Multi-color parametric solitons

In the previous sections, we have discussed the features of multiple parametric processes using the plane-wave and continuous-wave approximations. However, parametric interactions can strongly modify the dynamics of spatial beams or temporal pulses. The parametrically coupled waves in a medium with quadratic nonlinearity may experience mutual spatial focusing or temporal compression and lock together into a stationary state, *quadratic soliton* (see Sukhorukov [1988]; Torner [1998]; Kivshar [1997]; Etrich, Lederer, Malomed, Peschel, and Peschel [2000]; Torruellas, Kivshar, and Stegeman [2001]; Boardman and Sukhorukov [2001]; Buryak, Di Trapani, Skryabin, and Trillo [2002], and references therein).

The first analysis of solitons supported by multistep parametric interactions was reported by Azimov, Sukhorukov, and Trukhov [1987] who found that as many as seven waves can be trapped together, and such *multi-color solitons* may be remarkably stable, in particular in the presence of absorption. Since phase mismatch and strength of several parametric interactions can be engineered in nonlinear periodic structures (see Sec. 4), there exists a flexibility in controlling the soliton properties, making them useful for potential applications including all-optical switching. In this section, we overview the properties of multistep parametric solitons that can form under the conditions of cascaded THG, two-color FWM, frequency conversion, and FHG.

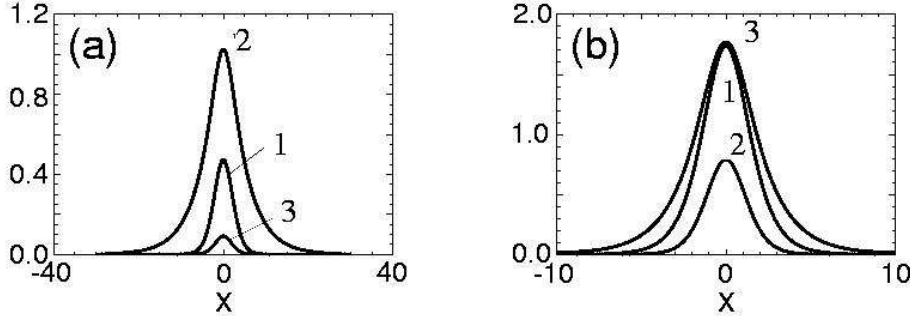


Figure 20: (a,b) Profiles of the THG parametric solitons for different values of phase mismatch (normalized units). Labels 1,2, and 3 indicate the number of harmonic. (Kivshar, Alexander, and Saltiel [1999])

5.1. THIRD-HARMONIC PARAMETRIC SOLITONS

Generation of the TH wave through cascaded SHG and SFG processes was discussed in Sec. 3.1. Komissarova and Sukhorukov [1996] demonstrated that these parametric interactions can result in simultaneous trapping of all the interacting waves and formation of a *three-colour parametric soliton*. Kivshar, Alexander, and Saltiel [1999] performed a detailed investigation of these solitons and demonstrated their stability under various conditions. Such solitons can be described by Eqs. (3.1) with additional terms accounting for beam diffraction,

$$\begin{aligned} \frac{dA_1}{dz} + \frac{i}{2k_1} \nabla_{\perp}^2 A_1 &= -i\sigma_1 A_2 A_1^* e^{-i\Delta k_{\text{SHG}} z} - i\sigma_3 A_3 A_2^* e^{-i\Delta k_{\text{SFG}} z}, \\ \frac{dA_2}{dz} + \frac{i}{2k_2} \nabla_{\perp}^2 A_2 &= -i\sigma_2 A_1^2 e^{i\Delta k_{\text{SHG}} z} - i\sigma_4 A_3 A_1^* e^{-i\Delta k_{\text{SFG}} z}, \\ \frac{dA_3}{dz} + \frac{i}{2k_3} \nabla_{\perp}^2 A_3 &= -i\sigma_5 A_2 A_1 e^{i\Delta k_{\text{SFG}} z}, \end{aligned} \quad (5.1)$$

where the contribution due to the direct THG process is neglected, assuming that the cascaded $\chi^{(2)}$ processes are dominant. The operator ∇_{\perp}^2 acts on the spatial dimensions in the transverse plane (perpendicular to the beam propagation direction z). Similar equations can describe the formation of temporal solitons, where nonlinearity compensates for both the group-velocity mismatch and second-order dispersion effects (Huang [2001]).

Stationary propagation of solitons is possible only when there is no energy exchange between the constituent waves; this requires that the individual phase velocities are synchronized due to nonlinear coupling. Such solutions of Eqs. (5.1) have the form $A_m(\mathbf{r}, z) = B_m(\mathbf{r}) e^{im\beta z}$, where β is the nonlinear propagation constant and $B_m(\mathbf{r})$ are the transverse soliton profiles. Spatial soliton properties were analyzed in the (1+1)-dimensional geometry, when the beam is confined by a planar waveguide and experiences diffraction only in one transverse direction so that $\nabla_{\perp}^2 = \partial^2 / \partial x^2$. There exist two families of single-hump solitons, however solutions with higher power are always unstable. Soliton examples from the low-power branch are shown in Fig. 20. It was also found that cascading interactions can lead to radiative decay of self-localized beams, however such quasi-solitons can demonstrate robust propagation for several diffraction length.

Lobanov and Sukhorukov [2002, 2003] developed a theoretical description of THG solitons in QPM structures, where all the frequency components oscillate along the propagation direction. The spectrum of these oscillations was determined analytically and numerically, and it was found that the solitons can be described by averaged equations with additional terms accounting for induced Kerr effects: self-phase modulation, cross-phase modulation, and third-harmonic generation.

5.2. TWO-COLOR PARAMETRIC SOLITONS

As discussed above in Sec. 3.3, two-colour multistep cascading can involve up to six steps corresponding to type I and type II interactions between two pairs of orthogonally polarized FF and SH waves. Existence of spatial quadratic solitons under these most general conditions was demonstrated by Boardman, Bontemps, and Xie [1998] who found that, by changing the FF polarization at the input, the SH output can be precisely controlled. A possibility for achieving beam steering and switching based on collision of two solitons was demonstrated as well.

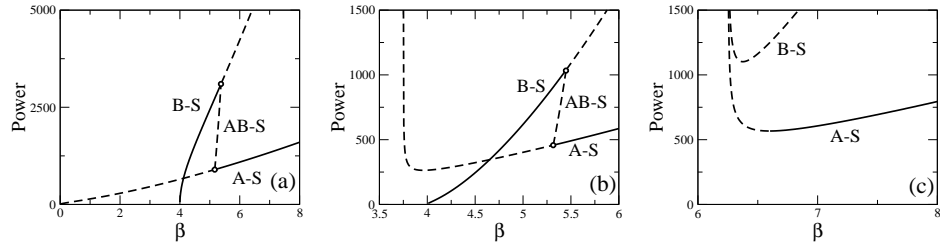


Figure 21: (a-c) Characteristic dependences of the total soliton power on the propagation constant corresponding to different phase mismatches for two-wave (A-S and B-S) and three-wave (AB-S) soliton families (normalized units). Solid lines show stable solitons, and dashed – unstable; open circles mark the bifurcation points. (the figures adapted from [Sukhorukov \[2000\]](#))

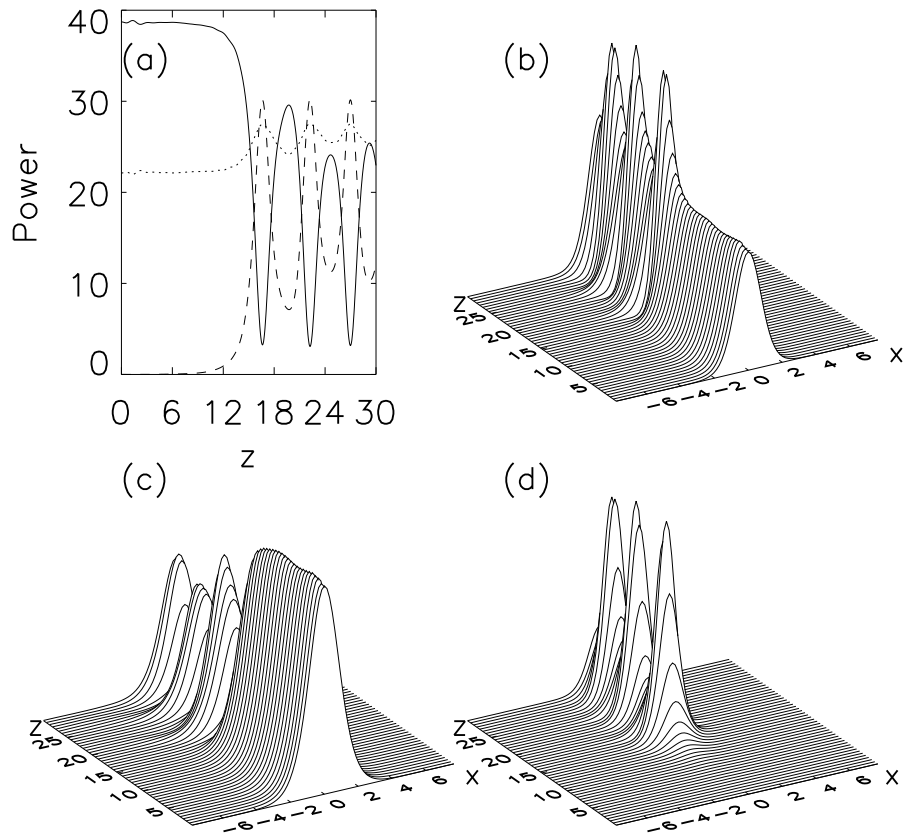


Figure 22: (a) Change of the normalized power in FF (A, solid) and SH (S, dotted) components, which initially constitute a two-wave soliton, and in the guided mode (B, dashed), demonstrating amplification of a guided wave. (b-d) Evolution of the intensity profiles for (b) the effective waveguide (SH), and (c,d) A and B FF components, respectively. ([Kivshar, Sukhorukov, and Saltiel \[1999\]](#))

The general case involving four waves coupled by six parametric processes requires three phase-matching conditions to be fulfilled simultaneously, and the respective components of the $\chi^{(2)}$ susceptibility tensor should also be nonzero. Formation of three-wave solitons which require two phase-matching conditions may be easier to achieve, as indicated by the experimental results in the plane-wave regime (see references in Sec. 3.3). [Kivshar, Sukhorukov, and Saltiel \[1999\]](#); [Sukhorukov \[2000\]](#) considered formation of solitons involving two FF components (A and B) that are coupled together through a single SH component (S). The soliton formation can be described by the following

set of coupled equations that are obtained in the slowly varying envelope approximation,

$$\begin{aligned} \frac{\partial A}{\partial z} + \frac{i}{2k_A} \nabla_{\perp}^2 A &= -i\sigma_{AS} S A^* e^{-i\Delta k_{AS} Z}, \\ \frac{\partial B}{\partial z} + \frac{i}{2k_B} \nabla_{\perp}^2 B &= -i\sigma_{BS} S B^* e^{-i\Delta k_{BS} Z}, \\ \frac{\partial S}{\partial z} + \frac{i}{2k_S} \nabla_{\perp}^2 S &= -i\sigma_{AS} A^2 e^{i\Delta k_{AS} Z} - i\sigma_{BS} B^2 e^{i\Delta k_{BS} Z}, \end{aligned} \quad (5.2)$$

where σ_{AS} and σ_{BS} are proportional to the elements of the second-order susceptibility tensor, as discussed in the previous sections, $\Delta k_{AS} = k_S - 2k_A$ and $\Delta k_{BS} = k_S - 2k_B$ are the wave-vector mismatch parameters for the A-S and B-S parametric interaction processes, respectively.

Similar to the case of the THG cascading, multi-component bright solitons are found in the form of stationary waves, which phases are locked together. When one of the FF waves is zero, then other two waves can form a type I quadratic soliton (A-S or B-S). However, these solitons may experience an instability associated with the amplification of the orthogonally polarized FF wave through the parametric decay instability of the SH component. Such changes of stability are associated with the bifurcation for two-wave to three-wave solitons, as shown in Fig. 21 for a (1+1)-dimensional case. We note that the Vakhitov-Kolokolov stability criterion ([Vakhitov and Kolokolov \[1973\]](#); [Pelinovsky, Buryak, and Kivshar \[1995\]](#)) can only be used as a necessary condition: branches with the negative power slope are unstable, but the positive slope does not guarantee stability.

Examples in Fig. 21 demonstrate the existence of stable solitons that have the same power but different polarizations of the FF waves. Such *multistability* is a sought-after property on nonlinear systems, since this may allow realization of controlled switching between different states. In Fig. 22, we illustrate the development of the soliton instability which results in a power exchange between the two FF components. Such type of polarization switching was earlier predicted for plane waves by [Assanto, Torelli, and Trillo \[1994\]](#).

The properties of two-color multistep cascading solitons were analyzed by [Towers, Sammut, Buryak, and Malomed \[1999\]](#); [Towers, Buryak, Sammut, and Malomed \[2000\]](#) for the case when two FF waves and the SH component are additionally coupled together through the type II parametric process. Due to this interaction, all solitons contain both FF waves, and transition between the states with different polarizations along the soliton family does not involve bifurcations. It was found that soliton multistability can be realized under appropriate conditions, both in planar (one-dimensional) and bulk (two-dimensional) configurations. On the other hand, [Towers, Buryak, Sammut, and Malomed \[2000\]](#) reported that no multistability occurs if the BB-S interaction is suppressed and the waves are coupled only through AA-S and AB-S processes.

5.3. SOLITONS DUE TO WAVELENGTH CONVERSION

Formation of spatial parametric solitons requires a strong coupling between the interacting waves, and this can be achieved when the parametric interactions are nearly phase-matched. In the cases of parametric THG and two-colour FWM, two (or even more) phase-matching conditions should be satisfied simultaneously. On the other hand, in the wavelength conversion scheme (see Sec. 3.2), only single phase-matching condition should be implemented, and this greatly simplifies the requirements for experimental observation of spatial beam localization and soliton formation under the conditions of multistep cascading. Indeed, the first experimental study was recently reported by [Couderc, Lago, Barthelemy, De Angelis, and Gringoli \[2002\]](#) who demonstrated that a multi-color soliton composed of a pump and its second harmonic creates an effective waveguide that can trap a weak probe beam which frequency is slightly detuned from the pump wave (see Fig. 23). This trapping is realized due to a parametric coupling of the probe with both the pump and harmonic waves, and additional side-band frequencies are generated in the process according to the principles of wavelength conversion. [Couderc, Lago, Barthelemy, De Angelis, and Gringoli \[2002\]](#) demonstrated that evolution of a weak probe is governed by the equation,

$$i \frac{\partial a}{\partial z} + \frac{1}{2k_1} \nabla_{\perp}^2 a + \delta\omega^2 \frac{1}{2} \frac{\partial^2 k}{\partial \omega^2} \bigg|_{\omega_1} a + \frac{\sigma^2}{\Delta k} (|A|^2 - |B|^2) a = 0, \quad (5.3)$$

where A and B are the profiles of mutually trapped pump wave and its second harmonic components, $\delta\omega$ is the frequency detuning of the probe, ω_1 and k_1 are the frequency and the wavenumber of the fundamental frequency wave, and Δk is the phase mismatch between the SH and FF components. The last term in Eq. (5.3) defines the profile of an effective waveguide which is experienced by the probe beam, and trapping can be realized when the overall sign is positive. It has been demonstrated in earlier studies that the FF component ($|A|^2$) dominates in a quadratic soliton when $\Delta k > 0$, whereas the SH component ($|B|^2$) becomes larger at negative mismatches, $\Delta k < 0$.

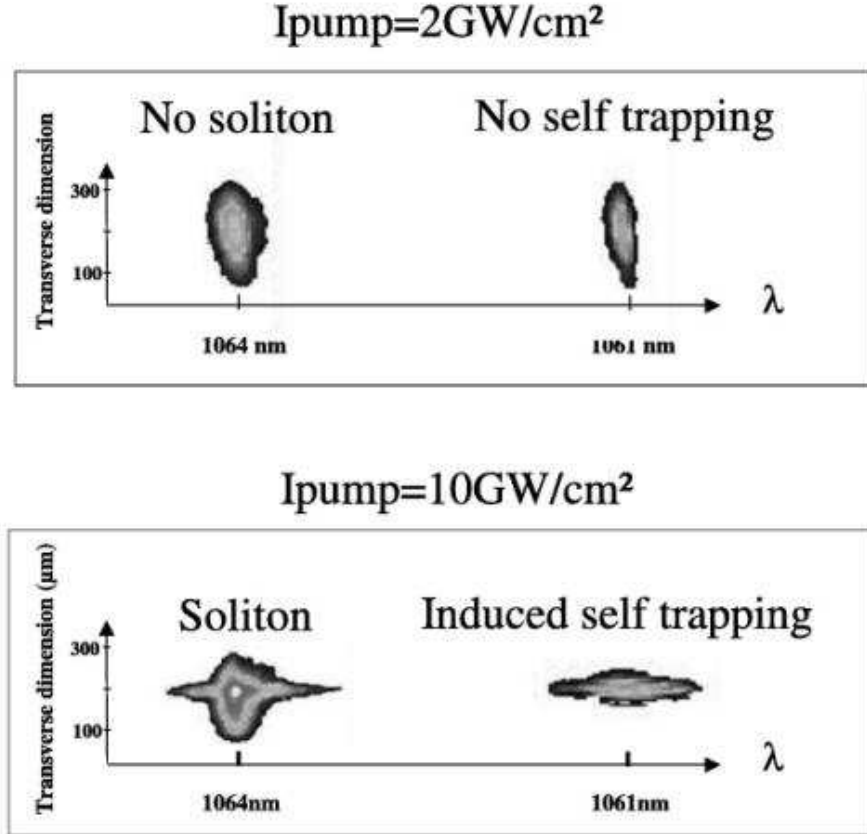


Figure 23: Beam profiles at the output of the 2cm long KTP crystal for low and high input intensities. Horizontal scale: wavelength; vertical scale: transverse dimension on the output pattern. Right part of the figure corresponds to the probe wave (1061 nm), the left part corresponds to the FF component of the soliton (pump at 1064 nm). (Couderc, Lago, Barthelemy, De Angelis, and Gringoli [2002])

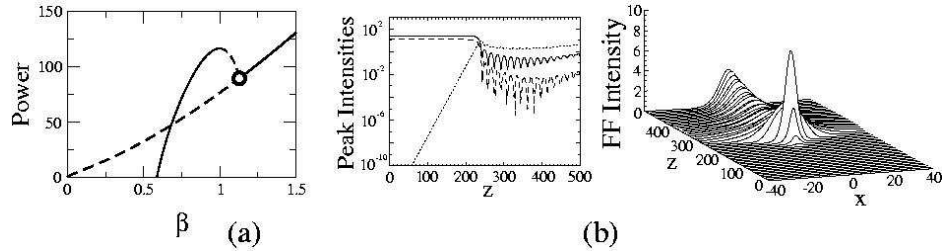


Figure 24: (a) Thick — two-wave (SH + FH), and black — three-wave solitons; solid and dashed lines mark stable and unstable solutions, respectively. Open circle is the bifurcation point; (b) Development of a decay instability of a two-wave soliton corresponding to $\beta = 1$ in plot (a), and generation of a three-component soliton. Dotted, solid, and dashed curves in the left plot show the FF, SH, and FH peak normalized intensities vs. distance, respectively. (Sukhorukov, Alexander, Kivshar, and Saltiel [2001])

Therefore, the probe can be trapped in both cases, however anti-waveguiding effect may occur for particular values of the mismatches and pump intensities.

5.4. OTHER TYPES OF MULTI-COLOR PARAMETRIC SOLITONS

Formation of spatial parametric solitons due to FHG in a planar waveguide configuration was analyzed theoretically by Sukhorukov, Alexander, Kivshar, and Saltiel [2001]. It was found that, similar to the case of two-color parametric

solitons (see Sec. 5.2), there can exist two-wave solitons (coupled second and fourth harmonics) and three-wave solitons containing all the three frequency components. Such coexistence of different solitons may give rise to multistability, as illustrated in Fig. 24(a). A two-wave soliton can exhibit parametric decay instability due to the energy transfer into the fundamental-frequency wave, this process is illustrated in Fig. 24(b).

Towers and Malomed [2002] performed a theoretical analysis of polychromatic solitons consisting of two low-frequency components ω_1 and ω_2 and three high-frequency waves, $2\omega_1$, $2\omega_2$, and $\omega_1 + \omega_2$. It was found that the power of a polychromatic soliton can be smaller compared to conventional two-wave parametric solitons, and this can be advantageous for applications. It was also demonstrated that polychromatic solitons can emerge after a collision of two-wave solitons, and soliton interactions may be used to implement a simple all-optical XOR logic gate.

§ 6. Conclusions

Parametric interactions and phase matching are the key concepts in nonlinear optics. The generation of new waves at the frequencies which are not accessible by standard sources and the efficient frequency conversion and manipulation are among the main goals of the current research in nonlinear optics. The QPM technique is becoming one of the leading technologies for the optical devices based on the parametric wave interaction; it allows generating new harmonics and can be made compatible with the operational wavelengths of optical communication systems.

In this paper, we have presented, for the first time to our knowledge, a systematic overview of the basic principles of the simultaneous phase matching of two (or more) parametric processes in different types of one- and two-dimensional nonlinear quadratic optical lattices, the so-called multistep parametric interactions. In particular, we have discussed different types of multiple phase-matched processes in the engineered QPM structures and two-dimensional nonlinear quadratic photonic crystals, as well as the properties of multi-color optical solitons generated by the multistep parametric processes. We have also summarized the most important experimental demonstrations for the multi-frequency generation due to multistep parametric processes. We believe that such a comprehensive summary of the up-to-date achievements will become a driving force for the future even more active research in this exciting field of nonlinear optics.

§ 7. Acknowledgements

This work was produced with the assistance of the Australian Research Council under the ARC Centers of Excellence Program. The Center for Ultra-high bandwidth Devices for Optical Systems (CUDOS) is an ARC Center of Excellence. Solomon Saltiel thanks the Nonlinear Physics Group for hospitality and the Research School of Physical Sciences and Engineering at the Australian National University for a grant of the senior visiting fellowship.

§ References

Akhmanov, S.A., 1977, High Order Optical Nonlinearities, in *Nonlinear Spectroscopy*, edited by N. Bloembergen (North-Holland, Amsterdam), volume 82 of *Enrico Fermi*, p. 239.

Akhmanov, S.A., A.N. Dubovik, S.M. Saltiel, I.V. Tomov, and V.G. Tunkin, 1974, Nonlinear optical effects of the fourth order in the field in a lithium formate crystal, *Pis'ma Zh. Éksp. Teor. Fiz.* **20**, 264–268 (in Russian) [English translation: *JETP Lett.* **20**, 117–118 (1974)].

Akhmanov, S.A., and R.V. Khokhlov, 1964, *Problemy Nelineinoi Optiki* (Inst. Nauch. Inform, Moscow) (in Russian).

Akhmanov, S.A., and R.V. Khokhlov, 1972, *Problems of Nonlinear Optics* (Gordon and Breach, New York).

Akhmanov, S.A., V.A. Martynov, S.M. Saltiel, and V.G. Tunkin, 1975, Nonresonant six-photon processes in a calcite crystal, *Pis'ma Zh. Éksp. Teor. Fiz.* **22**, 143–147 (in Russian) [English translation: *JETP Lett.* **22**, 65–67 (1975)].

Akhmanov, S.A., L.B. Meisner, S.T. Parinov, S.M. Saltiel, and V.G. Tunkin, 1977, Cubic nonlinear susceptibilities of crystals in optical range - signs and magnitudes of susceptibilities of crystals with and without inversion centers, *Zh. Éksp. Teor. Fiz.* **73**, 1710–1728 (in Russian) [English translation: *JETP* **46**, 898 (1977)].

Alekseev, K.N., and A.V. Ponomarev, 2002, Optical chaos in nonlinear photonic crystals, *Pis'ma Zh. Éksp. Teor. Fiz.* **75**, 206–210 [Reproduced in: *JETP Lett.* **75**, 174–178 (2002), DOI:[10.1134/1.1475717](https://doi.org/10.1134/1.1475717)]; Erratum: *Pis'ma Zh. Éksp. Teor. Fiz.* **75**, 464 (2002) [Reproduced in: *JETP Lett.* **76**, 401 (2002), DOI:[10.1134/1.1525125](https://doi.org/10.1134/1.1525125)].

Ammann, E.O., J.M. Yarborough, and J. Falk, 1971, Simultaneous optical parametric oscillation and second-harmonic generation, *J. Appl. Phys.* **42**, 5618–5634.

Andrews, R.A., H. Rabin, and C.L. Tang, 1970, Coupled parametric downconversion and upconversion with simultaneous phase matching, *Phys. Rev. Lett.* **25**, 605–608, DOI:[10.1103/PhysRevLett.25.605](https://doi.org/10.1103/PhysRevLett.25.605).

Asobe, M., O. Tadanaga, H. Miyazawa, Y. Nishida, and H. Suzuki, 2003, Multiple quasi-phase-matched LiNbO₃ wavelength converter with a continuously phase-modulated domain structure, *Opt. Lett.* **28**, 558–560.

Assanto, G., G.I. Stegeman, M. Sheik-Bahae, and E. Vanstryland, 1995, Coherent interactions for all-optical signal-processing via quadratic nonlinearities, *IEEE J. Quantum Electron.* **31**, 673–681, DOI:[10.1109/3.371942](https://doi.org/10.1109/3.371942).

Assanto, G., I. Torelli, and S. Trillo, 1994, All-optical processing by means of vectorial interactions in 2nd-order cascading - novel approaches, *Opt. Lett.* **19**, 1720–1722.

Astinov, V., K.J. Kubarych, C.J. Milne, and R.J.D. Miller, 2000, Diffractive optics implementation of six-wave mixing, *Opt. Lett.* **25**, 853–855.

Aytur, O., and Y. Dikmelik, 1998, Plane-wave theory of self-doubling optical parametric oscillators, *IEEE J. Quantum Electron.* **34**, 447–458.

Azimov, B.S., A.P. Sukhorukov, and D.V. Trukhov, 1987, Parametric multifrequency solitons - origination, collision and decay, *Izv. Akad. Nauk Ser. Fiz.* **51**, 229–233 (in Russian) [English translation: *Bull. Russ. Acad. Sci. Phys.* **51**, 19–23 (1987)].

Bakker, H.J., P.C.M. Planken, L. Kuipers, and A. Lagendijk, 1989, Simultaneous phase matching of three second-order nonlinear optical processes in LiNbO₃, *Opt. Commun.* **73**, 398–402, DOI:[10.1016/0030-4018\(89\)90179-X](https://doi.org/10.1016/0030-4018(89)90179-X).

Baldi, P., C.G. Trevino-Palacios, G.I. Stegeman, M.P. Demicheli, D.B. Ostrowsky, D. Delacourt, and M. Papuchon, 1995, Simultaneous generation of red, green and blue-light in room-temperature periodically poled lithium-niobate wave-guides using single-source, *Electron. Lett.* **31**, 1350–1351, DOI:[10.1049/el:19950953](https://doi.org/10.1049/el:19950953).

Banfi, G., I. Christiani, and V. Degiorgio, 2000, Wavelength shifting by cascaded second-order processes, *J. Opt. A-Pure Appl. Opt.* **2**, 260–267, DOI:[10.1088/1464-4258/2/4/303](https://doi.org/10.1088/1464-4258/2/4/303).

Banfi, G.P., P.K. Datta, V. Degiorgio, G. Donelli, D. Fortusini, and J.N. Sherwood, 1998, Frequency shifting through cascaded second-order processes in a N-(4-nitrophenyl)-L-prolinol crystal, *Opt. Lett.* **23**, 439–441.

Banfi, G.P., P.K. Datta, V. Degiorgio, and D. Fortusini, 1998, Wavelength shifting and amplification of optical pulses through cascaded second-order processes in periodically poled lithium niobate, *Appl. Phys. Lett.* **73**, 136–138, DOI:[10.1063/1.121734](https://doi.org/10.1063/1.121734).

Bang, O., C.B. Clausen, P.L. Christiansen, and L. Torner, 1999, Engineering competing nonlinearities, *Opt. Lett.* **24**, 1413–1415.

Banks, P.S., M.D. Feit, and M.D. Perry, 1999, High-intensity third-harmonic generation in beta barium borate through second-order and third-order susceptibilities, *Opt. Lett.* **24**, 4–6.

Banks, P.S., M.D. Feit, and M.D. Perry, 2002, High-intensity third-harmonic generation, *J. Opt. Soc. Am. B* **19**, 102–118.

Berger, V., 1998, Nonlinear photonic crystals, *Phys. Rev. Lett.* **81**, 4136–4139, DOI:[10.1103/PhysRevLett.81.4136](https://doi.org/10.1103/PhysRevLett.81.4136).

Berger, V., 1999, Photonic crystals for nonlinear optical frequency conversion, in *Confined Photon Systems: Fundamentals and Applications*, edited by H. Benisty, J.M. Gerard, R. Houdre, J. Rarity, and C. Weisbuch (Springer-Verlag, Berlin), volume 531 of *Lecture Notes in Physics*, pp. 366–392.

Biaggio, I., 1999, Nonlocal contributions to degenerate four-wave mixing in noncentrosymmetric materials, *Phys. Rev. Lett.* **82**, 193–196, DOI:[10.1103/PhysRevLett.82.193](https://doi.org/10.1103/PhysRevLett.82.193).

Biaggio, I., 2001, Degenerate four-wave mixing in noncentrosymmetric materials, *Phys. Rev. A* **64**, 063813–13, DOI:[10.1103/PhysRevA.64.063813](https://doi.org/10.1103/PhysRevA.64.063813).

Birch, J., M. Severin, U. Wahlstrom, Y. Yamamoto, G. Radnoci, R. Riklund, J.E. Sundgren, and L.R. Wallenberg, 1990, Structural characterization of precious-mean quasiperiodic Mo/V single-crystal superlattices grown by dual-target magnetron sputtering, *Phys. Rev. B* **41**, 10398–10407, DOI:[10.1103/PhysRevB.41.10398](https://doi.org/10.1103/PhysRevB.41.10398).

Bloembergen, N., 1982, Nonlinear optics and spectroscopy, *Rev. Mod. Phys.* **54**, 685–695, DOI:[10.1103/RevModPhys.54.685](https://doi.org/10.1103/RevModPhys.54.685).

Boardman, A.D., P. Bontemps, and K. Xie, 1998, Vector solitary optical beam control with mixed type I type II second-harmonic generation, *Opt. Quantum Electron.* **30**, 891–905, DOI:[10.1023/A:1006955210556](https://doi.org/10.1023/A:1006955210556).

Boardman, A.D., and A.P. Sukhorukov (eds.), 2001, *Soliton-Driven Photonics*, volume 31 of *NATO Science Series: II: Mathematics, Physics and Chemistry* (Kluwer, Boston).

Boardman, A.D., and K. Xie, 1997, Vector spatial solitons influenced by magneto-optic effects in cascadable nonlinear media, *Phys. Rev. E* **55**, 1899–1909, DOI:[10.1103/PhysRevE.55.1899](https://doi.org/10.1103/PhysRevE.55.1899).

Bosshard, C., I. Biaggio, Fischer. St, S. Follonier, and P. Gunter, 1999, Cascaded contributions to degenerate four-wave mixing in an acentric organic crystal, *Opt. Lett.* **24**, 196–198.

Bosshard, C., U. Gubler, P. Kaatz, W. Mazerant, and U. Meier, 2000, Non-phase-matched optical third-harmonic generation in noncentrosymmetric media: Cascaded second-order contributions for the calibration of third-order nonlinearities, *Phys. Rev. B* **61**, 10688–10701, DOI:[10.1103/PhysRevB.61.10688](https://doi.org/10.1103/PhysRevB.61.10688).

Bosshard, C., R. Spreiter, M. Zgonik, and P. Gunter, 1995, Kerr nonlinearity via cascaded optical rectification and the linear electro-optic effect, *Phys. Rev. Lett.* **74**, 2816–2819, DOI:[10.1103/PhysRevLett.74.2816](https://doi.org/10.1103/PhysRevLett.74.2816).

Boulanger, B., J.P. Feve, P. Delarue, I. Rousseau, and G. Marnier, 1999, Cubic optical nonlinearity of KTiOPO_4 , *J. Phys. B* **32**, 475–488, DOI:[10.1088/0953-4075/32/2/026](https://doi.org/10.1088/0953-4075/32/2/026).

Boyd, R.W., 1992, *Nonlinear Optics* (Academic Press, San Diego).

Bracken, J.A., and C.Q. Xu, 2003, All-optical wavelength conversions based on MgO-doped LiNbO_3 QPM waveguides using an EDFA as a pump source, *IEEE Photonics Technol. Lett.* **15**, 954–956.

Broderick, N.G.R., R.T. Bratfalean, T.M. Monro, D.J. Richardson, and C.M. de Sterke, 2002, Temperature and wavelength tuning of second-, third-, and fourth-harmonic generation in a two-dimensional hexagonally poled nonlinear crystal, *J. Opt. Soc. Am. B* **19**, 2263–2272.

Broderick, N.G.R., G.W. Ross, H.L. Offerhaus, D.J. Richardson, and D.C. Hanna, 2000, Hexagonally poled lithium niobate: a two-dimensional nonlinear photonic crystal, *Phys. Rev. Lett.* **84**, 4345–4348, DOI:[10.1103/PhysRevLett.84.4345](https://doi.org/10.1103/PhysRevLett.84.4345).

Burr, K.C., C.L. Tang, M.A. Arbore, and M.M. Fejer, 1997, High-repetition-rate femtosecond optical parametric oscillator based on periodically poled lithium niobate, *Appl. Phys. Lett.* **70**, 3341–3343, DOI:[10.1063/1.119164](https://doi.org/10.1063/1.119164).

Buryak, A.V., P. Di Trapani, D.V. Skryabin, and S. Trillo, 2002, Optical solitons due to quadratic nonlinearities: from basic physics to futuristic applications, *Phys. Rep.* **370**, 63–235, DOI:[10.1016/S0370-1573\(02\)00196-5](https://doi.org/10.1016/S0370-1573(02)00196-5).

Butcher, P.N., and D. Cotter, 1992, *The elements of Nonlinear Optics* (Cambridge, UK).

Butterworth, S.D., P.G.R. Smith, and D.C. Hanna, 1997, Picosecond Ti:sapphire-pumped optical parametric oscillator based on periodically poled LiNbO_3 , *Opt. Lett.* **22**, 618–620.

Capmany, J., 2001, Simultaneous generation of red, green, and blue continuous-wave laser radiation in Nd^{3+} -doped aperiodically poled lithium niobate, *Appl. Phys. Lett.* **78**, 144–146, DOI:[10.1063/1.1338495](https://doi.org/10.1063/1.1338495).

Capmany, J., V. Bermudez, D. Callejo, J.G. Sole, and E. Dieguez, 2000, Continuous wave simultaneous multi-self-frequency conversion in Nd^{3+} -doped aperiodically poled bulk lithium niobate, *Appl. Phys. Lett.* **76**, 1225–1227, DOI:[10.1063/1.125897](https://doi.org/10.1063/1.125897).

Cardakli, M.C., D. Gurkan, S.A. Havstad, A.E. Willner, K.R. Parameswaran, M.M. Fejer, and I. Brener, 2002, Tunable all-optical time-slot-interchange and wavelength conversion using difference-frequency-generation and optical buffers, *IEEE Photonics Technol. Lett.* **14**, 200–202.

Cardakli, M.C., A.B. Sahin, O.H. Adamczyk, A.E. Willner, K.R. Parameswaran, and M.M. Fejer, 2002, Wavelength conversion of subcarrier channels using difference frequency generation in a PPLN waveguide, *IEEE Photonics Technol. Lett.* **14**, 1327–1329.

Centini, M., G. D’Aguanno, M. Scalora, C. Sibilia, M. Bertolotti, M.J. Bloemer, and C.M. Bowden, 2001, Simultaneously phase-matched enhanced second and third harmonic generation, *Phys. Rev. E* **64**, 046606–5, DOI:[10.1103/PhysRevE.64.046606](https://doi.org/10.1103/PhysRevE.64.046606).

Chemla, D.S., R.F. Begley, and R.L. Byer, 1974, Experimental and theoretical studies of third-harmonic generation in the chalcopyrite CdGeAs_2 , *IEEE J. Quantum Electron.* **10**, 71–80.

Chen, B., and C.Q. Xu, 2004, Analysis of novel cascaded $\chi^{(2)}$ (SFG+DFG) wavelength conversions in quasi-phase-matched waveguides, *IEEE J. Quantum Electron.* **40**, 256–261, DOI:[10.1109/JQE.2003.823023](https://doi.org/10.1109/JQE.2003.823023).

Chen, B., C.Q. Xu, B. Zhou, and X.H. Tang, 2002, Analysis of cascaded second-order nonlinear interaction based on quasi-phase-matched optical waveguides, *IEEE J. Sel. Top. Quantum Electron.* **8**, 675–680.

Chen, Y.B., C. Zhang, Y.Y. Zhu, S.N. Zhu, H.T. Wang, and N.B. Ming, 2001, Optical harmonic generation in a quasi-phase-matched three-component Fibonacci superlattice LiTaO_3 , *Appl. Phys. Lett.* **78**, 577–579, DOI:[10.1063/1.1344226](https://doi.org/10.1063/1.1344226).

Chirkin, A.S., 2002, Entangled and squeezed photon states at consecutive and simultaneous quasi-phase-matched wave interactions, *J. Opt. B: Quantum Semicl. Opt.* **4**, S91–S97, DOI:[10.1088/1464-4266/4/3/361](https://doi.org/10.1088/1464-4266/4/3/361).

Chirkin, A.S., and A.V. Nikandrov, 2003, Generation of high frequency photons with sub-Poissonian statistics at consecutive interactions, *J. Opt. B: Quantum Semicl. Opt.* **5**, 169–174, DOI:[10.1088/1464-4266/5/2/309](https://doi.org/10.1088/1464-4266/5/2/309).

Chirkin, A.S., V.V. Volkov, G.D. Laptev, and E.Y. Morozov, 2000, Consecutive three-wave interactions in nonlinear optics of periodically inhomogeneous media, *Quantum Electron.* **30**, 847 (in Russian) [English translation: *Quantum Electron.* **30**, 847–858 (2000), DOI:[10.1070/qe2000v03n10ABEH001859](https://doi.org/10.1070/qe2000v03n10ABEH001859)].

Chou, M.H., I. Brener, M.M. Fejer, E.E. Chaban, and S.B. Christman, 1999, 1.5- μm -band wavelength conversion based on cascaded second-order nonlinearity in LiNbO_3 waveguides, *IEEE Photonics Technol. Lett.* **11**, 653–655.

Chou, M.H., I. Brener, G. Lenz, R. Scotti, E.E. Chaban, J. Shmulovich, D. Philen, S. Kosinski, K.R. Parameswaran, and M.M. Fejer, 2000, Efficient wide-band and tunable midspan spectral inverter using cascaded nonlinearities in LiNbO_3 waveguides, *IEEE Photonics Technol. Lett.* **12**, 82–84.

Chou, M.H., I. Brener, K.R. Parameswaran, and M.M. Fejer, 1999, Stability and bandwidth enhancement of difference frequency generation (DFG)-based wavelength conversion by pump detuning, *Electron. Lett.* **35**, 978–980, DOI:[10.1049/el:19990678](https://doi.org/10.1049/el:19990678).

Chou, M.H., K.R. Parameswaran, M.M. Fejer, and I. Brener, 1999, Multiple-channel wavelength conversion by use of engi-

neered quasi-phase-matching structures in LiNbO₃ waveguides, Opt. Lett. **24**, 1157–1159.

Chowdhury, A., S.C. Hagness, and L. McCaughan, 2000, Simultaneous optical wavelength interchange with a two-dimensional second-order nonlinear photonic crystal, Opt. Lett. **25**, 832–834.

Chowdhury, A., C. Staus, B.F. Boland, T.F. Kuech, and L. McCaughan, 2001, Experimental demonstration of 1535–1555-nm simultaneous optical wavelength interchange with a nonlinear photonic crystal, Opt. Lett. **26**, 1353–1355.

Couderc, V., E.L. Lago, A. Barthelemy, C. De Angelis, and F. Gringoli, 2002, Trapping of a weak probe through coupling with a two-color quadratic spatial soliton, Opt. Commun. **203**, 421–425, DOI:[10.1016/S0030-4018\(02\)01171-9](https://doi.org/10.1016/S0030-4018(02)01171-9).

Crespo, H., J.T. Mendonca, and A. Dos Santos, 2000, Cascaded highly nondegenerate four-wave-mixing phenomenon in transparent isotropic condensed media, Opt. Lett. **25**, 829–831.

Cristiani, I., G.P. Banfi, V. Degiorgio, and L. Tartara, 1999, Wavelength shifting of optical pulses through cascaded second-order processes in a lithium-niobate channel waveguide, Appl. Phys. Lett. **75**, 1198–1200, DOI:[10.1063/1.124640](https://doi.org/10.1063/1.124640).

Cristiani, I., V. Degiorgio, L. Soccia, F. Carbone, and M. Romagnoli, 2002, Polarization-insensitive wavelength conversion in a lithium niobate waveguide by the cascading technique, IEEE Photonics Technol. Lett. **14**, 669–671.

Cristiani, I., C. Liberale, V. Degiorgio, G. Tartarini, and P. Bassi, 2001, Nonlinear characterization and modeling of periodically poled lithium niobate waveguides for 1.5- μ m-band cascaded wavelength conversion, Opt. Commun. **187**, 263–270, DOI:[10.1016/S0030-4018\(00\)01099-3](https://doi.org/10.1016/S0030-4018(00)01099-3).

DeRossi, A., C. Conti, and G. Assanto, 1997, Mode interplay via quadratic cascading in a lithium niobate waveguide for all-optical processing, Opt. Quantum Electron. **29**, 53–63.

DeSalvo, R., D.J. Hagan, M. Sheik-Bahae, G. Stegeman, E.W. Vanstryland, and H. Vanherzele, 1992, Self-focusing and self-defocusing by cascaded 2nd-order effects in KTP, Opt. Lett. **17**, 28–30.

Dikmelik, Y., G. Akgun, and O. Aytur, 1999, Plane-wave dynamics of optical parametric oscillation with simultaneous sum-frequency generation, IEEE J. Quantum Electron. **35**, 897–912.

Ding, Y.J., X. Mu, and X. Gu, 2000, Efficient generation of coherent blue and green light based on frequency conversion in KTiOPO₄ crystals, J. Nonlinear Opt. Phys. Mater. **9**, 21–53, DOI:[10.1016/S0218-8635\(00\)00004-2](https://doi.org/10.1016/S0218-8635(00)00004-2).

Dmitriev, V.G., and S.G. Grechin, 1998, Multifrequency laser radiation harmonics generation in nonlinear crystals with regular domain structure, in *ICONO'98: Nonlinear Optical Phenomena*, edited by S.S. Chesnokov, V.P. Kandidov, and N.I. Koroteev, volume 3733 of *Proc. SPIE*, pp. 228–236, .

Dmitriev, V.G., G.G. Gurzadyan, and D.N. Nikogosyan, 1999, *Handbook of Nonlinear Optical Crystals*, volume 64 of *Springer Series in Optical Sciences* (Springer-Verlag, New York), 3rd rev. ed. edition.

Dmitriev, V.G., and R. Singh, 2003, Generation of polarization squeezed light in PPNC, arXiv physics/0308025.

Douillet, A., J.J. Zondy, G. Santarelli, A. Makdissi, and A. Clairon, 2001, A phase-locked frequency divide-by-3 optical parametric oscillator, IEEE Trans. Instrum. Meas. **50**, 548–551, DOI:[10.1109/19.918188](https://doi.org/10.1109/19.918188).

Du, Y., S.N. Zhu, Y.Y. Zhu, P. Xu, C. Zhang, Y.B. Chen, Z.W. Liu, N.B. Ming, X.R. Zhang, F.F. Zhang, and S.Y. Zhang, 2002, Parametric and cascaded parametric interactions in a quasiperiodic optical superlattice, Appl. Phys. Lett. **81**, 1573–1575, DOI:[10.1063/1.1502007](https://doi.org/10.1063/1.1502007).

Durfee, C.G., L. Misoguti, S. Backus, H.C. Kapteyn, and M.M. Murnane, 2002, Phase matching in cascaded third-order processes, J. Opt. Soc. Am. B **19**, 822–831.

Egorov, O.A., and A.P. Sukhorukov, 1998, New phenomena in three-wave interactions at multiple frequencies: complete wave energy exchange, Izv. Akad. Nauk Ser. Fiz. **62**, 2345–2353 (in Russian) [English translation: Bull. Russ. Acad. Sci. Phys. **62**, 1884–1891 (1998)].

Eschmann, A., and M.A.M. Marte, 1997, Detuning effects in competing $\chi^{(2)}$ nonlinearities, Quantum Semiclass. Opt. **9**, 247–255, DOI:[10.1088/1355-5111/9/2/011](https://doi.org/10.1088/1355-5111/9/2/011).

Etrich, C., F. Lederer, B. Malomed, T. Peschel, and U. Peschel, 2000, Optical solitons in media with quadratic nonlinearity, in *Progress in Optics*, edited by E. Wolf (North-Holland, Amsterdam), volume 41, pp. 483–568.

Fejer, M.M., 1998, Nonlinear optical frequency conversion: Material requirements, engineered materials, and quasi-phase-matching, in *Beam Shaping and Control with Nonlinear Optics*, edited by F. Kajzer and R. Reinisch (Plenum, New York), pp. 375–406.

Fejer, M.M., G.A. Magel, D.H. Jundt, and R.L. Byer, 1992, Quasi-phase-matched 2nd harmonic-generation - tuning and tolerances, IEEE J. Quantum Electron. **28**, 2631–2654.

Feve, J.P., B. Boulanger, and J. Douady, 2002, Specific properties of cubic optical parametric interactions compared to quadratic interactions, Phys. Rev. A **66**, 063817–11, DOI:[10.1103/PhysRevA.66.063817](https://doi.org/10.1103/PhysRevA.66.063817).

Feve, J.P., B. Boulanger, and Y. Guillien, 2000, Efficient energy conversion for cubic third-harmonic generation that is phase matched in KTiOPO₄, Opt. Lett. **25**, 1373–1375.

Fradkin-Kashi, K., and A. Arie, 1999, Multiple-wavelength quasi-phase-matched nonlinear interactions, IEEE J. Quantum Electron. **35**, 1649–1656.

Fradkin-Kashi, K., A. Arie, P. Urenski, and G. Rosenman, 2002, Multiple nonlinear optical interactions with arbitrary wave vector differences, *Phys. Rev. Lett.* **88**, 023903–4, DOI:[10.1103/PhysRevLett.88.023903](https://doi.org/10.1103/PhysRevLett.88.023903).

Gallo, K., and G. Assanto, 1999, Analysis of lithium niobate all-optical wavelength shifters for the third spectral window, *J. Opt. Soc. Am. B* **16**, 741–753.

Gallo, K., G. Assanto, and G.I. Stegeman, 1997, Efficient wavelength shifting over the erbium amplifier bandwidth via cascaded second order processes in lithium niobate waveguides, *Appl. Phys. Lett.* **71**, 1020–1022, DOI:[10.1063/1.119714](https://doi.org/10.1063/1.119714).

Gallo, K., R.T. Bratfalean, A.C. Peacock, N.G.R. Broderick, C.B.E. Gawith, L. Ming, P.G.R. Smith, and D.J. Richardson, 2003, Second-harmonic generation in hexagonally-poled lithium niobate slab waveguides, *Electron. Lett.* **39**, 75–76.

Ganeev, R.A., I.A. Kulagin, A.I. Ryasnyanskii, R.I. Tugushev, and T. Usmanov, 2003, The nonlinear refractive indices and nonlinear third-order susceptibilities of quadratic crystals, *Opt Spectrosc Engl Trans* **94**, 561–568, DOI:[10.1134/1.1570482](https://doi.org/10.1134/1.1570482).

Gao, S.M., C.X. Yang, and G.F. Jin, 2004, Flat broad-band wavelength conversion based on sinusoidally chirped optical superlattices in lithium niobate, *IEEE Photonics Technol. Lett.* **16**, 557–559, DOI:[10.1109/LPT.2003.823102](https://doi.org/10.1109/LPT.2003.823102).

Grechin, S.G., and V.G. Dmitriev, 2001a, Quasi-phase-matching conditions for a simultaneous generation of several harmonics of laser radiation in periodically poled crystals, *Kvantov. Elektron.* **31**, 933–936 (in Russian) [English translation: *Quantum Electron.* **31**, 933–936 (2001), DOI:[10.1070/QE2001v031n10ABEH002079](https://doi.org/10.1070/QE2001v031n10ABEH002079)].

Grechin, S.G., and V.G. Dmitriev, 2001b, Second harmonic generation in periodically poled crystals for two types of interaction, *Kvantov. Elektron.* **31**, 929–932 (in Russian) [English translation: *Quantum Electron.* **31**, 929–932 (2001), DOI:[10.1070/QE2001v031n10ABEH002078](https://doi.org/10.1070/QE2001v031n10ABEH002078)].

Grechin, S.G., V.G. Dmitriev, and Yu.V. Yur'ev, 1999, Second-harmonic generation under conditions of simultaneous phase-matched and quasi-phase-matched interactions in nonlinear crystals with a regular domain structure, *Kvantov. Elektron.* **26**, 155–157 (in Russian) [English translation: *Quantum Electron.* **29**, 155–157 (1999), DOI:[10.1070/qe1999v029n02ABEH001437](https://doi.org/10.1070/qe1999v029n02ABEH001437)].

Gu, B.Y., B.Z. Dong, Y. Zhang, and G.Z. Yang, 1999, Enhanced harmonic generation in aperiodic optical superlattices, *Appl. Phys. Lett.* **75**, 2175–2177, DOI:[10.1063/1.124956](https://doi.org/10.1063/1.124956).

Gu, B.Y., Y. Zhang, and B.Z. Dong, 2000, Investigations of harmonic generations in aperiodic optical superlattices, *J. Appl. Phys.* **87**, 7629–7637, DOI:[10.1063/1.373433](https://doi.org/10.1063/1.373433).

Gu, X.H., R.Y. Korotkov, Y.J. Ding, J.U. Kang, and J.B. Khurgin, 1998, Observation of backward sum-frequency generation in periodically poled lithium niobate, *Opt. Commun.* **155**, 323–326, DOI:[10.1016/S0030-4018\(98\)00385-X](https://doi.org/10.1016/S0030-4018(98)00385-X).

Gu, X.H., M. Makarov, Y.J. Ding, J.B. Khurgin, and W.P. Risk, 1999, Backward second-harmonic and third-harmonic generation in a periodically poled potassium titanyl phosphate waveguide, *Opt. Lett.* **24**, 127–129.

Harel, R., W.H. Burkett, G. Lenz, E.E. Chaban, K.R. Parameswaran, M.M. Fejer, and I. Brener, 2002, Interchannel cross talk caused by pump depletion in periodically poled LiNbO₃ waveguide wavelength converters, *J. Opt. Soc. Am. B* **19**, 849–851.

He, J., S.H. Tang, Y.Q. Qin, P. Dong, H.Z. Zhang, C.H. Kang, W.X. Sun, and Z.X. Shen, 2003, Two-dimensional structures of ferroelectric domain inversion in LiNbO₃ by direct electron beam lithography, *J. Appl. Phys.* **93**, 9943–9946, DOI:[10.1063/1.1575918](https://doi.org/10.1063/1.1575918).

He, J.L., J. Liao, H. Liu, J. Du, F. Xu, H.T. Wang, S.N. Zhu, Y.Y. Zhu, and N.B. Ming, 2003, Simultaneous cw red, yellow, and green light generation, "traffic signal lights", by frequency doubling and sum-frequency mixing in an aperiodically poled LiTaO₃, *Appl. Phys. Lett.* **83**, 228–230, DOI:[10.1063/1.1592635](https://doi.org/10.1063/1.1592635).

He, J.L., J. Liu, G.Z. Luo, Y.L. Jia, J.X. Du, C.S. Guo, and S.N. Zhu, 2002, Blue generation in a periodically poled LiTaO₃ by frequency tripling an 1342 nm Nd:YVO₄ laser, *Chin. Phys. Lett.* **19**, 944–946, DOI:[10.1088/0256-307X/19/7/319](https://doi.org/10.1088/0256-307X/19/7/319).

Hebling, J., E.J. Mayer, J. Kuhl, and R. Szipocs, 1995, Chirped-mirror dispersion-compensated femtosecond optical parametric oscillator, *Opt. Lett.* **20**, 919–921.

Hooper, B.A., D.J. Gauthier, and J.M.J. Madey, 1994, 4th-harmonic generation in a single lithium-niobate crystal with cascaded 2nd-harmonic generation, *Appl. Optics* **33**, 6980–6984.

Huang, C.P., Y.Y. Zhu, S.N. Zhu, and N.B. Ming, 2002, Generation of three primary colours through coupled quasi-phase-matched processes, *J. Phys. Condens. Matter* **14**, 13899–13904, DOI:[10.1088/0953-8984/14/50/315](https://doi.org/10.1088/0953-8984/14/50/315).

Huang, G.X., 2001, Temporal optical solitons via multistep $\chi^{(2)}$ cascading, *Chin. Phys.* **10**, 418–423, DOI:[10.1088/1009-1963/10/5/311](https://doi.org/10.1088/1009-1963/10/5/311).

Ishizuki, H., T. Suhara, M. Fujimura, and H. Nishihara, 2001, Wavelength-conversion type picosecond optical switching using a waveguide QPM-SHG/DFG device, *Opt. Quantum Electron.* **33**, 953–961, DOI:[10.1023/A:1017542911327](https://doi.org/10.1023/A:1017542911327).

Ivanov, R., K. Koynov, and S. Saltiel, 2002, Efficiency of cascaded third harmonic generation in single quadratic crystal in focused beam, *Opt. Commun.* **212**, 397–403, DOI:[10.1016/S0030-4018\(02\)02007-2](https://doi.org/10.1016/S0030-4018(02)02007-2); Erratum: *Opt. Commun.* **218**, 197–198 (2003), DOI:[10.1016/S0030-4018\(03\)01201-X](https://doi.org/10.1016/S0030-4018(03)01201-X).

Jaque, D., J. Capmany, and J. Garcia Sole, 1999, Red, green, and blue laser light from a single Nd:YAl₃(BO₃)₄ crystal based on laser oscillation at 1.3 μ m, *Appl. Phys. Lett.* **75**, 325–327, DOI:[10.1063/1.124364](https://doi.org/10.1063/1.124364).

Johansen, S.K., S. Carrasco, L. Torner, and O. Bang, 2002, Engineering of spatial solitons in two-period QPM structures, *Opt. Commun.* **203**, 393–402, DOI:[10.1016/S0030-4018\(02\)01130-6](https://doi.org/10.1016/S0030-4018(02)01130-6).

Karaulanov, T., and S.M. Saltiel, 2003, Efficient collinear third-harmonic generation in a single two-dimensional nonlinear photonic crystal, in *12th International School on Quantum Electronics: Laser Physics and Applications*, edited by P.A. Atanasov, A.A. Serafetinides, and I.N. Kolev (SPIE, USA), volume 5226 of *Proc. SPIE*, pp. 114–118, .

Kartaloglu, T., and O. Aytur, 2003, Femtosecond self-doubling optical parametric oscillator based on KTiOAsO_4 , *IEEE J. Quantum Electron.* **39**, 65–67.

Kartaloglu, T., Z.G. Figen, and O. Aytur, 2003, Simultaneous phase matching of optical parametric oscillation and second-harmonic generation in aperiodically poled lithium niobate, *J. Opt. Soc. Am. B* **20**, 343–350.

Kartaloglu, T., K.G. Koprulu, and O. Aytur, 1997, Phase-matched self-doubling optical parametric oscillator, *Opt. Lett.* **22**, 280–282.

Kildal, H., and G.W. Iseler, 1979, Higher-order nonlinear processes in CdGeAs_2 , *Phys. Rev. B* **19**, 5218–5222, DOI:[10.1103/PhysRevB.19.5218](https://doi.org/10.1103/PhysRevB.19.5218).

Kim, M.S., and C.S. Yoon, 2002, Theoretical analysis of third-harmonic generation via direct third-order and cascaded second-order processes in $\text{CsLiB}_6\text{O}_{10}$ crystals, *Phys. Rev. A* **65**, 033831–9, DOI:[10.1103/PhysRevA.65.033831](https://doi.org/10.1103/PhysRevA.65.033831).

Kivshar, Yu.S., 1997, Quadratic solitons: past, present, and future, in *Advanced Photonics with Second-Order Optically Nonlinear Processes*, edited by A.D. Boardman, L. Pavlov, and S. Tanev (Kluwer, Boston), volume 61 of *NATO Science Series. 3. High Technology*, pp. 451–475.

Kivshar, Yu.S., T.J. Alexander, and S. Saltiel, 1999, Spatial optical solitons resulting from multistep cascading, *Opt. Lett.* **24**, 759–761.

Kivshar, Yu.S., A.A. Sukhorukov, and S.M. Saltiel, 1999, Two-color multistep cascading and parametric soliton-induced waveguides, *Phys. Rev. E* **60**, R5056–R5059, DOI:[10.1103/PhysRevE.60.R5056](https://doi.org/10.1103/PhysRevE.60.R5056).

Kobayashi, Y., and K. Torizuka, 2000, Measurement of the optical phase relation among subharmonic pulses in a femtosecond optical parametric oscillator, *Opt. Lett.* **25**, 856–858.

Komissarova, M.V., and A.P. Sukhorukov, 1993, Properties of an optical parametric oscillator with multiple frequencies, *Kvantov. Elektron.* **20**, 1025–1027 (in Russian) [English translation: *Quantum Electron.* **23**, 893–895 (1993)].

Komissarova, M.V., and A.P. Sukhorukov, 1996, Parametric processes in the interference of several channels of wave interaction, *Laser Phys.* **6**, 1034–1039.

Komissarova, M.W., A.P. Sukhorukov, and V.A. Tereshkov, 1997, On parametric amplification of traveling waves with multiple frequencies, *Izv. Akad. Nauk Ser. Fiz.* **61**, 2298–2302 (in Russian) [English translation: *Bull. Russ. Acad. Sci. Phys.* **61**, 1808–1812 (1997)].

Konotop, V.V., and V. Kuzmiak, 1999, Simultaneous second- and third-harmonic generation in one-dimensional photonic crystals, *J. Opt. Soc. Am. B* **16**, 1370–1376.

Koprulu, K.G., T. Kartaloglu, Y. Dikmelik, and O. Aytur, 1999, Single-crystal sum-frequency-generating optical parametric oscillator, *J. Opt. Soc. Am. B* **16**, 1546–1552.

Koynov, K., and S. Saltiel, 1998, Nonlinear phase shift via multistep $\chi^{(2)}$ cascading, *Opt. Commun.* **152**, 96–100, DOI:[10.1016/S0030-4018\(98\)00114-X](https://doi.org/10.1016/S0030-4018(98)00114-X).

Kunimatsu, D., C.Q. Xu, M.D. Pelusi, X. Wang, K. Kikuchi, H. Ito, and A. Suzuki, 2000, Subpicosecond pulse transmission over 144 km using midway optical phase conjugation via a cascaded second-order process in a LiNbO_3 waveguide, *IEEE Photonics Technol. Lett.* **12**, 1621–1623.

Laurell, F., J.B. Brown, and J.D. Bierlein, 1993, Simultaneous generation of UV and visible light in segmented KTP waveguides, *Appl. Phys. Lett.* **62**, 1872–1874, DOI:[10.1063/1.109528](https://doi.org/10.1063/1.109528).

Lee, C.K., J.Y. Zhang, J.Y. Huang, and C.L. Pan, 2003, Generation of femtosecond laser pulses tunable from 380 nm to 465 nm via cascaded nonlinear optical mixing in a noncollinear optical parametric amplifier with a type-I phase matched BBO crystal, *Opt. Express* **11**, 1702–1708.

Lee, D.H., M.E. Klein, J.P. Meyn, R. Wallenstein, P. Gross, and K.J. Boller, 2003, Phase-coherent all-optical frequency division by three, *Phys. Rev. A* **67**, 013808–13, DOI:[10.1103/PhysRevA.67.013808](https://doi.org/10.1103/PhysRevA.67.013808).

Lee, T.W., and S.C. Hagness, 2003, Pseudo-Spectral Time-Domain Analysis of Second Harmonic Generation in 2-D Nonlinear Photonic Crystals, in *Annual Meeting of the IEEE Lasers and Electro-Optics Society* (IEEE), pp. 194–195, .

Liao, J., J.L. He, H. Liu, H.T. Wang, S.N. Zhu, Y.Y. Zhu, and N.B. Ming, 2003, Simultaneous generation of red, green, and blue quasi-continuous-wave coherent radiation based on multiple quasiphase-matched interactions from a single, aperiodically-poled LiTaO_3 , *Appl. Phys. Lett.* **82**, 3159–3161, DOI:[10.1063/1.1570941](https://doi.org/10.1063/1.1570941).

Liu, W., J.Q. Sun, and J. Kurz, 2003, Bandwidth and tunability enhancement of wavelength conversion by quasi-phase-matching difference frequency generation, *Opt. Commun.* **216**, 239–246, DOI:[10.1016/S0030-4018\(02\)02336-2](https://doi.org/10.1016/S0030-4018(02)02336-2).

Liu, Z.W., Y. Du, J. Liao, S.N. Zhu, Y.Y. Zhu, Y.Q. Qin, H.T. Wang, J.L. He, C. Zhang, and N.B. Ming, 2002, Engineering

of a dual-periodic optical superlattice used in a coupled optical parametric interaction, *J. Opt. Soc. Am. B* **19**, 1676–1684.

Liu, Z.W., S.N. Zhu, Y.Y. Zhu, Y.Q. Qin, J.L. He, C. Zhang, H.T. Wang, N.B. Ming, X.Y. Liang, and Z.Y. Xu, 2001, Quasi-cw ultraviolet generation in a dual-periodic LiTaO₃ superlattice by frequency tripling, *Jpn. J. Appl. Phys.* **40**, 6841–6844, DOI:[10.1143/JJAP.40.6841](https://doi.org/10.1143/JJAP.40.6841).

Lobanov, V.E., and A.P. Sukhorukov, 2002, Dynamics of trapping of three harmonics into spatial soliton in quadratic periodically inverted crystals, *Izv. Akad. Nauk Ser. Fiz.* **66**, 1783–1786 (in Russian).

Lobanov, V.E., and A.P. Sukhorukov, 2003, Hybrid parametric solitons in nonlinear photonic crystals, *Izv. Vyssh. Uchebn. Zaved. Radiofiz.* **45**, 407–414 (in Russian) [English translation: *Radiophys. Quantum Electron.* **45**, 323–329 (2003)].

Lodahl, P., M. Bache, and M. Saffman, 2000, Spiral intensity patterns in the internally pumped optical parametric oscillator, *Phys. Rev. Lett.* **85**, 4506–4509, DOI:[10.1103/PhysRevLett.85.4506](https://doi.org/10.1103/PhysRevLett.85.4506).

Lodahl, P., M. Bache, and M. Saffman, 2001, Spatiotemporal structures in the internally pumped optical parametric oscillator, *Phys. Rev. A* **63**, 023815–12, DOI:[10.1103/PhysRevA.63.023815](https://doi.org/10.1103/PhysRevA.63.023815).

Lodahl, P., and M. Saffman, 1999, Pattern formation in singly resonant second-harmonic generation with competing parametric oscillation, *Phys. Rev. A* **60**, 3251–3261, DOI:[10.1103/PhysRevA.60.3251](https://doi.org/10.1103/PhysRevA.60.3251).

Longhi, S., 2001a, Hexagonal patterns in multistep optical parametric processes, *Opt. Lett.* **26**, 713–715.

Longhi, S., 2001b, Multiphase patterns in self-phase-locked optical parametric oscillators, *Eur. Phys. J. D* **17**, 57–66, DOI:[10.1007/s100530170037](https://doi.org/10.1007/s100530170037).

Longhi, S., 2001c, Spiral waves in a class of optical parametric oscillators, *Phys. Rev. E* **63**, 055202–4, DOI:[10.1103/PhysRevE.63.055202](https://doi.org/10.1103/PhysRevE.63.055202).

Luo, G.Z., S.N. Zhu, J.L. He, Y.Y. Zhu, H.T. Wang, Z.W. Liu, C. Zhang, and N.B. Ming, 2001, Simultaneously efficient blue and red light generations in a periodically poled LiTaO₃, *Appl. Phys. Lett.* **78**, 3006–3008, DOI:[10.1063/1.1371245](https://doi.org/10.1063/1.1371245).

Marte, M.A.M., 1995a, Nonlinear dynamics and quantum noise for competing $\chi^{(2)}$ nonlinearities, *J. Opt. Soc. Am. B* **12**, 2296–2303.

Marte, M.A.M., 1995b, Sub-poissonian twin beams via competing nonlinearities, *Phys. Rev. Lett.* **74**, 4815–4818, DOI:[10.1103/PhysRevLett.74.4815](https://doi.org/10.1103/PhysRevLett.74.4815).

McGowan, C., D.T. Reid, Z.E. Penman, M. Ebrahimzadeh, W. Sibbett, and D.H. Jundt, 1998, Femtosecond optical parametric oscillator based on periodically poled lithium niobate, *J. Opt. Soc. Am. B* **15**, 694–701.

Meredith, G.R., 1981, Cascading in optical third-harmonic generation by crystalline quartz, *Phys. Rev. B* **24**, 5522–5532, DOI:[10.1103/PhysRevB.24.5522](https://doi.org/10.1103/PhysRevB.24.5522).

Misoguti, L., S. Backus, C.G. Durfee, R. Bartels, M.M. Murnane, and H.C. Kapteyn, 2001, Generation of broadband VUV light using third-order cascaded processes, *Phys. Rev. Lett.* **87**, 013601–4, DOI:[10.1103/PhysRevLett.87.013601](https://doi.org/10.1103/PhysRevLett.87.013601).

Moore, G.T., K. Koch, M.E. Dearborn, and M. Vaidyanathan, 1998, A simultaneously phase-matched tandem optical parametric oscillator, *IEEE J. Quantum Electron.* **34**, 803–810.

Morozov, E.Y., and A.S. Chirkin, 2003, Consecutive parametric interactions of light waves with aliquant frequencies, *J. Opt. A-Pure Appl. Opt.* **5**, 233–238, DOI:[10.1088/1464-4258/5/3/315](https://doi.org/10.1088/1464-4258/5/3/315).

Mu, X.D., X.H. Gu, M.V. Makarov, Y.J. Ding, J.Y. Wang, I.Q. Wei, and Y.G. Liu, 2000, Third-harmonic generation by cascading second-order nonlinear processes in a cerium-doped KTiOPO₄ crystal, *Opt. Lett.* **25**, 117–119.

Myers, L.E., R.C. Eckardt, M.M. Fejer, R.L. Byer, W.R. Bosenberg, and J.W. Pierce, 1995, Quasi-phase-matched optical parametric oscillators in bulk periodically poled LiNbO₃, *J. Opt. Soc. Am. B* **12**, 2102–2116.

Ni, P., B. Ma, X. Wang, B. Cheng, and D. Zhang, 2003, Second-harmonic generation in two-dimensional periodically poled lithium niobate using second-order quasiphase matching, *Appl. Phys. Lett.* **82**, 4230–4232, DOI:[10.1063/1.1579856](https://doi.org/10.1063/1.1579856).

Nikandrov, A.V., and A.S. Chirkin, 2002a, Entangled quantum states in consecutive and cascade nonlinear optical processes, *J. Russ. Laser Res.* **23**, 81–91, DOI:[10.1023/A:1014235615491](https://doi.org/10.1023/A:1014235615491).

Nikandrov, A.V., and A.S. Chirkin, 2002b, The formation of a light field with suppressed photon fluctuations by nonlinear optical methods, *Pis'ma Zh. Éksp. Teor. Fiz.* **76**, 333–336 (in Russian) [English translation: *JETP Lett.* **76**, 275–278 (2002), DOI:[10.1134/1.1520620](https://doi.org/10.1134/1.1520620)].

Nitti, S., H.M. Tan, G.P. Banfi, and V. Degiorgio, 1994, Induced 3rd-order nonlinearity via cascaded 2nd-order effects in organic-crystals of MBA-NP, *Opt. Commun.* **106**, 263–268, DOI:[10.1016/0030-4018\(94\)90334-4](https://doi.org/10.1016/0030-4018(94)90334-4).

Norton, A.H., and C.M. de Sterke, 2003a, Optimal poling of nonlinear photonic crystals for frequency conversion, *Opt. Lett.* **28**, 188–190.

Norton, A.H., and C.M. de Sterke, 2003b, Two-dimensional poling patterns for 3rd and 4th harmonic generation, *Opt. Express* **11**, 1008–1014.

Orlov, R.Yu., A.P. Sukhorukov, and I.V. Tomov, 1972, Simultaneous generation of second and third optical harmonics in a crystal, *Annuaire de L'Universite de Sofia Faculte de Physique* **64-65**, 283–288 (in Russian).

Pasiskevicius, V., S.J. Holmgren, S. Wang, and F. Laurell, 2002, Simultaneous second-harmonic generation with two orthog-

onal polarization states in periodically poled KTP, Opt. Lett. **27**, 1628–1630.

Pelinovsky, D.E., A.V. Buryak, and Yu.S. Kivshar, 1995, Instability of solitons governed by quadratic nonlinearities, Phys. Rev. Lett. **75**, 591–595, DOI:[10.1103/PhysRevLett.75.591](https://doi.org/10.1103/PhysRevLett.75.591).

Petrov, G.I., O. Albert, J. Etchepare, and S.M. Saltiel, 2001, Cross-polarized wave generation by effective cubic nonlinear optical interaction, Opt. Lett. **26**, 355–357.

Petrov, G.I., O. Albert, N. Minkovski, J. Etchepare, and S.M. Saltiel, 2002, Experimental and theoretical investigation of generation of a cross-polarized wave by cascading of two different second-order processes, J. Opt. Soc. Am. B **19**, 268–279.

Petrov, V., and F. Noack, 1995, Frequency upconversion of tunable femtosecond pulses by parametric amplification and sum-frequency generation in a single nonlinear crystal, Opt. Lett. **20**, 2171–2173.

Pfister, O., J.S. Wells, L. Hollberg, L. Zink, D.A. Van Baak, M.D. Levenson, and W.R. Bosenberg, 1997, Continuous-wave frequency tripling and quadrupling by simultaneous three-wave mixings in periodically poled crystals: application to a two-step 1.19–10.71- μ m frequency bridge, Opt. Lett. **22**, 1211–1213.

Powers, P.E., R.J. Ellingson, W.S. Pelouch, and C.L. Tang, 1993, Recent advances of the Ti:sapphire-pumped high-repetition-rate femtosecond optical parametric oscillator, J. Opt. Soc. Am. B **10**, 2162–2167.

Qin, Y.Q., Y.Y. Zhu, C. Zhang, and N.B. Ming, 2003, Theoretical investigations of efficient cascaded third-harmonic generation in quasi-phase-matched and -mismatched configurations, J. Opt. Soc. Am. B **20**, 73–82.

Qin, Y.Q., Y.Y. Zhu, S.N. Zhu, and N.B. Ming, 1998, Quasi-phase-matched harmonic generation through coupled parametric processes in a quasiperiodic optical superlattice, J. Appl. Phys. **84**, 6911–6916, DOI:[10.1063/1.368988](https://doi.org/10.1063/1.368988).

Qiu, P., and A. Penzkofer, 1988, Picosecond third-harmonic light generation in beta -BaB₂O₄, Appl. Phys. B **45**, 225–236.

Reintjes, J.F., 1984, *Nonlinear Optical Parametric Processes in Liquids and Gasses* (Academic Press, New York).

Romero, J.J., D. Jaque, J.G. Sole, and A.A. Kaminskii, 2002, Simultaneous generation of coherent light in the three fundamental colors by quasicylindrical ferroelectric domains in Sr_{0.6}Ba_{0.4}(NbO₃)₂, Appl. Phys. Lett. **81**, 4106–4108, DOI:[10.1063/1.1523156](https://doi.org/10.1063/1.1523156).

Rostovtseva, V.V., S.M. Saltiel, A.P. Sukhorukov, and V.G. Tunkin, 1980, Higher optical harmonics generation in focused beams, Kvantov. Elektron. **7**, 1081–1088 (in Russian) [English translation: Quantum Electron. **10**, 616 (1980)].

Rostovtseva, V.V., A.P. Sukhorukov, V.G. Tunkin, and S.M. Saltiel, 1977, Higher harmonics generation by cascade processes in focused beams, Opt. Commun. **22**, 56–60, DOI:[10.1016/0030-4018\(77\)90246-2](https://doi.org/10.1016/0030-4018(77)90246-2).

Saltiel, S., and Y. Deyanova, 1999, Polarization switching as a result of cascading of two simultaneously phase-matched quadratic processes, Opt. Lett. **24**, 1296–1298.

Saltiel, S., and Yu.S. Kivshar, 2000a, Phase matching in nonlinear $\chi^{(2)}$ photonic crystals, Opt. Lett. **25**, 1204–1206; Errata: Opt. Lett. **25**, 1612 (2000).

Saltiel, S., K. Koynov, Y. Deyanova, and Yu.S. Kivshar, 2000, Nonlinear phase shift resulting from two-color multistep cascading, J. Opt. Soc. Am. B **17**, 959–965.

Saltiel, S.M., and Yu.S. Kivshar, 2000b, Phase-matching for nonlinear optical parametric processes with multistep cascading, Bulgarian J. Phys. **27**, 57–64.

Saltiel, S.M., and Yu.S. Kivshar, 2002, All-optical deflection and splitting by second-order cascading, Opt. Lett. **27**, 921–923.

Schiller, S., G. Breitenbach, R. Paschotta, and J. Mlynek, 1996, Subharmonic-pumped continuous-wave parametric oscillator, Appl. Phys. Lett. **68**, 3374–3376, DOI:[10.1063/1.116508](https://doi.org/10.1063/1.116508).

Schiller, S., and R.L. Byer, 1993, Quadruply resonant optical parametric oscillation in a monolithic total-internal-reflection resonator, J. Opt. Soc. Am. B **10**, 1696–1707.

Schreiber, G., H. Suche, Y.L. Lee, W. Grundkotter, V. Quiring, R. Ricken, and W. Sohler, 2001, Efficient cascaded difference frequency conversion in periodically poled Ti : LiNbO₃ waveguides using pulsed and cw pumping, Appl. Phys. B **73**, 501–504, DOI:[10.1007/s003400100708](https://doi.org/10.1007/s003400100708).

Shen, Y.R., 1984, *The Principles of Nonlinear Optics* (John Wiley and Sons, New York).

Shi, B., and X. Wang, 2002, Nonlinear photonic band-gap structure with extremely high efficiency for third-harmonic generation, Appl. Phys. Lett. **80**, 3667–3669, DOI:[10.1063/1.1480120](https://doi.org/10.1063/1.1480120).

Slyusarev, S., T. Ikegami, and S. Ohshima, 1999, Phase-coherent optical frequency division by 3 of 532-nm laser light with a continuous-wave optical parametric oscillator, Opt. Lett. **24**, 1856–1858.

Smithers, M.E., and E.Y.C. Lu, 1974, Quantum theory of coherent spontaneous and stimulated emissions, Phys. Rev. A **9**, 790–801, DOI:[10.1103/PhysRevA.9.790](https://doi.org/10.1103/PhysRevA.9.790).

Stegeman, G.I., D.J. Hagan, and L. Torner, 1996, $\chi^{(2)}$ cascading phenomena and their applications to all-optical signal processing, mode-locking, pulse compression and solitons, Opt. Quantum Electron. **28**, 1691–1740; Corrigendum: Opt. Quantum Electron. **29**, 532 (1997).

de Sterke, M., S.M. Saltiel, and Yu.S. Kivshar, 2001, Efficient collinear fourth-harmonic generation by two-channel multistep cascading in a single two-dimensional nonlinear photonic crystal, Opt. Lett. **26**, 539–541.

Sukhorukov, A.A., 2000, Approximate solutions and scaling transformations for quadratic solitons, *Phys. Rev. E* **61**, 4530–4539, DOI:[10.1103/PhysRevE.61.4530](https://doi.org/10.1103/PhysRevE.61.4530).

Sukhorukov, A.A., T.J. Alexander, Yu.S. Kivshar, and S.M. Saltiel, 2001, Multistep cascading and fourth-harmonic generation, *Phys. Lett. A* **281**, 34–38, DOI:[10.1016/S0375-9601\(01\)00106-2](https://doi.org/10.1016/S0375-9601(01)00106-2).

Sukhorukov, A.P., 1988, *Nonlinear Wave Interactions in Optics and Radiophysics* (Nauka, Moscow) (in Russian).

Sukhorukov, A.P., and I.V. Tomov, 1970, On simultaneous synchronous generation of the second and the third harmonics in crystals in quadratic nonlinearity, *Izv. Vyssh. Uchebn. Zaved. Radiofiz.* **13**, 266–270 (in Russian).

Sun, J., and W. Liu, 2003, Multiwavelength generation by utilizing second-order nonlinearity of LiNbO_3 waveguides in fiber lasers, *Opt. Commun.* **224**, 125, DOI:[10.1016/S0030-4018\(03\)01727-9](https://doi.org/10.1016/S0030-4018(03)01727-9).

Sundheimer, M.L., A. Villeneuve, G.I. Stegeman, and J.D. Bierlein, 1994a, Cascading nonlinearities in KTP wave-guides at communications wavelengths, *Electron. Lett.* **30**, 1400–1401, DOI:[10.1049/el:19940966](https://doi.org/10.1049/el:19940966).

Sundheimer, M.L., A. Villeneuve, G.I. Stegeman, and J.D. Bierlein, 1994b, Simultaneous generation of red, green and blue-light in a segmented KTP wave-guide using a single-source, *Electron. Lett.* **30**, 975–976, DOI:[10.1049/el:19940674](https://doi.org/10.1049/el:19940674).

Taima, T., K. Komatsu, T. Kaino, C.P. Franceschina, L. Tartara, G.P. Banfi, and V. Degiorgio, 2003, Third-order nonlinear optical properties of 2-adamantylamino-5-nitropyridine caused by cascaded second-order nonlinearity, *Opt. Mater.* **21**, 83–86, DOI:[10.1016/S0925-3467\(02\)00118-0](https://doi.org/10.1016/S0925-3467(02)00118-0).

Takagi, Y., and S. Muraki, 2000, Third-harmonic generation in a noncentrosymmetrical crystal: direct third-order or cascaded second-order process?, *J. Lumines.* **87**, 865–867, DOI:[10.1016/S0022-2313\(99\)00445-7](https://doi.org/10.1016/S0022-2313(99)00445-7).

Tan, H., G.P. Banfi, and A. Tomaselli, 1993, Optical frequency mixing through cascaded 2nd-order processes in beta-barium borate, *Appl. Phys. Lett.* **63**, 2472–2474, DOI:[10.1063/1.110453](https://doi.org/10.1063/1.110453).

Tomov, I.V., B. Van Wonterghem, and P.M. Rentzepis, 1992, Third-harmonic generation in barium borate, *Appl. Optics* **31**, 4172–4174.

Torner, L., 1998, Spatial solitons in quadratic nonlinear media, in *Beam Shaping and Control with Nonlinear Optics*, edited by F. Kajzer and R. Reinisch (Plenum, New York), pp. 229–258.

Torruellas, W.E., Yu.S. Kivshar, and G.I. Stegeman, 2001, Quadratic solitons, in *Spatial Optical Solitons*, edited by S. Trillo and W.E. Torruellas (Springer-Verlag, New York), volume 82 of *Springer Series in Optical Sciences*, pp. 127–168.

Towers, I., A.V. Buryak, R.A. Sammut, and B.A. Malomed, 2000, Quadratic solitons resulting from double-resonance wave mixing, *J. Opt. Soc. Am. B* **17**, 2018–2025.

Towers, I., R. Sammut, A.V. Buryak, and B.A. Malomed, 1999, Soliton multistability as a result of double-resonance wave mixing in $\chi^{(2)}$ media, *Opt. Lett.* **24**, 1738–1740.

Towers, I.N., and B.A. Malomed, 2002, Polychromatic solitons in a quadratic medium, *Phys. Rev. E* **66**, 046620–7, DOI:[10.1103/PhysRevE.66.046620](https://doi.org/10.1103/PhysRevE.66.046620).

Trevino-Palacios, C.G., G.I. Stegeman, P. Baldi, and M.P. De Micheli, 1998, Wavelength shifting using cascaded second-order processes for WDM applications at $1.55 \mu\text{m}$, *Electron. Lett.* **34**, 2157–2158, DOI:[10.1049/el:19981459](https://doi.org/10.1049/el:19981459).

Trevino-Palacios, C.G., G.I. Stegeman, M.P. Demicheli, P. Baldi, S. Nouh, D.B. Ostrowsky, D. Delacourt, and M. Papuchon, 1995, Intensity-dependent mode competition in 2nd-harmonic generation in multimode wave-guides, *Appl. Phys. Lett.* **67**, 170–172, DOI:[10.1063/1.114656](https://doi.org/10.1063/1.114656).

Trillo, S., and G. Assanto, 1994, Polarization spatial chaos in 2nd-harmonic generation, *Opt. Lett.* **19**, 1825–1827.

Unsbo, P., 1995, Phase conjugation by cascaded second-order nonlinear-optical processes, *J. Opt. Soc. Am. B* **12**, 43–48.

Vaidyanathan, M., R.C. Eckardt, V. Dominic, L.E. Myers, and T.P. Grayson, 1997, Cascaded optical parametric oscillations, *Opt. Express* **1**, 49–53.

Vakhitov, N.G., and A.A. Kolokolov, 1973, Stationary solutions of the wave equation in the medium with nonlinearity saturation, *Izv. Vyssh. Uchebn. Zaved. Radiofiz.* **16**, 1020–1028 (in Russian) [English translation: *Radiophys. Quantum Electron.* **16**, 783–789 (1973)].

Varanavicius, A., A. Dubietis, A. Berzanskis, R. Danielius, and A. Piskarskas, 1997, Near-degenerate cascaded four-wave mixing in an optical parametric amplifier, *Opt. Lett.* **22**, 1603–1605.

Volkov, V.V., and A.S. Chirkin, 1998, Quasi-phase-matched parametric amplification of waves with low-frequency pumping, *Kvantov. Elektron.* **25**, 101–102 (in Russian) [English translation: *Quantum Electron.* **28**, 95–96 (1998), DOI:[10.1070/qe1998v028n02ABEH001152](https://doi.org/10.1070/qe1998v028n02ABEH001152)].

Volkov, V.V., G.D. Laptev, E.Yu. Morozov, I.I. Naumova, and A.S. Chirkin, 1998, Consecutive quasi-phase-matched generation of the third harmonic of the radiation from an Nd:YAG laser in a periodically poled Y:LiNbO_3 crystal, *Kvantov. Elektron.* **25**, 1046–1048 (in Russian) [English translation: *Quantum Electron.* **28**, 1020–1021 (1998), DOI:[10.1070/qe1998v028n11ABEH001377](https://doi.org/10.1070/qe1998v028n11ABEH001377)].

Wang, C.C., and E.L. Baardsen, 1969, Optical third harmonic generation using mode-locked and non-mode-locked lasers, *Appl. Phys. Lett.* **15**, 396–397, DOI:[10.1063/1.1652874](https://doi.org/10.1063/1.1652874).

Wang, X.H., and B.Y. Gu, 2001, Nonlinear frequency conversion in 2D $\chi^{(2)}$ photonic crystals and novel nonlinear double-circle construction, *Eur. Phys. J. B* **24**, 323–326, DOI:[10.1007/s10051-001-8681-6](https://doi.org/10.1007/s10051-001-8681-6).

Xu, C.Q., and B. Chen, 2004, Cascaded wavelength conversions based on sum-frequency generation and difference-frequency generation, *Opt. Lett.* **29**, 292–294.

Xu, Z.Y., X.Y. Liang, J. Li, A.Y. Yao, X.C. Lin, D.F. Cui, and L.A. Wu, 2002, Violet to infrared multiwavelength generation in periodically poled lithium niobate pumped by a Q-switched Nd:YVO₄ laser, *Chin. Phys. Lett.* **19**, 801–803, DOI:[10.1088/0256-307X/19/6/318](https://doi.org/10.1088/0256-307X/19/6/318).

Yablonovitch, E., C. Flytzanis, and N. Bloembergen, 1972, Anisotropic interference of three-wave and double two-wave frequency mixing in GaAs, *Phys. Rev. Lett.* **29**, 865–868, DOI:[10.1103/PhysRevLett.29.865](https://doi.org/10.1103/PhysRevLett.29.865).

Yang, X.L., and S.W. Xie, 1995, Expression of 3rd-order effective nonlinear susceptibility for 3rd-harmonic generation in crystals, *Appl. Optics* **34**, 6130–6135.

Zeng, X.L., X.F. Chen, Y.P. Chen, Y.X. Xia, and Y.L. Chen, 2003, Observation of all-optical wavelength conversion based on cascaded effect in periodically poled lithium niobate waveguide, *Opt. Laser Technol.* **35**, 187–190, DOI:[10.1016/S0030-3992\(02\)00170-6](https://doi.org/10.1016/S0030-3992(02)00170-6).

Zgonik, M., and P. Gunter, 1996, Cascading nonlinearities in optical four-wave mixing, *J. Opt. Soc. Am. B* **13**, 570–576.

Zhang, C., H. Wei, Y.Y. Zhu, H.T. Wang, S.N. Zhu, and N.B. Ming, 2001, Third-harmonic generation in a general two-component quasiperiodic optical superlattice, *Opt. Lett.* **26**, 899–901.

Zhang, C., Y.Y. Zhu, S.X. Yang, Y.Q. Qin, S.N. Zhu, Y.B. Chen, H. Liu, and N.B. Ming, 2000, Crucial effects of coupling coefficients on quasi-phase-matched harmonic generation in an optical superlattice, *Opt. Lett.* **25**, 436–438.

Zhang, C., Y.Y. Zhu, S.N. Zhu, and N.B. Ming, 2001, Coupled quasi-phase-matched high-order harmonic generation, *J. Opt. A-Pure Appl. Opt.* **3**, 317–320, DOI:[10.1088/1464-4258/3/5/301](https://doi.org/10.1088/1464-4258/3/5/301).

Zhang, X., J. Hebling, J. Kuhl, W.W. Ruhle, L. Palfalvi, and H. Giessen, 2002, Femtosecond near-IR optical parametric oscillator with efficient intracavity generation of visible light, *J. Opt. Soc. Am. B* **19**, 2479–2488.

Zhang, X.P., J. Hebling, A. Bartels, D. Nau, J. Kuhl, W.W. Ruhle, and H. Giessen, 2002, 1-GHz-repetition-rate femtosecond optical parametric oscillator, *Appl. Phys. Lett.* **80**, 1873–1875, DOI:[10.1063/1.1461870](https://doi.org/10.1063/1.1461870).

Zhang, X.P., J. Hebling, J. Kuhl, W.W. Ruhle, and H. Giessen, 2001, Efficient intracavity generation of visible pulses in a femtosecond near-infrared optical parametric oscillator, *Opt. Lett.* **26**, 2005–2007.

Zhao, L.M., B.Y. Gu, Y.S. Zhou, and F.H. Wang, 2003, Coupled third harmonic generations and multiple mode effects in aperiodic optical superlattices with a finite lateral width, *J. Appl. Phys.* **94**, 1882–1891, DOI:[10.1063/1.1585122](https://doi.org/10.1063/1.1585122).

Zhou, B., C.Q. Xu, and B. Chen, 2003, Comparison of difference-frequency generation and cascaded $\chi^{(2)}$ based wavelength conversions in LiNbO₃ quasi-phase-matched waveguides, *J. Opt. Soc. Am. B* **20**, 846–852.

Zhu, S., Y.Y. Zhu, and N.B. Ming, 1997, Quasi-phase-matched third-harmonic generation in a quasiperiodic optical superlattice, *Science* **278**, 843–846, DOI:[10.1126/science.278.5339.843](https://doi.org/10.1126/science.278.5339.843).

Zhu, Y.Y., and N.B. Ming, 1999, Dielectric superlattices for nonlinear optical effects, *Opt. Quantum Electron.* **31**, 1093–1128, DOI:[10.1023/A:1006932103769](https://doi.org/10.1023/A:1006932103769).

Zhu, Y.Y., R.F. Xiao, J.S. Fu, G.K.L. Wong, and N.B. Ming, 1998, Third harmonic generation through coupled second-order nonlinear optical parametric processes in quasiperiodically domain-inverted Sr_{0.6}Ba_{0.4}Nb₂O₆ optical superlattices, *Appl. Phys. Lett.* **73**, 432–434, DOI:[10.1063/1.121890](https://doi.org/10.1063/1.121890).

Zondy, J.J., 2003, Stability of the self-phase-locked pump-enhanced singly resonant parametric oscillator, *Phys. Rev. A* **67**, 035801–4, DOI:[10.1103/PhysRevA.67.035801](https://doi.org/10.1103/PhysRevA.67.035801).

Zondy, J.J., A. Douillet, A. Tallet, E. Ressayre, and M. Le Berre, 2001, Theory of self-phase-locked optical parametric oscillators, *Phys. Rev. A* **63**, 023814–14, DOI:[10.1103/PhysRevA.63.023814](https://doi.org/10.1103/PhysRevA.63.023814).